Finanziato dall'Unione europea NextGenerationEU
Ministero dell'Università e della Ricerca
Italiadomani PIANO NAZIONALE DI RIPRESA E RESILIENZA

UNIVERSITÀ DEGLI STUDI DEL SANNIO Benevento

Department of Science and Technology

Ph.D. course in

Science and Technology for Environmental and Health

XXXVIII CYCLE

Omics approaches for identifying novel molecular targets of metabolic alterations

"Modulation of hepatic metabolism and autophagy in MASLD"

Tutor

Prof. Maria Moreno

Co-Tutor

Prof. Antonia Giacco

PhD student

Nicla Scopigno

PhD Course Coordinator

Prof. Marina Paolucci

Academic Year 2024-2025

Table of Contents

Abbreviations

8-OHdG: 8-hydroxy-2'-deoxyguanosine

AALD: alcohol-associated liver disease

ACC: acetyl-CoA carboxylase

ACSL4: acyl-CoA synthetase long chain family member 4

ADP: adenosine diphosphate

ADRP: adipose differentiation-related protein

AF2: ligand-independent activating domain

AKT: serine-threonine protein kinase

AMPK: 5' AMP-activated protein kinase

ANT: adenine nucleotide translocator

APE: apurinic/apyrimidinic endonuclease

ATG14: autophagy-related protein 14

ATG5: autophagy related protein 5

ATG7: autophagy-related protein 7

ATG9: autophagy related protein 9

ATP: adenosine triphosphate

BAT: brown adipose tissue

BCL-2: B-cell-leukemia/lymphoma 2

BCL-XL: B-cell Lymphoma-extra large

BW: body weight

CD36: cluster of differentiation 36

cGAS: cyclic GMP-AMP synthase

cGMP: cyclic guanosine monophosphate

ChREBP: carbohydrate response element-binding protein

CL: cardiolipin

CMA: chaperone-mediated autophagy

Co-As: coactivators

Co-Rs: corepressors

COX: cytochrome c oxidase

CPS1: carbamoyl phosphate synthetase 1

CPT1: carnitine palmitoyltransferase 1

CRY1: cryptochrome-1

CYP7A: cholesterol 7α-hydroxylase

D1: type I deiodinase

D2: type II deiodinase

D3: type III deiodinase

DAG: diacylglycerol

DAMPs: damage-associated molecular patterns

DBD: DNA- binding domain

DILI: drug-induced liver injury

DNL: de novo lipogenesis

DRP1: dynamin-related protein 1

ER: endoplasmic reticulum

ERR: estrogen-related receptor

ETC: electron transport chain

FADH2: flavine adenine dinucleotide

FASN: fatty acid synthase

FATP: fatty acid transport protein

FFA: free fatty acid

FIS1: fission protein 1

FOXO1: forkhead box protein O1

FXR: farnesoid X receptor

G3PDH: glycerol-3-phosphate dehydrogenase

GDNF: glial cell line-derived neurotrophic

GLP-1: glucagon-like peptide-1

GPX: glutathione peroxidase

GSH: glutathione

GSK3β: glycogen synthase kinase 3β

H_2O_2: hydrogen peroxide

HCC: hepatocellular carcinoma

HFD: high fat diet

HMGCR: 3-hydroxy-3-methyl-glutaryl-coenzyme A reductase

HMGCS1: 3-hydroxy-3-methylglutaryl-CoA synthase 1

HW: heart weight

hPOBs: human primary osteoblasts

HPT axis: hypothalamic-pituitary-thyroid axis

HSC70: heat shock cognate 70 kDa protein

HSCs: hepatic stellate cells

IKBα: inhibitor of kappa B alpha

IL-1β: interleukin-1 beta

IL-6: interleukin-6

IL-10: interleukin-10

IRS1/2: insulin receptor substrates 1 and 2

KFERQ: specific pentapeptide motif 'Lysine- Phenylalanine- Glutamic Acid- Arginine - Glutamine

LAMP-2A: lysosome-associated membrane protein 2A

LBD: ligand-binding domain

LC3II: microtubule-associated protein 1 Light Chain 3B

LDL: low-density lipoprotein

LDLr: low-density lipoprotein receptor

LXL: liver X receptor

MAPK: mitogen-activated protein kinase

MASH: metabolic dysfunction-associated steatohepatitis

MASLD: metabolic dysfunction-associated steatotic liver disease

MCT8: monocarboxylate transporter 8

MCTs: monocarboxylate transporters

MDA: malondialdehyde

MFF: mitochondrial fission factor

MFN1: mitochondrial fusion protein mitofusin-1

MFN2: mitochondrial fusion protein mitofusin-2

mGDP: mitochondrial Glycerol-3-Phosphate Dehydrogenase

MPTP: mitochondrial permeability transition pore

MQC: mitochondrial quality control

mtDNA: mitochondrial DNA

mTOR: mammalian target of rapamycin complex 1

NADH: nicotinamide adenine dinucleotide

NAFLD: non-alcoholic fatty liver disease

NASH: non-alcoholic steatohepatitis

NF-κB: nuclear factor-kappa B

NIS: sodium iodide symporter

NLRP3: NOD-like receptor protein 3

NLS: nuclear localization signal

NO: nitric oxide

NOX 4: NADPH oxidase 4

NPCs: non-parenchymal cells

NR: nuclear receptor

NRF-1: nuclear respiratory factor 1

NRF2: nuclear respiratory factor 2

NTIS: non-thyroidal illness syndrome

OGG1: 8-Oxoguanine Glycosylase 1

OMA1: OMA1 zinc metallopeptidase

OPA1: optic atrophy 1

OXPHOS: oxidative phosphorylation

P/O ratio: phosphate/oxygen ratio

P62: Sequestosome 1

PARKIN: E3 ubiquitin-protein ligase Parkin.

PCKε: protein kinase C isoforms ε

PGC-1α: peroxisome proliferator-activated receptor gamma coactivator 1-alpha

PI3K: phosphatidylinositol 3-kinase

PINK1: PTEN-induced kinase 1

PNPLA3: patatin-like phospholipase domain containing 3

POLγ: DNA polymerase gamma

PPARα: peroxisome proliferator-activated receptor alpha

PRDX3: peroxiredoxin 3

RMR: resting metabolic rate

ROS: reactive oxygen species

rT3: reverse T3

RUBICON: run domain beclin-1 interacting and cysteine-rich containing protein

RXRs: retinoid X receptors

SCD1: stearoyl-CoA desaturase-1

SERCA: sarco/endoplasmic reticulum Ca^{2+}-ATPase

SIRT3: sirtuin 3

SOCS3: suppressor of Cytokine Signaling 3

SOD: superoxide dismutase

SPOT14: thyroid hormone-inducible hepatic protein (THRSP)

SREBP-1c: sterol regulatory element-binding protein-1c

STING: stimulator of interferon genes

T2: 3,5-diiodotironina

T2DM: type 2 diabetes mellitus

T3: triiodotironina

T4: thyroxine

TB-1: Tat-Beclin 1

TBK1: TANK-binding kinase

TC: cholesterol

TFAM: mitochondria transcription factor A

TFE3: transcription factor E3

TFEB: transcription factor EB

TG: triglycerides

TH: thyroid hormon

THRA: thyroid hormone receptor alpha

THRB: thyroid hormone receptor beta

Thrα: thyroid hormone receptor alpha

Thrβ: thyroid hormone receptor beta

TNF-α: tumor necrosis factor-alpha

TOM20: translocase of Outer Mitochondrial Membrane 20

TPO: thyroid peroxidase

TREs: thyroid hormone response elements

TRs: thyroid hormone receptors

TRα: thyroid hormone receptor isoform α

TRβ: thyroid hormone receptor isoform β

TSH: thyroid stimulating hormone

UCP1: uncoupling protein 1

UCP2: uncoupling protein 2

UCP3: uncoupling protein 3

ULK1: unc-51 Like Autophagy Activating Kinase 1.

VLDL: very low-density lipoprotein

VPS34: vacuolar protein sorting 34

WAT: white adipose tissue

Abstract

Metabolic dysfunction-associated steatotic liver disease (MASLD) is a high prevalent chronic liver disorder driven by ectopic lipid accumulation in hepatocytes and closely associated with obesity, type 2 diabetes, and metabolic syndrome. Current therapeutic approaches mainly target systemic metabolic risk factors and fail to directly address the hepatic molecular mechanisms underlying disease progression, particularly mitochondrial dysfunction, highlighting the need for more targeted therapeutic strategies. Increasing evidence indicates that alterations in mitochondrial homeostasis and autophagy play a central role in MASLD pathogenesis, supporting the need for innovative, mechanism-based therapeutic approaches.

Thyroid hormones play a key role in hepatic lipid metabolism and mitochondrial function and therefore represent attractive therapeutic candidates. While 3,5,3'-triiodo-L-thyronine (T3) potently stimulates lipid oxidation and energy expenditure, its clinical use is limited by systemic thyrotoxic effects. In contrast, 3,5-diiodo-L-thyronine (T2), a naturally occurring T3 metabolite, exerts tissue-selective – predominantly hepatic – metabolic effects without disrupting systemic thyroid homeostasis, acting mainly through non-genomic mechanisms that directly modulate mitochondrial function.

Autophagy dysfunction further contributes to MASLD pathogenesis by impairing lipid droplet clearance (lipophagy) and removal of damaged mitochondria (mitophagy). Tat-Beclin 1 (Tb), a peptide known as an "autophagy inducer", represents a pharmacological approach to restore autophagic flux. The combined targeting of mitochondrial metabolism and autophagy may therefore offer complementary therapeutic benefits.

This study investigated whether pharmacological modulation of hepatic mitochondrial metabolism and autophagy counteracts MASLD progression. A mouse model of human MASLD was induced by 19 weeks of high-fat diet (HFD, 50% fat). HFD-fed mice were treated short-term (10 days) with the iodothyronines T3 and T2, and Tb, administered alone and in combination with T2.

The project was structured around three main aims: (I) to establish and validate the HFD-induced MASLD model and assess the effects of pharmacological interventions on the whole body metabolic phenotype; (II) to characterise hepatic processes, including redox homeostasis, mitochondrial DNA damage and repair mechanisms, and their modulation by pharmacological interventions; (III) to investigate mitochondrial dysfunction-driven inflammatory signalling, mitochondrial quality control mechanisms (MQC - biogenesis, dynamics, and mitophagy), and autophagy, with an in depth analysis of mitochondrial function and electron transport chain composition.

After 19 weeks of HFD feeding, mice developed overt MASLD, characterized by dyslipidaemia, insulin resistance, hepatic steatosis, and a hypothyroid state, accompanied by oxidative stress, inflammation, impaired autophagy, disrupted MQC, and defective mitochondrial bioenergetics.

Both T3 and T2 showed beneficial effects, reducing adiposity and hepatic lipid accumulation, and improving insulin signalling, fatty acid oxidation, and lipophagy. Moreover, both iodothyronines reduced mtDNA oxidative damage. However, their mechanisms of action differed substantially. T3 stimulated autophagy, mitochondrial biogenesis, and mitophagy, promoting mitochondrial turnover and enhancing respiratory capacity to sustain the hypermetabolic state induced by T3 itself, thereby highlighting limitations to its therapeutic use. The antioxidant, anti-inflammatory, and lipid-lowering effects mediated by T2 were much more pronounced than with the other treatments. In addition, T2 modulated MQC by promoting mitochondrial fusion and mitophagy, and induced mitochondrial respiratory capacity by direct modulation of the electron transport chain.

Histological analysis revealed that Tb reduced hepatic steatosis severity by enhancing autophagy- mediated, clearance of lipid droplets without affecting mitochondrial processes, including mitochondrial quality control. Notably, beyond its established role as autophagy inducer, Tb was shown for the first time, to reduce mtDNA oxidative damage by stimulating the base excision repair system, similarly to iodothyronines.

The combined administration of Tb and T2 produced an overall beneficial effect on MASLD by combining autophagy-mediated cell clearance with T2-driven metabolic optimisation of mitochondrial function. However, the effects of the combined treatments were not always synergistic, suggesting that simultaneous modulation of autophagy and mitochondrial metabolism may involve complex regulatory interactions.

Overall, the reported data identify mitochondrial dysfunction and impaired quality control as a central pathogenic node in MASLD and highlight the therapeutic potential of strategies targeting mitochondrial metabolism and autophagic pathways. Among the pharmacological approaches investigated, T2 emerged as the most effective and well-tolerated intervention, while its combination with an autophagy inducer such as Tb opens new perspectives for multi-target therapeutic strategies in MASLD.

Chapter I: Pathophysiology of MASLD

Metabolic dysfunction-associated steatotic liver disease (MASLD), previously referred to as non-alcoholic fatty liver disease (NAFLD), is a hepatic condition characterized by an abnormal accumulation of triglycerides within hepatocytes in the context of metabolic dysfunction (Scorletti et al., 2022; Lazarus et al., 2022).

The spectrum of disease encompasses simple steatosis through to steatohepatitis, fibrosis, cirrhosis and, in some cases, progression to hepatocellular carcinoma (Lazarus et al., 2022).

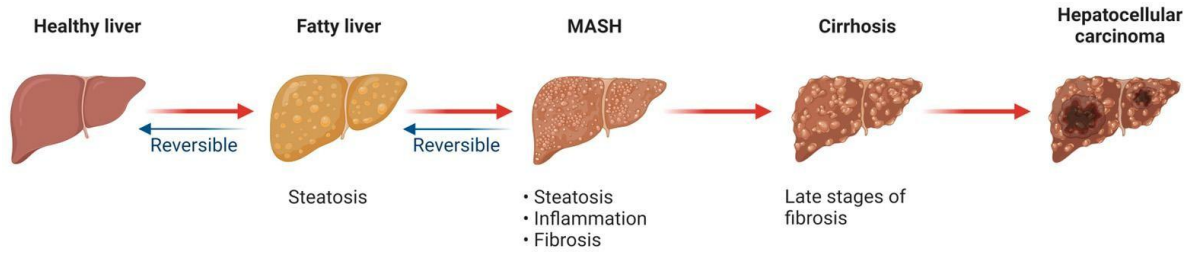

Figure 1. Progression of metabolic dysfunction-associated steatotic liver disease (MASLD). (Radosavljevic et al., 2024).

The change in terminology was driven by the need to address several limitations of the original one and to better characterize the disease and its associated risk factors.

NAFLD was originally introduced as a diagnosis of exclusion to distinguish lipid-driven liver disease from alcohol-induced injury; however, defining a condition by what it is not has several limitations. To overcome these limitations, experts employed the Delphi method to establish a new nomenclature and definition that is both inclusive and representative. This process was sled by three major organizations: the American Association for the Study of Liver Diseases (AASLD), the European Association for the Study of the Liver (EASL), and the Asociacion Latinoamericana para el Estudio del Higado (ALEH). In collaboration with regulatory agencies, patient advocacy groups, and multidisciplinary medical experts, these organizations reached a consensus: the term “steatotic liver disease” (SLD) was adopted as an umbrella category encompassing all liver disorders characterized by steatosis (Tilg et al., 2010; Baselli et al., 2022). Within this classification, MASLD refers to steatotic liver disease occurring in the presence of at least one cardiometabolic risk factor. This modification redirects clinical and scientific attention toward metabolic drivers rather than the exclusion of alcohol alone as a defining criterion. In addition to MASLD and alcohol-associated liver disease (ALD), the

updated framework recognises an intermediate condition termed metabolic dysfunction and alcohol-related liver disease (MetALD), which identifies individuals exhibiting metabolic risk factors alongside moderate alcohol consumption (Rinella et al. 2023). By shifting the diagnostic focus toward metabolic dysfunction, MASLD better aligns with mechanistic research exploring insulin resistance, lipid handling, mitochondrial dysfunction, and endocrine regulators of hepatic metabolism. This is particularly relevant for studies investigating thyroid hormone (TH) signalling in the liver, as in this case, since TH play a key role in lipid oxidation, mitochondrial function and metabolic homeostasis—processes central to steatosis development.

MASLD is a complex and heterogeneous metabolic disorder driven by the interplay of multiple, tightly interconnected pathophysiological processes. These include alterations in hepatic lipid metabolism (Syed-Abdul 2023), insulin resistance (Maldonado-Rojas et al., 2024), mitochondrial dysfunction (Radosavljevic et al., 2024), chronic oxidative stress and low-grade inflammation (Zhou et al., 2025). Rather than acting independently, these mechanisms interact synergistically, creating a self-perpetuating network that promotes hepatic lipid accumulation, hepatocellular injury, and progressive metabolic dysfunction.

1.1 Metabolic dysregulation and hepatic lipid metabolism in MASLD

Risk factors for MASLD include obesity, insulin resistance, hypertension, and hypertriglyceridemia, and the progressive increase in its global prevalence closely parallels the rise in metabolic disorders (Li et al., 2024). Disorders of lipid metabolism are the primary cause of fatty liver, as MASLD is predominantly characterized by excessive triglyceride accumulation in hepatocytes (Fuchs et al., 2022).

When the storage capacity of subcutaneous adipose tissue is exceeded, lipid accumulation shifts towards visceral depots, which become a major source of free fatty acid (FFA) efflux to the liver. This is further aggravated by adipocyte hypertrophy and insulin resistance, which enhance lipolysis and increase the delivery of circulating FFAs to hepatocytes independently of diabetes status. Dietary intake additionally contributes to hepatic lipid burden by providing exogenous FFAs and carbohydrates that fuel de novo lipogenesis (DNL) (Sheikh et al., 2025). The role of diet in increasing the influx of dietary FFAs and carbohydrates is also outstanding. Under such systemic changes, the liver becomes the major target organ dysfunction due to altered insulin signalling, increased lipogenesis, and mitochondrial or microsomal dysfunction (Zhang et al., 2021; Chauvier et al., 2007). In MASLD, hepatocellular lipid accumulation, mainly as

triglycerides, results from an imbalance between lipid input and output. FFAs are the main substrate for triglyceride synthesis by esterification (Linton et al., 2005).

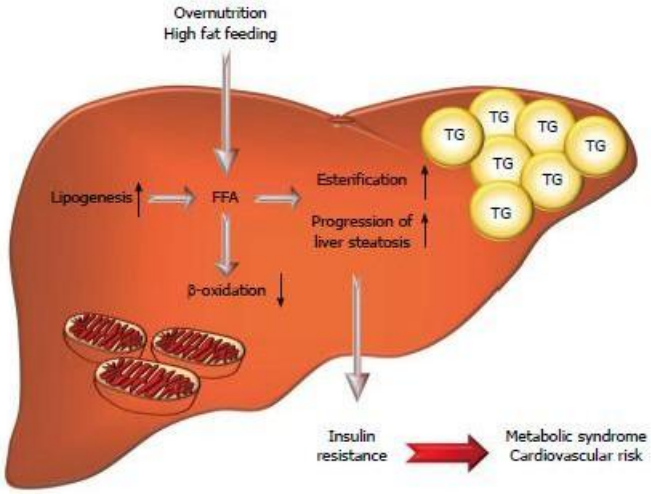

Figure 2. Hepatic lipid partitioning and liver and systemic metabolic damages in nonalcoholic fatty liver disease. Hepatic lipid partitioning and liver and systemic metabolic damages in nonalcoholic fatty liver disease.
Chronic overnutrition/hyperlipidemic feeding causes fat retention in hepatocytes that, in turn, results in alteration of fat uptake, de novo synthesis (lipogenesis) and oxidation with a significant imbalance of lipid homeostasis. This can subsequently induce insulin-resistance, metabolic syndrome and cardiovascular diseases. (Coppola et al., 2014).

Under physiological conditions, several mechanisms maintain lipid homeostasis. Conversely, when FFA influx surpasses the hepatocyte capacity for oxidation and export, as in MASLD, triglyceride storage increases and metabolic stress develops. Initially, the esterification of FFAs into triglycerides serves as a protective mechanism to prevent the accumulation of toxic lipid intermediates. However, sustained excess FFA delivery results in the accumulation of bioactive lipid species, such as diacylglycerols, which impair insulin signalling and disrupt metabolic homeostasis (Park et al., 2020). Hepatic fatty acid uptake is mediated by specific membrane-associated transporters, including fatty acid transport proteins (FATPs), particularly FATP2 and FATP5 (Pohl et al., 2004), as well as the fatty acid translocase CD36. Increased hepatic expression and membrane localization of CD36 have been reported in MASLD and metabolic dysfunction–associated steatohepatitis (MASH), contributing to excessive fatty acid influx and intracellular lipid accumulation (Zhang et al., 2025). Experimental inhibition of CD36 activity or palmitoylation has been shown to attenuate hepatic steatosis, highlighting its role as a key regulator of lipid uptake (Zhao et al., 2018). Similarly, dysregulation of lipogenic pathways plays a central role in triglyceride deposition. De novo lipogenesis is driven by the upregulation

of key enzymes, including acetyl-CoA carboxylase (ACC) and fatty acid synthase (FAS), whose expression and activity are increased in MASLD. These enzymes are transcriptionally regulated by sterol regulatory element-binding protein-1c (SREBP-1c) and carbohydrate-responsive element-binding protein (ChREBP), which are activated in response to hyperinsulinemia and nutrient excess (Simões et al., 2021).

As lipid overload persists, mitochondrial overload and dysfunction develop, with impaired β-oxidation leading to excessive production of reactive oxygen species (ROS) (Koliaki et al., 2015). Key regulators of mitochondrial fatty acid oxidation, such as carnitine palmitoyltransferase 1 (CPT1), may become functionally impaired in advanced stages of disease, further exacerbating lipid accumulation and oxidative stress (Begriche et al., 2013; Koliaki et al., 2015). ROS accumulation triggers oxidative stress, endoplasmic reticulum dysfunction, and activation of pro-inflammatory and stress-related signalling pathways (Greatorex et al., 2023). In this context, lipotoxicity develops as hepatocytes are exposed not only to FFAs but also to toxic lipid metabolites that promote cell injury, inflammation and death. Lipotoxicity has therefore been proposed as a key mechanism driving the transition from simple steatosis to steatohepatitis (MASH), as it induces hepatocellular damage via endoplasmic reticulum stress, activation of inflammatory cascades and cell death pathways (Shi et al., 2023; Dewidar et al., 2023).

1.2 Insulin Resistance and Type 2 Diabetes Mellitus: a link between hepatic and systemic disease

Insulin resistance represents a central pathogenic mechanism in the development and progression of MASLD and constitutes a critical link between hepatic steatosis and systemic metabolic dysfunction (Miller et al., 2025). Under physiological conditions, insulin suppresses hepatic gluconeogenesis, promotes glycogen storage, and tightly regulates lipid metabolism by limiting de novo lipogenesis and ensuring balanced lipid turnover (Uehara et al., 2023). The insulin signalling in hepatocytes is initiated by the activation of the insulin receptor and downstream phosphorylation of insulin receptor substrates (IRS1 and IRS2) (White 1979), leading to the activation of the phosphatidylinositol 3-kinase (PI3K/AKT) pathway (Folli et al. 1992). This signalling cascade suppresses hepatic gluconeogenesis through inhibition of FOXO1 activity and regulates lipid metabolism by modulating glycogen synthesis and lipogenesis (Haeusler et al., 2014). In insulin-resistant states, this regulatory control is disrupted. Excess intracellular lipid accumulation and lipotoxic intermediates, such as

diacylglycerols and ceramides, activate novel and conventional protein kinase C (PCK) isoforms, particularly PKCε (Samuel et al., 2004). PKCε is the predominant PKC isoform activated in liver following fat feeding, which inhibits IRS1/2 function through serine phosphorylation, thereby attenuating downstream PI3K/AKT signalling (Samuel et al., 2007). Consequently, insulin-mediated suppression of gluconeogenesis is blunted, while lipogenic pathways remain inappropriately active. This condition promotes increased glucose output together with enhanced de novo lipogenesis, contributing to triglyceride accumulation within hepatocytes and worsening steatosis (Petersen et al., 2018). Accordingly, the use of a specific PKCε antisense oligonucleotide that knocking down PKCε expression in the liver protected rats from lipid-induced hepatic insulin resistance despite increases in hepatic lipid content (Samuel et al., 2007). Several studies confirmed the key interaction between DAG, activation of PKCε, and hepatic insulin resistance in numerous rodent models of NAFLD-associated hepatic insulin resistance (Birkenfeld et al., 2011a; Choi et al., 2007b; Erion et al., 2009; Jornayvaz et al., 2011).

At the post-receptor level, impaired AKT activation results in reduced phosphorylation of key downstream targets, including glycogen synthase kinase 3β (GSK3β), leading to altered glycogen metabolism and persistent activation of FOXO1, which drives the transcription of gluconeogenesis genes. In parallel, chronic nutrient excess and hyperinsulinemia activate mTOR signalling, further exacerbating metabolic dysregulation and contributing to impaired autophagic responses (Gross et al., 2008; Titchenelle et al., 20015; Laplante et al., 2012).

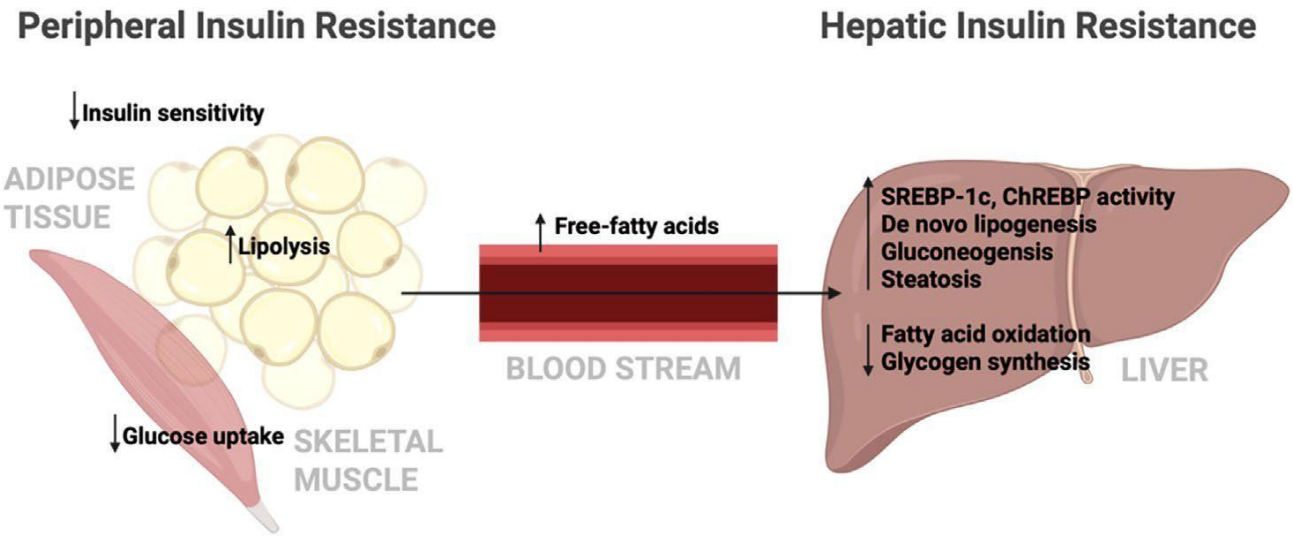

Figure 3. Interplay between peripheral and hepatic insulin resistance in MASLD pathogenesis. Peripheral insulin resistance increases circulation free fatty acids and hyperinsulinemia, which in turn drive hepatic insulin resistance, gluconeogenesis and lipogenesis. These processes promote steatosis, mitochondrial dysfunction and progression from MASLD to MASH (Miller et al., 2025).

Peripheral insulin resistance, particularly in adipose tissue and skeletal muscle, results in compensatory hyperinsulinemia and profoundly alters lipid metabolism. In insulin-resistant adipocytes, the antilipolytic action of insulin is blunted, leading to increased basal and stimulated lipolysis and excessive release of free fatty acids (FFAs) into the circulation. This enhanced FFA flux toward the liver significantly contributes to hepatic lipid overload, independently of overt hyperglycemia or diabetes status, and impairs hepatic lipid oxidation (Wilcox 2005). The resulting hormonal and metabolic imbalance stimulates the activation of key hepatic lipogenic transcription factors promoting de novo lipogenesis (Barbhuiya et al., 2025; Zhang et al., 2024). When coupled with impaired lipid oxidation and increased influx of FFAs, this metabolic environment strongly favours the development of hepatic steatosis and consequent lipotoxicity. Thus, insulin resistance acts as a driving force that connects systemic metabolic disturbances with hepatic lipid accumulation and inflammation.

Type 2 diabetes mellitus represents the clinical culmination of systemic insulin resistance and is characterized by chronic hyperglycemia resulting from impaired insulin action combined with progressive β-cell dysfunction (DeFronzo et al., 2015). In the context of MASLD, persistent hepatic insulin resistance contributes to fasting hyperglycemia by sustaining inappropriate gluconeogenesis, while compensatory hyperinsulinemia further drives hepatic de novo lipogenesis (Petersen & Shulman 2018). Hepatic steatosis, in turn, exacerbates glucose dysregulation by impairing hepatic insulin clearance and amplifying inflammatory and lipotoxic signalling pathways (Birkenfeld & Shulman 2014). Clinical and epidemiological studies consistently demonstrate that MASLD is highly prevalent among individuals with T2DM and that the presence of diabetes markedly increases the risk of progression to steatohepatitis, advanced fibrosis, and hepatocellular carcinoma (Younossi et al., 2016; Mantovani et al., 2020). Accordingly, MASLD and type 2 diabetes mellitus (T2DM) are linked by a bidirectional relationship, in which hepatic lipid accumulation worsens systemic insulin resistance, while chronic hyperglycemia and hyperinsulinemia further accelerate hepatic metabolic dysfunction. Together, these mechanisms identify the liver as a central regulator of whole-body glucose homeostasis and underscore insulin resistance as both a driver and a consequence of MASLD (Miller et al., 2025).

1.3 From hepatic fat accumulation to mitochondrial oxidative stress

When the oxidative and secretory capacity of hepatocytes is exceeded, excessive FFA oxidation within mitochondria leads to the overproduction of reactive oxygen species (ROS), which in turn induce oxidative stress, organelle dysfunction and activation of apoptotic pathways (Simões et al 2021). Thus, mitochondrial dysfunction emerges as a central mechanism in the pathogenesis and progression of MASLD (Pierantonelli et al., 2019).

Mitochondria are essential organelles responsible for a wide range of cellular functions, such as energy production through oxidative phosphorylation (OXPHOS). This process takes place within the inner mitochondrial membrane and consists of a sequence of enzymatic reactions that generate adenosine triphosphate (ATP), the primary energy-supplying molecule for cells (Casanova et al., 2023). During OXPHOS, electrons derived from nutrient oxidation are transferred through a series of protein complexes (complexes I to V) in the mitochondrial electron transport chain (ETC). As the electrons move along the ETC, the energy released is used to pump protons (H+) from the mitochondrial matrix into the intermembrane space, creating an electrochemical proton gradient. ATP synthase (Complex V) utilizes this proton motive force to convert adenosine diphosphate (ADP) into ATP (Whang et al., 2024). Through this mechanism, mitochondria supply the energy required for numerous cellular processes, including muscle contraction, biosynthesis, and active transport (Tang et al., 2020). When mitochondrial activity is disrupted, particularly when OXPHOS efficiency declines and electron leakage from the ETC increases, mitochondria become a major source of reactive oxygen species (ROS) (Chen et al., 2023).

Mitochondrial oxidative stress arises from an imbalance between the production of ROS and the capacity of cellular antioxidant defences to neutralise them. The progression of oxidative stress involves a cascade of interconnected mechanisms: the electron leakage from the ETC leads to the formation of superoxide radicals, which are converted into other ROS such as hydrogen peroxide (H_2O_2). Under physiological conditions, mitochondrial antioxidant defenses, including superoxide dismutase (SOD), catalase, and glutathione peroxidase (GPX), work along with non-enzymatic antioxidants like glutathione (GSH) to neutralize ROS and maintain redox balance (Kowalczyk et al., 2021; Jomova et al., 2023). However, when the levels of ROS surpass the capabilities of these defence mechanisms, mitochondrial proteins, lipids and DNA are subjected to oxidative damage. This damage compromises mitochondrial function and integrity, further escalating ROS production in a vicious cycle of oxidative stress. The

repercussions of oxidative stress can have widespread effects on cellular function and contribute to the pathogenesis of various diseases (Kowalczyk et al., 2021; Veskovic et al., 2019).

1.4 Mitochondrial dysfunction drives MASLD progression

Mitochondrial dysfunction is a central mechanism in the pathogenesis and progression of MASLD. Mitochondria comprise for up to 18% of a hepatocyte total volume and play a crucial role in hepatic metabolism by providing energy through β-oxidation and oxidative phosphorylation (Pohl et al., 2004). Given the liver high metabolic demand, hepatocellular function is critically dependent on mitochondrial efficiency and integrity.

In MASLD, sustained lipid overload and oxidative stress disrupt mitochondrial function, leading to decreased β-oxidation, electron transport chain (ETC) dysfunction, reduced ATP synthesis, excessive ROS generation and mtDNA damage (Pohl et al., 2004; Simões et al., 2021). Under these conditions, mitochondria shift from being efficient energy-producing organelles to major sources of intracellular ROS, as electron leakage from ETC complexes increases markedly (Murphy 2009). The resulting overproduction of superoxide radicals and hydrogen further amplifies oxidative stress and compromises mitochondrial bioenergetic capacity (Radosavljevic et al., 2024).

Excessive ROS production promotes lipid peroxidation of mitochondrial membranes, alters membrane fluidity, and impairs the activity of key mitochondrial enzymes, thereby exacerbating ETC dysfunction and reinforcing a vicious cycle of oxidative damage (Kowalczyk et al., 2021; Begriche et al., 2013). In parallel, mitochondrial DNA (mtDNA)—due to its close proximity to the ETC and lack of protective istones—is particularly vulnerable to oxidative lesions, which impair the transcription of mitochondrially encoded ETC subunits and further aggravate defects in oxidative phosphorylation (Yakes & Van Houten 1997; Simões et al., 2021).

A central trigger of this pathological cycle is the accumulation of long-chain FFAs within hepatocytes. Elevated FFA availability increases mitochondrial substrate load and drives excessive flux through β-oxidation, overwhelming mitochondrial oxidative capacity and favouring incomplete fatty acid oxidation (Koliaki et al., 2015; Begriche et al., 2013). This metabolic overload not only enhances ROS production but also disrupts mitochondrial coupling efficiency, further reducing ATP generation and promoting hepatocellular energy stress (Pessayre et al., 2012). Collectively, these alterations position mitochondrial dysfunction as a critical mediator linking lipid overload, oxidative stress, and metabolic impairment in MASLD,

thereby creating a permissive environment for inflammation, cell injury, and disease progression.

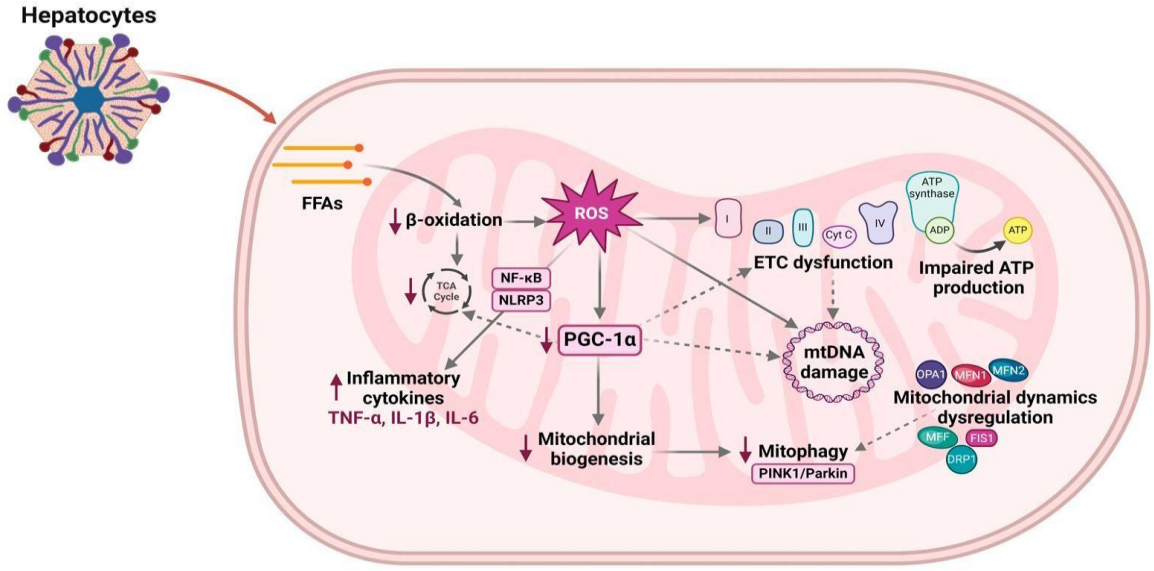

Figure 4. Mechanisms of mitochondrial dysfunction in MASLD. Abbreviations: FFAs, free fatty acids; ROS, reactive oxygen species; ETC, electron transport chain; Cyt C, cytochrome c; mtDNA, mitochondrial DNA; PGC-1α, peroxisome proliferator-activated receptor-γ coactivator 1α; NF-κB, nuclear factor-kappa B; NLRP3, nucleotide-binding oligomerization domain-like receptor 3; TNF-α, tumor necrosis factor-alpha; IL-1β, interleukin-1 beta; IL-6, interleukin-6; PINK1, PTEN-induced kinase 1; FIS1, fission protein 1; MFF, mitochondrial fission factor; DRP1, dynamin-related protein 1; OPA1, optic atrophy 1; MFN1, mitofusin 1; MFN2, mitofusin 2. (Radosavljevic et al., 2024).

1.5 Inflammation in MASLD progression: the role of mitochondrial damage-associated molecular patterns (mtDAMPs)

Chronic hepatocellular injury and mitochondrial dysfunction represent key triggers for the activation of inflammatory responses in MASLD, playing a central role in disease progression from simple steatosis to steatohepatitis and fibrosis. Multiple cells have shown to communicate with each other, contributing to disease progression through the release and exchange of various forms of damage-associated molecular patterns (DAMPs) during or after cell death. Normally DAMPs originate from the plasma membrane, nucleus, endoplasmic reticulum, and cytoplasm (Di Micco et al., 2016; Grootjans et al., 2014; Meares et al., 2014). However, mitochondria, as the primary organelle responsible for regulating energy metabolism and cell death, also participate in the production of various DAMPs (Billingham et al., 2022; Wenceslau et al., 2014; Muñoz-Planillo et al., 2013). These mito-DAMPs are recognized as danger signals by

themselves, as well as by neighbouring or distant cells, serving as important mediators of cell communication in liver diseases (Beucher et al., 2024).

In detail, cellular stress, such as an excess of reactive oxygen species (ROS) as seen in MASLD, can destabilise the mitochondrial permeability transition pore (MPTP), causing the leakage of cytochrome c, adenosine triphosphate (ATP), cardiolipin (CL), carbamoyl phosphate synthetase 1 (CPS1), and mtDNA (Krysko et al., 2011) into the cytoplasm (Kent et al., 2021; Chen et al., 2025; Shao et al., 2024).

Among mtDAMPs, cytosolic mtDNA promotes innate immune responses within the liver, by activating pattern recognition receptors, including cyclic GMP-AMP synthase (cGAS)-stimulator of interferon genes (STING)-TANK-binding kinase (TBK1) which triggers subsequent pro-inflammatory signalling pathways (Chen et al., 2016). cGAS-STING functions as the predominant sensor of viral and bacterial DNA in the cytoplasm of infected cells. In recent years, several studies have demonstrated that the cGAS-STING signalling axis can also be activated by endogenous DNA (Roers et al., 2016, Chen et al., 2016; Barber et al., 2015), as well as mtDNA. In an HCC mouse model, mtDNA translocated into the cytoplasm and activated the cGAS-STING pathway, which subsequently mediated T cell anti-tumor function (Shi et al., 2024). Similarly, endogenous mtDNA or released exogenous forms also stimulated the activation of the NOD-like receptor protein 3 (NLRP3) inflammasome and inflammatory responses in macrophages (Swanson et al., 2019; West et al., 2017).

Furthermore, ROS can modulate inflammatory signalling pathways, including nuclear factor-kappa B (NF-κB) and nucleotide-binding oligomerization domain-like receptor 3 (NLRP3) inflammasome, leading to increased production of inflammatory cytokines such as interleukin-1 beta (IL-1β), interleukin-6 (IL-6), and tumor necrosis factor-alpha (TNF-α) (Liu et al., 2023). TNF-α further amplifies oxidative stress and inflammation by activating MAPK pathways, which stimulate additional ROS production. This establishes a vicious cycle of inflammation and oxidative damage. Moreover, pro-inflammatory cytokines activate Kupffer cells, intensifying immune responses and contributing to progressive hepatocellular damage in MASLD (Luo et al., 2021). In addition, emerging evidence indicates that ultrastructural abnormalities and disturbances in mitochondrial dynamics—particularly impaired fission and fusion—are associated with more severe stages of MASLD and MASH. The inability to efficiently remove damaged mitochondria through mitophagy leads to their accumulation within hepatocytes, further exacerbating oxidative stress and impairing energy metabolism (Gelen et al., 2023). This progressive failure of mitochondrial quality control ultimately compromises the liver capacity to maintain metabolic homeostasis, resulting in hepatocellular

death, inflammation, and fibrosis. Collectively, these mitochondrial alterations represent a critical nexus between metabolic overload, oxidative injury, and cellular dysfunction, underscoring the central role of mitochondrial impairment in the evolution of MASLD to its more advanced, fibrotic forms.

1.6 Impaired Mitochondrial Quality Control (MQC) in MASLD

Mitochondrial Quality Control (MQC) comprises a multifaceted set of processes that protect mitochondria from damage and prevent the accumulation of defective mitochondria. Those processes mainly involve three distinct, tightly regulated mechanisms: biogenesis, dynamics, and mitophagy (Atici et al., 2023; Ng et al., 2021). MQC is essential for maintaining mitochondrial integrity and function in metabolically active tissues such as the liver, where mitochondria are crucial for energy production, lipid oxidation, and cellular signalling. Mitochondrial dysfunction is a central pathological feature of MASLD, resulting from defects in several aspects of MQC and reduced efficiency of the electron transport chain (ETC) (Einer et al., 2018; Koliaki et al., 2015; Li et al., 2019; Tumova et al., 2016). Consequently, disruption of MQC mechanisms contributes directly to hepatocellular injury and disease progression in MASLD.

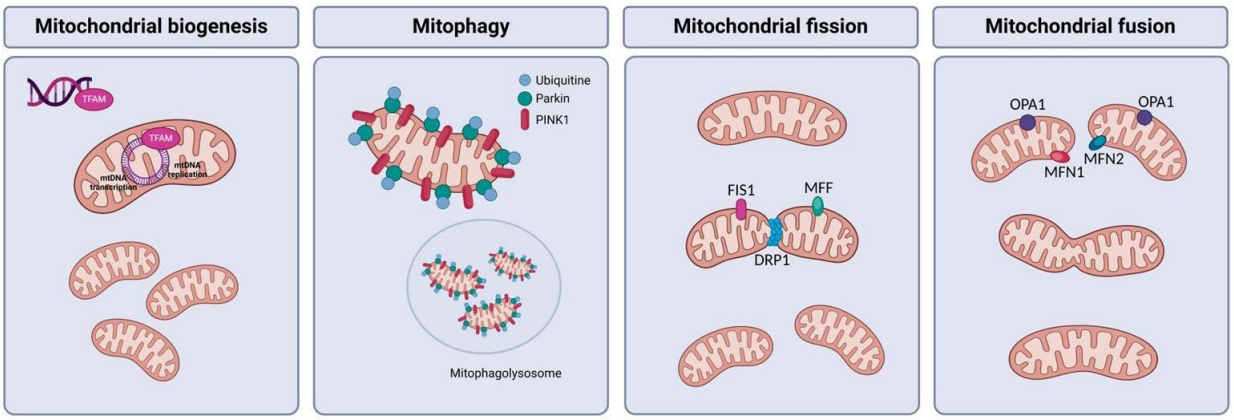

Figure 5. Mitochondrial quality control (MQC) mechanisms. TFAM, mitochondrial transcription factor A; mtDNA, mitochondrial DNA; PINK1, PTEN-induced kinase 1; FIS1, fission protein 1; MFF, mitochondrial fission factor; DRP1, dynamin-related protein 1; OPA1, optic atrophy 1; MFN1, mitofusin 1; MFN2, mitofusin 2. (Radosavljevic et al., 2024).

Mitochondrial biogenesis is a highly complex process through which cells generate new mitochondria to meet their energy demands and maintain cellular homeostasis (Liu et al., 2025).

It requires the coordinated synthesis and assembly of mitochondrial proteins, lipids and DNA (Popov 2020). A key regulator of this process is mitochondrial transcription factor A (TFAM), which binds to mtDNA, promoting its transcription and packaging into nucleoids, which are essential for maintaining mtDNA stability and proper mitochondrial function. TFAM expression is regulated by peroxisome proliferator-activated receptor-γ coactivator 1α (PGC-1α), thereby linking nuclear regulation of mitochondrial biogenesis to the maintenance and expression of mtDNA (Clapier et al., 2008). Additional transcription factors exert a significant influence by activating promoters of mitochondrial genes, such as nuclear respiratory factor 1 (NRF-1), nuclear respiratory factor 2 (NRF-2), and members of the estrogen-related receptor (ERR) (Tang et al., 2020; Ding et al., 2021). PGC-1α also induces SIRT3 and PPARα, optimising oxidative phosphorylation. The long-chain acyl- CoA synthetase family member ACSL4 is highly expressed in liver tissue of patients with MASLD and is positively correlated with hepatocyte steatosis and fibrosis. ACSL4 inhibits PGC-1α, thereby reducing β-oxidation and ATP synthesis, as well as mt-biogenesis (Fu et al., 2025).

Mitochondria are highly dynamic organelles, changing their shape through processes of fusion and fission. The balance between fusion and fission is regulated by various proteins encoded by nuclear genes (Green et al., 2022).

Mitochondrial fusion is a process through which individual mitochondria create an interconnected network, merging their membranes and contents, forming larger and more functional ones. This process is mediated by specific proteins. Key proteins involved in mitochondrial fusion are mitofusin 1 (MFN1), mitofusin 2 (MFN2) and optic atrophy 1 (OPA1) (Chen et al., 2023). MFN1 and MFN2 are localized on the outer mitochondrial membrane and mediate the tethering and fusion of adjacent mitochondria, whereas OPA1 is localized on the inner membrane and regulates the fusion of inner membranes (Gao et al., 2021). MASLD downregulates MNF2, impairing ER-mitochondrial phosphatidylserine transfer and exacerbating ER stress. Reduced MNF1/2 and OPA 1 correlate with MASH severity (Elbadawy et al., 2023).

Mitochondrial fission is a process during which a single mitochondrion divides into two or more smaller mitochondria. It is regulated by the activity of dynamin-related protein 1 (DRP1), a GTPase that assembles into spirals around the mitochondrion at constriction sites. The recruitment of DRP1 is facilitated by mitochondrial fission factor (MFF) and fission protein (FIS1). DRP1 drives the constriction of the outer mitochondrial membrane, leading to mitochondrial division (Fenton et al., 2022). DRP1 upregulation correlates with MASLD: Mdivi-1 and (Drp1 inhibitor) and metformin normalise fission by modulating AMPK signalling

(Elbadawy et al., 2023). Rhein, an anthraquinone compound isolated from rhubarb, inhibits Drp1, enhancing PINK1/Parkin mitophagy and reducing apoptosis (Li et al., 2020).

Through mitochondrial fission, cells can selectively eliminate damaged mitochondria through mitophagy. This is a specialized form of autophagy that selectively targets damaged or dysfunctional mitochondria, maintaining quality control and cellular homeostasis. Mitophagy is typically initiated in response to cellular stress, such as oxidative stress, nutrient deprivation, or mitochondrial dysfunction (Roca-Agujetas et al., 2019). Key regulators of mitophagy include PTEN-induced kinase 1 (PINK1) and Parkin, which identify damaged mitochondria and tagging them for degradation. In MASLD, there is an interactive relationship between mitophagy and lipotoxicity; the reduced PINK1/Parkin expression compromises mitochondrial autophagy, accelerating cytochrome c release and MPTP opening. In both in vitro and in vivo models, the anthocyanin cation anthocyanin-3-O-glucoside has been shown to bolster the condition of MASLD by enhancing PINK/Parkin-mediated mitophagy (Dias et al., 2025).

Collectively, impaired MQC represents a convergence point at which lipid overload, oxidative stress, and mitochondrial dysfunction intersect, sustaining hepatocellular injury and facilitating the progression from simple steatosis to more advanced stages of MASLD, including MASH and fibrosis. Through MQC, cells maintain mitochondrial integrity, prevent the accumulation of dysfunctional organelles, and limit the release of harmful mitochondrial components that could activate cell death pathways or exacerbate disease progression. However, when the MQC system becomes overwhelmed or dysregulated, the capacity for mitochondrial repair and renewal is lost. Persistent oxidative stress disrupts mitochondrial dynamics, leading to excessive pathological fission—driven by hyperactivation of DRP1—and reduced fusion, due to the loss of MFN2 and OPA1. Mitophagy is also severely compromised: the PINK1/Parkin pathway becomes dysfunctional, leading to accumulation of dysfunctional mitochondria and further amplification of oxidative stress and inflammatory signalling (Youle & van der Bliek 2012).

Chapter II: Thyroid Hormones and 3,5-Diiodo-L-Thyronine (T2)

Thyroid hormones are synthesized in the colloid internal part of the thyroid follicles. Iodine is reduced to iodide ion in the intestine, where it enters the bloodstream and is absorbed into the epithelial thyroid cells through a Na+/I- symporter-mediated mechanism (NIS) (Dai et al., 1996). Iodide is oxidised and incorporated into the glycoprotein thyroglobulin by thyroid peroxidase (TPO), forming mono- and di-iodinated tyrosine residues. Coupling of two diiodotyrosines produces thyroxine (T4 or 3,5,3',5'-tetraiodothyronine), whereas the coupling of one monoiodotyrosine and one diiodotyrosine yields triiodothyronine (T3 or 3,5,3'-triiodo-L-thyronine) (Yen et al., 2001).

TH release into the circulation is regulated by the hypothalamic-pituitary–thyroid axis and is tightly controlled through negative feedback. T4 and T3 in the bloodstream are bound to transport proteins, with only a small, ''unbound'' or ''free'' fraction being biologically active. The functions of these proteins most probably include: (a) ensuring a constant supply of TH to the cells and tissues by preventing urinary loss, (b) protecting the organism against abrupt changes in thyroid-hormone production and/or degradation, and (c) ultimately protecting against iodine deficiency. (Yen et al., 2001).

All the circulating T4 is secreted by the thyroid gland, whereas most (about 80%) of the systemic T3 is generated by deiodination of T4, making local activation a crucial regulatory step for tissue-specific TH action.

Thyroid-hormone deiodination is mediated by three iodothyronine deiodinases: type I deiodinase (D1), preferentially expressed in the liver but also present in kidney, thyroid, and pituitary, contributes substantially to circulating T3 levels and supports hepatic metabolic activity; type II deiodinase (D2), present in the central nervous system, anterior pituitary, brown adipose tissue, and placenta, converts T4 to T3 locally to ensure adequate intracellular hormone availability; type III deiodinase (D3), present in the central nervous system, placenta, skin, and fetal tissue, is able to deiodinate exclusively at the inner ring of T4 and T3, leading to the formation of 3,3',5'-T3 or reverse T3 (rT3) (Darras et al., 2012). Overall, deiodinase enzymes finely regulate thyroid hormone activation and inactivation: D1 and D2 mediate the conversion of T4 to the biologically active T3, whereas D3 and, in part, D1 are responsible for the generation of metabolites such as rT3 and 3,3'-T2 (Fig. 6).

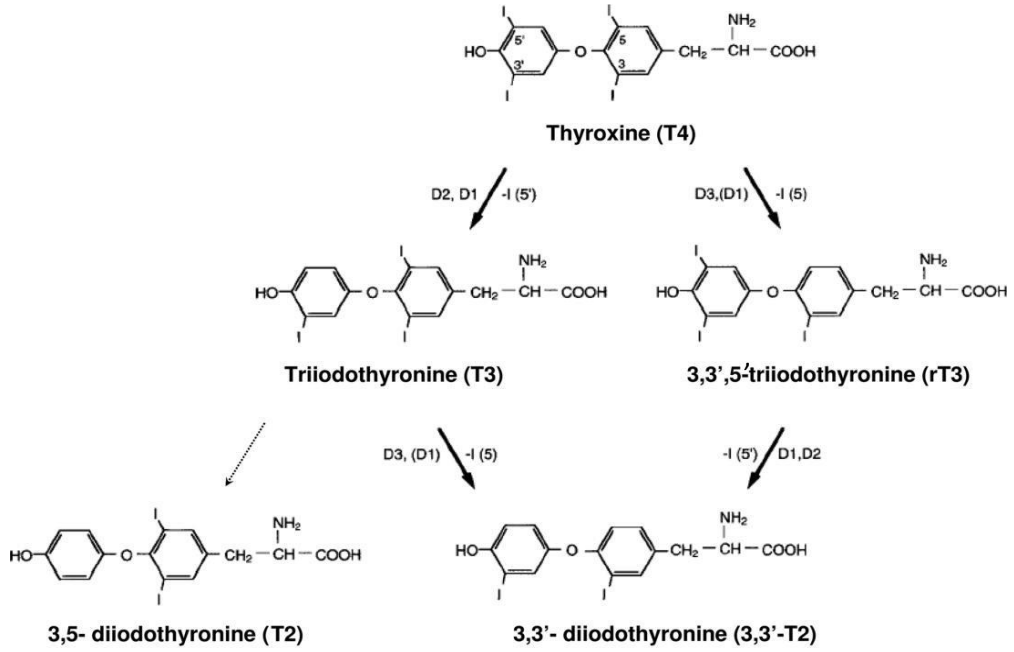

Figure 6. The sequential monodeiodination cascade: production of triiodothyronine (T3); rT3; 3,3'-T2; 3,5-T2; and 3',5'-T2 by stepwise deiodination of thyroxine (T4). The broken arrow indicates unknown pathway(s) (Moreno et al., 2008).

Approximately 80-85% of T3, classically considered the active hormone, is generated by D1, primarily in the liver and kidneys. The peripheral generation of rT3 is estimated to account for 95% of all the rT3 produced by the body (Moreno et al., 2008; Chopra et al., 1976). D1 and D3 are also involved in the further degradation of iodothyronines to distinct diiodothyronines: 3,5-diiodothyronine (3,5-T2); 3,3'-T2 and 3',5'- diiodothyronine (3',5'-T2). These, in turn, can be transformed into monoiodothyronine (T1) and subsequently into thyronine (T0).

Uptake of TH into peripheral tissues is mediated by specific membrane transporter proteins, among which the monocarboxylate transporter (MCTs) family deserves special attention. Fourteen members of this family have been recognized so far, but only 6 of them transport TH. MCT8 is currently known to be highly specific only for TH (Friesema et al., 2003), whereas MCT10 also has the ability to carry different types of amino acid.

These transporters regulate the intracellular bioavailability of TH and thereby influence tissue-specific metabolic responses. Defects in TH transport, activation or receptor signalling can therefore impair hepatic TH action, setting the stage for metabolic alterations that favour lipid accumulation and liver dysfunction (Marino et al., 2025).

2.1 Thyroid hormones actions: genomic and nongenomic actions

TH act via two distinct pathways: (Dai et al., 1996) genomic or long-term effects and (Yen et al., 2001) and short-term effects. The genomic actions of TH start in the nucleus by binding to thyroid receptor (TRs), while non-genomic ones are initiated in several cell compartment likewise plasma membrane, cytoplasm and mitochondria.

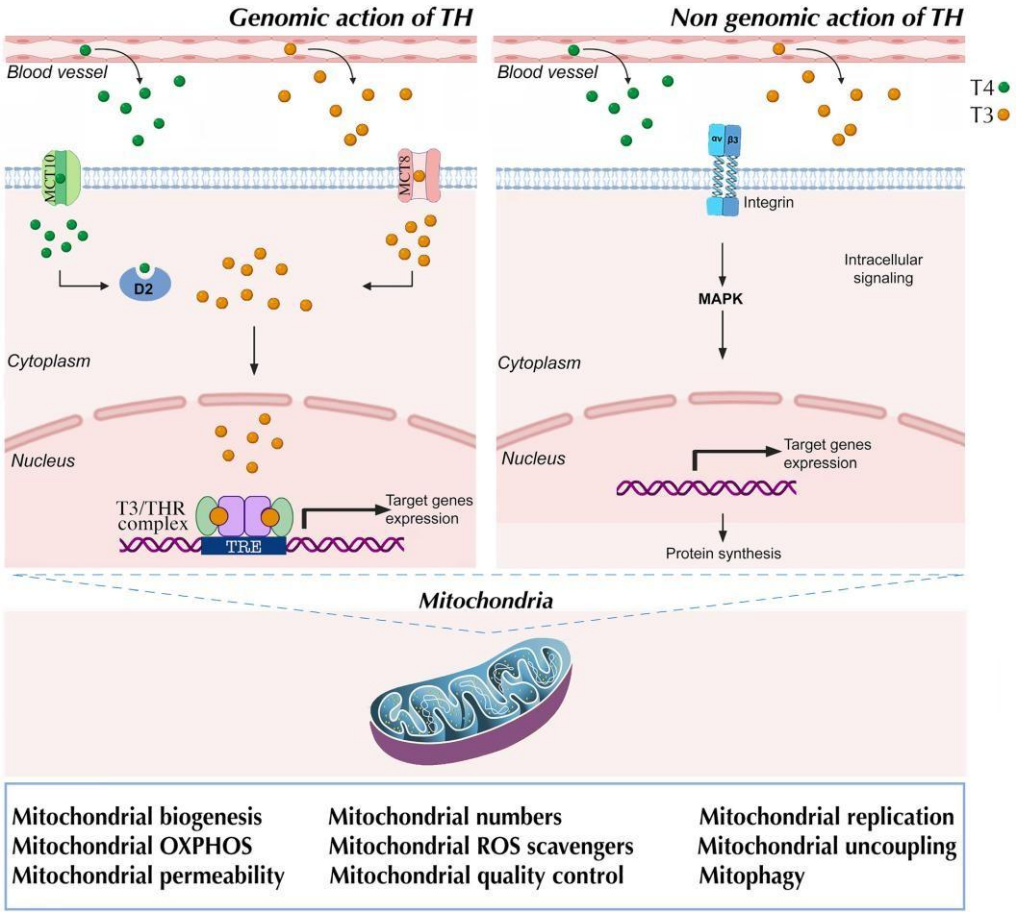

Figure 7. Thyroid Hormones have a deep influence on mitochondria functioning via genomic and non-genomic mechanisms (Sagliocchi et al., 2024).

2.1.1 Genomic actions of thyroid hormones

Thyroid hormones play critical roles in metabolism, tissue differentiation, and growth, and are required for the normal function of nearly all tissues. Early studies by Tata and colleagues (Tata et al., 1962; Tata et al., 1963) showed that THs mainly target the cell nucleus, leading to the

identification for specific nuclear receptors of THs (TRs), afterwards found in various tissues and cells (Lazar, 2003; Oppenheimer et al., 1972; Oppenheimer et al., 1987).

Nuclear hormone receptors are part of a large family of transcription factors and are master regulators of transcriptional programmes that integrate the homeostatic control of almost all biological processes, including development, reproduction, cell growth, metabolism, immunity and inflammation (Yen 2001). They regulate gene expression in response to small lipophilic compounds such as THs, steroids, oxysterols, and fatty acids. These molecules directly bind to the nuclear receptor (NR) ligand-binding domain and trigger conformational changes. The recruitment of distinct sets of coregulators (i.e. coactivators and corepressors) than determines whether a given NR will activate or repress the transcription of target genes (McKenna et al., 2009).

TRs are associated with chromatin and bind THs with high affinity and specificity. They can be prebound to thyroid hormone response elements (TREs) located in the promoter regions of target genes. The formation of TH-TR-TRE complex is the critical initial step in the positive or negative regulation of target gene transcription and, subsequently, protein synthesis.

TRs are encoded by the THRA and THRB genes, giving rise to multiple receptor isoforms, including TRα1, TRα2, TRβ1 and TRβ2. Among these, TRα1 and TRβ1 are the main T3-binding isoforms, whereas TRα2 lacks T3-binding capacity.

TRα1 is predominantly expressed in cardiac and skeletal muscle, brown adipose tissue (BAT) and the brain (Hodin et al., 1990), whereas TRα2 shows a broader distribution, with higher levels in the brain, testis, kidney, and BAT (Buzzard et al., 2000). TRβ1 is mainly expressed in the liver, kidney and brain, while TRβ2 is restricted to the anterior pituitary, specific hypothalamic nuclei and the cochlea, reflecting specialized roles in neuroendocrine regulation (Lazar et al., 1990; Cook et al., 1992; Lechan et al., 1993; Bradley et al., 1994).

TRs are composed of a single polypeptide chain with different functional domains (Evans 1988). The aminoterminal domains vary among TR isoforms. They act as transcription regulators and contain a ligand-independent activating domain, known as AF2, which is exposed when the ligand binds the receptor. In the middle of the chain is a highly conserved region known as the DNA-binding domain (DBD). This region contains almost 70 amino acids forming a “zinc-finger” domain, which interacts directly with a specific DNA segment, known as TREs, localized in the promoter of the target gene.

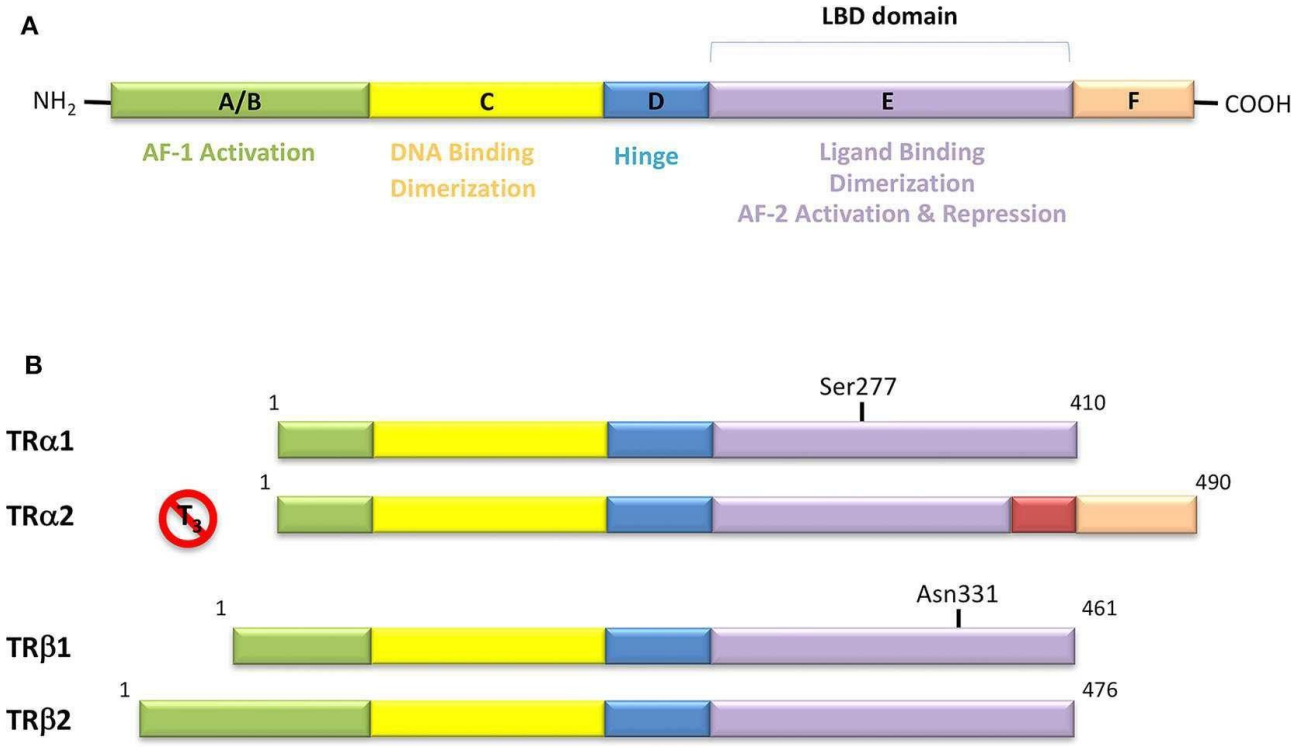

Figure 8. Thyroid Hormone receptor structure and functional region (Soprano et al., 2020). (A) Domain organization of Thyroid Hormone Receptors (TRs) and functional regions. The TR is a member of the nuclear receptor (NR) protein family. The NRs share a common modular structure, which contains a variable A/B N-terminal region, a central conserved DNA-binding domain (DBD), a less conserved ligand-binding domain (LBD), and a linker region between the DBD and LBD. The N-terminal region harbors the activation function-1 (AF-1), which is independent of the LBD-ligand interaction. Within the LBD lies the activation function-2 (AF-2), with it referring to the recruitment of transcriptional activators in a ligand-dependent manner. (B) Schematic representation of the different isoforms of thyroid hormone receptor. These are two distinct TR genes (alpha and beta) that expressed as two differentially spliced isoforms (α1 and α2, β1 and β2, respectively). TRα1 and TRβ1 are the predominant ligand binding forms in most tissues. Each receptor isoform conforms to the three-domain structure (NTD, BDB, and LBD) that is typical of NRs. The length of receptors is indicated just above the receptor diagrams. TRα2 cannot bind T3 because it contains a 122-amino acid carboxy terminus that replaces a region in TRα1 that is critical for TH binding (Saponaro et al., 2020).

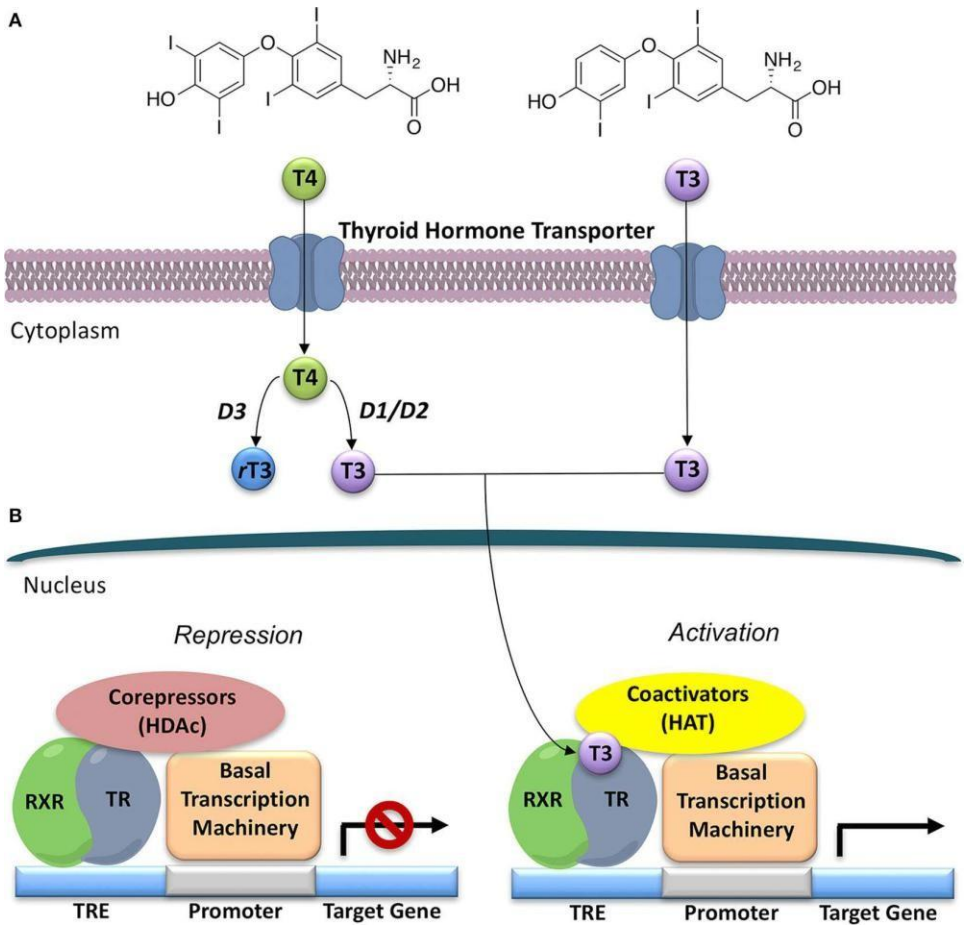

Figure 9. General model for thyroid hormone (T3) generation and action in the nucleus. (A) Thyroxine (T4), the prevalent form of thyroid hormone (TH) produced by the thyroid gland, once released is converted to T3, the major form of TH, by deiodinases 1 and 2 (D1 and D2). Deiodinase 3 (D3) converts T4 to the inactive rT3. (B) Thyroid Hormone Receptors (TRs) act as transcriptional factors that regulate a wide variety of genes. Unliganded TR, often as a heterodimer with retinoic X receptor (RXR), binds to a thyroid hormone response element (TRE) on DNA and then recruits co-repressors and their associated histone de-acetylases (HDACs); thus, repressing gene expression. T3 binding to the ligand-binding domain (LBD) promotes a conformational change in TR that leads to co-repressor release and recruitment of co-activators, and associated histone acetyl-transferases (HATs). This alteration in co-factor binding leads to recruitment of polymerase III and the onset of gene transcription (Saponaro et al., 2020).

The carboxyl-terminal ligand-binding domain (LBD) binds THs and interacts with DNA transcriptional coregulators, including corepressors (Co-Rs) and coactivators (Co-As) (Lonard et al., 2007). This region is also involved in homodimerization of TRs and their heterodimerization with other members of the receptor superfamily. TRs bind to TREs both as homodimers and as heterodimers with other members of the receptor superfamily, such as RXRs, vitamin D receptor, and all subtypes of the retinoic receptors. In particular, heterodimerization with RXR increases TRs binding to TREs, the efficacy of TR response to T3, and the transcriptional activation (Zhang et al., 1993).

The coregulators (Co-A and Co-R) influence the activation of TRs. In the absence of T3, the unliganded TR binds to TRE as a heterodimer with RXR. The association of unliganded

TR/RXR with Co-R results in the repression of basal transcriptional activity. Upon ligand activation of TRs, the transcriptional block imposed by a corepressor complex located on TR-TRE is removed, thereby permitting the transcription of T3-regulated genes (Cheng et al., 2010).

However, many TR target genes display the opposite gene expression activation, as they are expressed or repressed in the absence or presence of TH, respectively.

2.1.2 Nongenomic actions of thyroid hormones

For many years, thyroid hormones were thought to exert their biological effects exclusively through genomic mechanisms, specifically via transcriptional regulation of target genes following direct interaction of T3 with nuclear TRs bound to chromatin. However, in the early 1980s, several researchers discovered that THs could regulate biological pathways without direct genomic interaction. These findings led to the recognition of rapid, or non-genomic, effects of thyroid hormones.

Thyroid hormones exert their biological functions not only through classical genomic mechanisms, which involve the binding of T3 to TRs and the consequent transcriptional modulation of specific genes, but also through nongenomic actions that begin at the plasma membrane, mitochondria, or cytoplasm (Davis et al., 2016; Cheng et al., 2010). These actions are characterized by rapid onset (within minutes or a few hours), independence from gene transcription and protein synthesis, and the involvement of receptors that may share structural homologies with nuclear TRs or be completely devoid of them (Davis et al., 2011). Notably, although initiated outside the nucleus, the activation of extranuclear receptors and signalling pathways can ultimately converge on the regulation of transcriptional activity, thereby functionally linking nongenomic and genomic mechanisms of thyroid hormone action.

Among extranuclear thyroid hormone receptors, some studies have demonstrated that plasma membrane-initiated actions begin at a binding site on integrin aVb3, a heterodimer protein that interacts both with extracellular matrix proteins and thyroid hormones (Bergh et al., 2005; Cody et al., 2007). It was shown that the hormone-binding domain comprises two binding sites. One site binds only T3 and activates the phosphatidylinositol 3-kinase (PI3K) signalling pathway, which can promote downstream effects including cytoplasm-to-nucleus translocation of TRα1 and transcription of the hypoxia-inducible factor-1a gene. In contrast, the second site binds both T3 and T4, with a higher affinity for T4, and primarily activates MAPK1 and MAPK2 kinases

signalling pathways (Bergh et al., 2005; Lin et al., 2011). Short-term and genomic effects thus integrate and cooperate, so that the non-genomic effects activate signalling pathways necessary for the regulation of gene expression (Siergrist-Kaiser et al., 1990; Ordonez-Moran et al., 2009).
In addition to plasma membrane receptors, several extranuclear TH binding sites are present in the cytoplasm and mitochondria. Notably, four truncated proteins, p43, p33, p30 and p28, are encoded by the same mature mRNA that also gives rise to TRα1, through alternative translation initiation (Bigler et al., 1988). The full-length TRα1 protein contains two nuclear localization signals (NLSs) together with several mitochondrial import signals (Carazo et al., 2012) that are probably not active when both NLSs are present. In contrast, truncated isoforms, lack one or both NLSs, and their localization could therefore be influenced by other signals (Giammarco et al., 2020).
In human primary osteoblasts (hPOBs) and mouse osteoblast-like MC3T3 cells, the TRα1 truncated isoform p30 was inserted into the inner leaflet of the plasma membrane, where it binds THs and activates multiple signalling pathways, including nitric oxide synthase (NOS), protein kinase G II (PKGII), and mitogen-activated protein kinases (MAPKs). Activation of these cascades results in increased intracellular levels of calcium ions, nitric oxide (NO), and cyclic guanosine monophosphate (cGMP), ultimately promoting osteoblast and osteocyte proliferation (Kalyanaraman et al., 2014).
Beyond cytoplasmic and membrane-initiated actions, accumulating evidence indicates that THs also exert direct effects on mitochondria. The presence of specific binding sites for T3 in the mitochondrial inner membrane was first reported in the 1970s and later confirmed by other investigators (Sterling & Milch, 1975; Goglia et al., 1981).
In rat liver mitochondria, the truncated TRα isoform p43 was found to be localized into mitochondrial matrix (Wrutniak et al., 1995). In mitochondrial transcription experiments, it was observed that p43 over-expression induced a large increase in both mitochondrial activity and mitochondriogenesis; these effects can be abolished by deleting the DNA-binding domain of the protein (Wrutniak-Cabello et al., 2017). In addition, the p28 isoform was found in the mitochondrial inner membrane and showed a higher affinity for T3 than full-length and p43, however its precise biological function remains incompletely understood (Wrutniak-Cabello et al., 2017).
Importantly, the genomic and nongenomic actions of THs cannot be considered as two separated phenomena. Instead, extensive crosstalk exists between extranuclear signalling pathways and nuclear transcriptional regulation. For example, T4 can modulate intracellular trafficking of proteins, including hormone receptors, thereby indirectly influencing nuclear

events (Lin et al., 2009; Davis et al., 2016). Moreover, TH-mediated interplay occurs between the nuclear and the mitochondrial genomes (Wirth et al., 2017). This multilayered network of genomic and nongenomic actions significantly expands the repertoire of cellular processes regulated by thyroid hormones and provides a conceptual framework for understanding their roles in physiology and disease. The complexity of TH signalling is further increased by the presence of bioactive TH metabolites, such as 3,5-T2, whose actions will be discussed below.

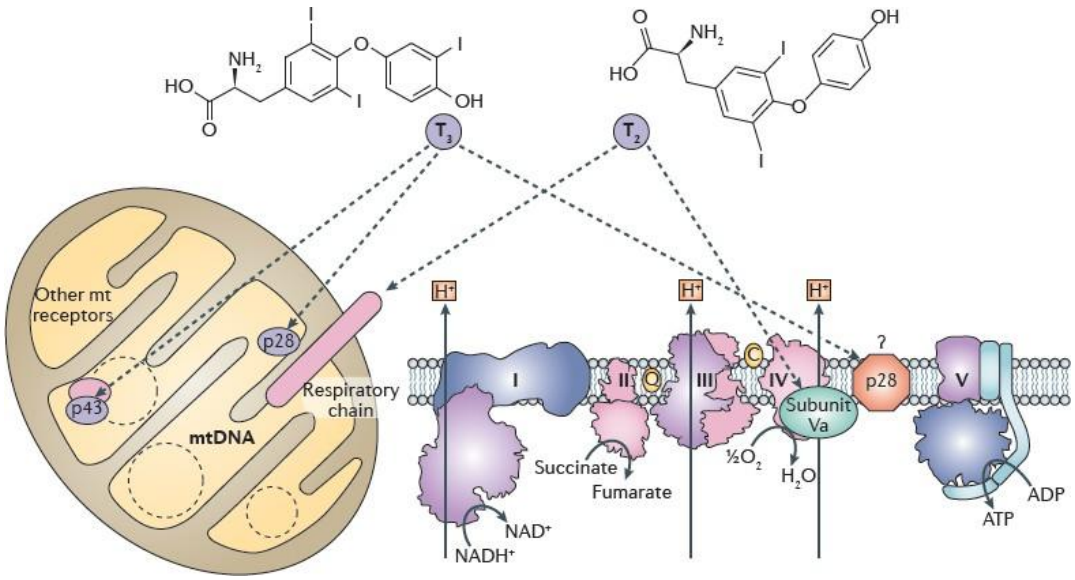

Figure 10. Mechanisms of direct actions of iodothyronines T3 and T2 on mitochondria. Left, cross-section of intact mitochondrion (mt); right, schematic view of mitochondrial membrane (Davis et al., 2015).

2.2 Metabolic effects of THs

THs regulate metabolic processes important for normal growth and development. They are important modulators of many metabolic processes, being strictly associated with the regulation of energy balance, mainly through their effects on the brain, white and brown adipose tissue, skeletal muscle, liver.

2.2.1 Basal metabolic rate

T3 is the main modulator of basal metabolism, increasing oxygen consumption, heat production, and mitochondrial activity (Brent 2012; Mullur et al., 2014). Through multiple mechanisms of action, T3 increases ATP production and stimulates the energy expenditure required to maintain ionic balance and basic cellular functions (Clausen et al., 1991). A key component of this effect derives from the stimulation of Na^+/K^+-ATPase and Ca^{2+}-ATPase (SERCA) activities, which consume energy to maintain sodium, potassium, and calcium gradients across cellular membranes (Simonides et al., 2001). Beyond sustaining normal cellular homeostasis, this process entails a considerable energy cost. This continuous ATP turnover contributes significantly to thermogenesis, with part of the heat generated arising from the so-called "calcium cycle" (Jiang et al., 2000).

At the mitochondrial level, thyroid hormones modulate the efficiency of oxidative phosphorylation by increasing the permeability of the inner mitochondrial membrane to protons, thus partially uncoupling the respiratory chain from ATP synthesis. This "proton leak" mechanism enhances mitochondrial respiration and accelerates energy expenditure, dissipating excess chemical energy as heat (Silva 2006; Gregory et al., 1991). In addition, T3 induces the expression of mitochondrial enzymes such as mitochondrial glycerol-3-phosphate dehydrogenase (mGPD), which transfers reducing equivalents from the cytosol to the mitochondria, thereby sustaining cellular respiration and thermogenesis. As a result, hypothyroidism is characterized by reduced metabolic rate, diminished ATP turnover, and impaired heat production, whereas hyperthyroidism amplifies ATP synthesis and thermogenesis, reflecting the profound systemic impact of thyroid hormone action on cellular metabolism (Silva, 2006; Harper et al., 2008; Cannon et al., 2004).

2.2.2 Regulation of body weight

Increased thyroid activity leads to greater resting energy expenditure, with more intense lipid and carbohydrate oxidation, promoting weight loss and maintaining caloric intake. Conversely, decreased thyroid hormones lead to a slowing of metabolic processes, reduced lipolysis, and a greater tendency toward fat accumulation, contributing to weight gain. It is important to note, however, that weight changes are not exclusively due to fat mass: hypothyroidism frequently causes water retention, linked to the accumulation of glycosaminoglycans in tissues, a phenomenon that affects body weight independently of caloric intake (Brent, 2012).

Furthermore, thyroid hormones influence appetite and systemic hormonal balance, interacting with insulin, cortisol, and leptin, thus contributing to the modulation of feeding behaviour and substrate metabolism (Iwen et al., 2018). Overall, the effect on body weight is the result of the interaction between energy expenditure, metabolic regulation, and neuroendocrine mechanisms that govern hunger, satiety, and nutrient utilization**.**

2.2.3 Cholesterol and triglycerides metabolism

The regulation of lipid metabolism by thyroid hormones depends largely on the action of T3 in the liver, mediated by the nuclear receptor TRβ (Rocha et al., 2008), demonstrated in mice carrying a dominant-negative mutation in Thrβ, the ThrβPV/PV mice (Araki et al., 2009). T3 lowers LDL cholesterol by stimulating the expression of the LDL receptor and thereby promoting the removal of cholesterol from the blood (Lopez et al., 2007).
In addition, TH influences cholesterol metabolism, affecting fatty acid β-oxidation and modulating cholesterol synthesis (Goldstein et al., 2006). Regarding triglycerides, thyroid hormones regulate both the production and catabolism of triglyceride-rich lipoproteins. T3 stimulates the expression of lipoprotein lipases and promotes the peripheral clearance of triglycerides (Kuusi et al., 1988). Another effect of T3 is the up-regulation of apolipoprotein AV (ApoAV), which plays a major role in TG regulation (Prieur et al., 2005). Indeed, increased levels of ApoAV have been associated with decreased levels of TGs (Rensen et al., 2005).

2.2.4 Fatty acids metabolism

Thyroid hormones play a key role in regulating fatty acid metabolism, intervening in both the mobilization of lipid reserves and the processes of lipid oxidation and synthesis. In adipose tissue, TH promotes lipolysis by activating hormone-sensitive lipase and increasing the sensitivity of adipocytes to catecholamines (Oppenheimer et al., 1991). This action facilitates the release of free fatty acids (FFAs) into the circulation, making them available as energy substrates for metabolically active tissues. Conversely, in the liver and muscle, T3 stimulates mitochondrial and peroxisomal β-oxidation, increasing the body's ability to utilize fatty acids as a primary energy source and promoting improved overall metabolic efficiency (Liu & Brent 2010).

Recently, it has been shown that thyroid hormones also regulate lipid droplet turnover within hepatocytes through a process termed lipophagy – the autophagic degradation of lipid droplets (Sinha et al., 2012, 2017, 2019). The mechanism is not fully characterised, but its combination with β-oxidation could become significant in the context of lipid excess.

2.2.5 Carbohydrate metabolism

Thyroid hormones regulate also carbohydrate metabolism, influencing both glucose availability and its utilization in peripheral tissues. Under physiological conditions, T3 enhances intestinal glucose absorption and facilitates its entry into cells by increasing the activity of transporters and enzymes involved in glycolysis. In the liver, T3 stimulates both glycogenolysis and gluconeogenesis, promoting increased endogenous glucose production and contributing to maintaining plasma glucose concentrations in situations of high energy demand. Conversely, thyroid hormones increase tissue sensitivity to catecholamines, amplifying the adrenergic response that supports glucose mobilization during periods of metabolic stress (Mullur et al., 2014).

However, alterations in thyroid function can compromise glucose homeostasis. In hyperthyroidism, excessive thyroid hormone action accelerates hepatic glucose production and insulin degradation, reducing its bioavailability and promoting the development of insulin resistance and hyperglycaemia. (Al-Shoumer et al., 2006). Conversely, hypothyroidism is associated with reduced glucose turnover, a reduced insulin response, and a slowing of glycolysis and gluconeogenesis, with a possible tendency toward hypoglycaemia (Kalra, Unnikrishnan, & Sahay 2014). Overall, the action of thyroid hormones on carbohydrates appears to be a finely regulated mechanism, in which hormonal balance is essential to ensure adequate metabolic control.

2.2.6 Thyroid hormones and mitochondrial efficiency

THs are key regulators of cellular energy metabolism and exert profound effects on mitochondrial efficiency. The calorigenic effect of TH, a hallmark of thyroid hormone physiology, is achieved through a partial dissociation of electron transport from ATP synthesis, thus reducing the P/O ratio (Hess et al., 1951; Lardy et al., 1951). Two mitochondrial mechanisms have been proposed to explain the molecular basis of TH-induced metabolic

inefficiency: proton leak across the inner mitochondrial membrane and redox slipping. During this mechanism, protons escape from the inner mitochondrial membrane without being used to pump ATP, resulting in oxygen consumption that does not produce energy. This intrinsic loss of protons through the electron transport system causes energy to be dissipated as heat (Lanni et al., 2016). TH modulates proton leak through both genomic and non-genomic actions, influencing key mitochondrial proteins. In the brown adipose tissue (BAT), THs enhance UCP1-dependent uncoupling by increasing local T3 production via DIO2 and promoting UCP1 transcription through TRα and TRβ (de Jesus et al., 2001).

Other structurally-UCP1-related proteins are activated by TH. UCP2 and UCP3 modulate ROS production and oxidative stress, thereby helping to maintain redox balance and prevent lipid-induced mitochondrial injury (Lombardi et al., 2010; Goglia et al., 2003).

In the liver, TH regulates uncoupling primarily through the adenine nucleotide translocator (ANT), increasing the activity and content of this protein (Dummler et al., 1996; Schönfeld et al., 1997). These findings indicate that the TH-induced increase in mitochondrial proton conductance in the liver is driven by enhanced ANT activity and elevated sensitivity to fatty acid–mediated proton leak.

Finally, TH enhance oxygen consumption (Hess et al., 1951; Lardy et al., 1951), stimulate thermogenesis (Herz et al., 2019; Krause 2020), and increase metabolic flexibility, highlighting their pivotal role in mitochondrial bioenergetics and their potential therapeutic relevance in metabolic diseases (Lanni et al., 2016).

2.3 THs regulate MQC and autophagy

Thyroid hormones are master regulators of mitochondrial quality control by balancing biogenesis, dynamics, and mitophagy to ensure optimal cellular energy metabolism. It is widely reported that T3 stimulates the expression of master regulators such as PGC1 a, NRF1 and TFAM to increase the number and function of mitochondria (Wulf et al., 2008; Garstka et al., 2003). In soleus of hyperthyroid mice, T3-mediated mitochondrial activity and biogenesis linked to autophagy activation via ROS-AMPK-ULK1 improves mitochondrial function (Lesmana et al., 2016). Similarly, in brown adipose tissues from hyperthyroid mice, T3 has been reported to act on mitochondrial respiration, autophagic flux, mitophagy, and mitochondrial biogenesis (Yau et al., 2019).

The ability of TH to activate several forms of autophagy (from mitophagy to lipophagy) has been in depth analysed. T3 induces mitophagy by activating Beclin1, PTEN Induced Kinase (Pink)/Parkin (Park), and Microtubule-associated protein 1A/1B-light chain 3 (LC3) pathways to counteract ROS-inflicted cell damage and death (Chi et al., 2019). Sinha and co-workers demonstrated, in vivo/in vitro, that mitophagy is necessary also for sustaining efficient oxidative phosphorylation induced by T3, under high-energy demand: in liver of mice, indeed, this iodothyronine induces concomitantly mitophagy and mitochondria renewal (Sinha et al., 2012). Moreover TH, have been shown to be able to induce in liver lipophagy mobilizing lipids from lipids droplets towards β-oxidation to provide substrates maintaining a hypermetabolic state (Sinha et al., 2012; Iannucci et al., 2017). Until now, there are no mechanistic studies that correlate directly TH administration with fusion/fission processes. A very few studies reported that T3 by contemporary promoting mitochondrial fission, through DRP1 overexpression, and biogenesis, contributes to the formation of smaller, more dynamic mitochondria and to the clearance of damaged mitochondria (Forini et al., 2019; Na et al., 2020).

2.4 THs and MASLD

TH play a central role in regulating of energy homeostasis and in the metabolism of lipids, carbohydrates, proteins, and minerals. Their effects are widespread across multiple organ systems, but the liver represents one of the primary targets of TH action (Kowalik et al., 2018; Gionfra et al., 2019).

Alterations in thyroid function can lead to significant disturbances in lipid metabolism; for example, hypothyroidism is often associated with hypercholesterolemia, which is recognized as one of the mechanisms linking impaired TH action to the pathogenesis of MASLD (Chung et al., 2012). Reduced circulating TH levels have been consistently reported in MASLD patients (Bohinc et al., 2014), and experimental studies have demonstrated that even moderate hypothyroidism increases susceptibility to hepatic steatosis (Ferradino et al., 2017). Transcriptomic analyses of liver tissue from individuals with MASLD undergoing bariatric surgery revealed a marked down-regulation of genes involved in RNA metabolism, protein synthesis, and mitochondrial function — pathways that are normally under positive regulation by TH (Pihlajamäki et al., 2009). Both human and rodent studies have also shown decreased intrahepatic T3 levels in MASLD, suggesting impaired local activation of thyroid hormones in the steatotic liver (Bohinc et al., 2014; Bruinstroop et al., 2018).

Functionally, thyroid hormones regulate multiple layers of hepatic metabolism. They enhance de novo lipogenesis through coordinated activation of lipogenic transcription factors, while simultaneously promoting fatty acid oxidation, VLDL secretion, and lipoprotein remodelling, ensuring that lipid synthesis and disposal remain balanced (Mullur et al., 2014; Damiano et al., 2017). TH also increase hepatic insulin sensitivity and regulate gluconeogenesis, helping to stabilise systemic glucose levels. These effects are mediated by thyroid hormone receptors, particularly TRβ, which plays a dominant role in hepatic lipid homeostasis (Yan et al., 2022). TRβ also interacts with other nuclear receptors—including PPARα, LXR, and FXR—integrating TH signalling with fatty acid oxidation, cholesterol metabolism, and bile acid pathways (Mullur et al., 2014). Disturbances in this network contribute to hepatocellular lipid accumulation, oxidative stress, and inflammation, key hallmarks of MASLD. Observational studies have further shown that elevated TSH levels, even within the upper-normal range, correlate with higher MASLD prevalence and severity, including advanced fibrosis (Guo et al., 2018; Mantovani et al., 2018). This suggests that thyroid dysfunction contributes not only to steatosis but also to disease progression. Recent mechanistic studies reinforce this link by demonstrating that TH regulate hepatic autophagy and lipophagy, essential processes for the breakdown of triglyceride droplets and damaged organelles (Sinha et al., 2017; Sinha et al., 2012). Impaired autophagy is a recognized feature of MASLD and contributes to mitochondrial dysfunction, ROS accumulation, activation of inflammatory pathways, and stellate cell stimulation—all central to the transition from simple steatosis to steatohepatitis.

2.5 3,5-diiodo-L-thyronine or T2

Thyroid hormones are pivotal in the regulation of differentiation, growth, and metabolism. In recent decades, substantial evidences have been collected demonstrating a possible bioactive role for endogenous thyroid hormone derivatives. The main characteristic of these molecules is the rapid onset of their effects, probably due to the involvement of a nongenomic pathway. Previously, these compounds were considered inactive thyroid hormone breakdown products. However, several reports have recently shown that they have relevant effects in the regulation of lipid metabolism, energy balance and thermogenesis. Among these compounds, T2, an endogenous metabolite of T3, has attracted rising interest as a peripheral mediator of several TH metabolic effects.

At the beginning of the 1980s, early experimental observations suggested that not only triiodothyronine (T3) but also its metabolite 3,3′-diiodothyronine (3,3′-T2) could bind to high-affinity intracellular sites located in the inner mitochondrial membranes (Goglia et al., 1980). Although both 3,3′-T2 and 3,5-T2 are naturally occurring diiodothyronines derived from T3, they differ markedly in their biological activity and tissue specificity. Early studies mainly focused on 3,3′-T2 because it was the first iodothyronine shown to bind mitochondrial membranes with high affinity (Goglia et al., 1980). However, more recent evidence has revealed that 3,5-T2 exerts far greater metabolic potency, particularly in stimulating hepatic oxygen consumption, lipid oxidation, and mitochondrial respiration (Moreno et al., 2002; Lanni et al., 2005; Lombardi et al., 2015).

Unlike 3,3′-T2, whose physiological significance remains uncertain and whose effects appear modest, 3,5-T2 acts as an active thyroid hormone metabolite capable of inducing rapid, non-genomic responses at the mitochondrial level (Arnold et al., 1998; Goglia 2005). These observations have shifted research attention toward 3,5-T2 as the principal bioactive derivative mediating thyroid hormone–dependent control of hepatic energy metabolism and as a promising target for therapeutic exploration in metabolic disorders (Senese et al., 2018; de Lange et al., 2021).

2.6 Mechanisms underlying the anti-steatotic and hypolipidemic effects of T2.

T2 exerts marked hypolipidemic and hepatometabolic effects through coordinated regulation of mitochondrial function, lipid handling, and cellular energy sensing-actions particularly relevant from both physiological and pharmacological perspectives, as observed in several animal models. Dietary modulation is well-established approach to studying hepatic metabolism, as changes in nutritional status profoundly affect lipid signalling networks and mitochondrial function (Moreno et al., 2003; de Lange et al., 2007). Animal models fed a high-fat diet (HFD) closely reproduce the metabolic disorders associated with human overnutrition, including obesity, dyslipidemia, insulin resistance, and ectopic fat deposition. In vivo studies in these models of diet-induced obesity and high-fat feeding consistently demonstrate that administration of T2 prevents or markedly attenuates visceral adipose tissue expansion and hepatic steatosis, reduces triglyceride accumulation, and improves systemic lipid profile by promoting a metabolic shift towards enhanced fatty acid oxidation (Lanni et al., 2005; Mollica et al., 2009; de Lange et al., 2011; Moreno et al., 2001). These improvements are accompanied

by reductions in circulating triglyceride and cholesterol levels, effects mechanistically linked to increased mitochondrial β-oxidation, activation of the carnitine palmitoyl-transferase (CPT) system, enhanced respiratory chain activity, and improved hepatic oxidative capacity (Silvestri et al., 2010; de Lange et al., 2011). Consistent with these findings, Mollica et al. demonstrated in a high-fat diet model that T2 rapidly reverses hepatic steatosis by enhancing mitochondrial fatty acid oxidation, reducing oxidative stress, and improving mitochondrial efficiency, identifying mitochondria as a primary target of T2 metabolic action (Mollica et al., 2009).

Proteomic and metabolic analyses further show that T2 induces broad remodelling of hepatic pathways, including fatty-acid metabolism, ketogenesis, amino-acid metabolism, urea cycle activity, and stress-response pathways, with mitochondria representing the most responsive compartment. These adaptations collectively counteract HFD-induced mitochondrial dysfunction, reduce oxidative stress and lipid peroxidation, and improve metabolic flexibility (Silvestri et al., 2010).

The systemic hypolipidemic effects elicited by T2 under HFD conditions depend in part on its direct action on the liver, where it modulates lipid and glucose metabolism under conditions of fat overload through both AMPK activation and SIRT1, an important metabolic regulator (Picard et al., 2004; Feige et al., 2008; de Lange et al., 2011). In HFD rats, T2 was demonstrated to (i) rapidly increase hepatic nuclear SIRT1 activity and (ii), through SIRT1-activation, deacetylate PGC-1α and SREBP-1c with a concomitant upregulation of genes involved in mitochondrial biogenesis and fatty acid oxidation, and downregulation of lipogenic genes (de Lange et al., 2011). This process reduces hepatic triglyceride storage, improves insulin sensitivity and attenuates of systemic dyslipidemia (de Lange et al., 2011).

Complementary mechanistic insights have been obtained through cellular systems that allow dissection of direct hepatocyte-autonomous effects. Studies by Grasselli and colleagues in high-fat diet and fatty liver rat models demonstrated that T2 markedly attenuates hepatic steatosis by reprogramming liver lipid handling toward enhanced oxidative flux and reduced de novo lipogenesis (Grasselli et al., 2008; Grasselli et al., 2012). In isolated rat hepatocytes, iodothyronines exerted direct, cell-autonomous effects on excess triglyceride storage, reducing intracellular lipid accumulation independently of systemic endocrine influences. T2 stimulated mitochondrial β-oxidation and limited lipid deposition through modulation of oxidative pathways, including activation of PPARα-related signalling, confirming a direct hepatic metabolic action (Grasselli et al., 2011).

In steatotic hepatocyte models, T2 promoted triglyceride mobilization from lipid droplets and enhanced mitochondrial fatty acid oxidation through up-regulation of CPT1, very long-chain

acyl-CoA dehydrogenase (VLCAD) and uncoupling protein 2 (UCP2), thereby shifting lipid composition towards less lipotoxic species and protecting hepatocytes from saturated fatty acid–induced lipotoxicity (Grasselli et al., 2014).

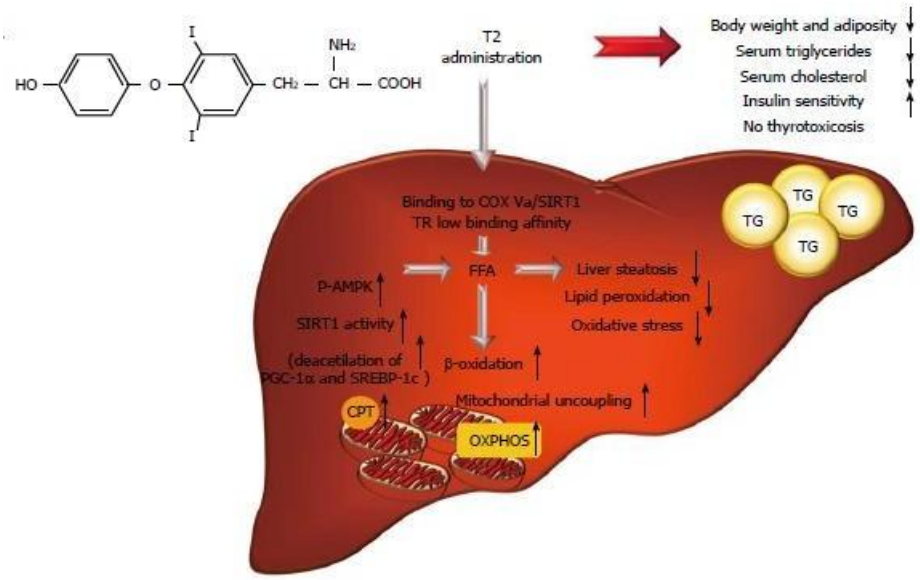

Figure 11. A summary of key events and molecular pathways underlying T2**.** T2: 3,5-diiodo-L-thyronine; TR: Thyroid hormone receptor; COX Va: Cytochrome-*c* oxidase Va subunit; FFA: Free fatty acid; TG: Triglyceride; P-AMPK: Phosphorylated AMP-activated protein kinase; SIRT1: NAD+-dependent deacetylase sirtuin 1; PGC-1α: Peroxisome proliferator-activated receptor γ coactivator; SREBP- 1c: Sterol response element binding protein-1c; CPT: Carnitine palmitoyltransferase system; OXPHOS: Oxidative phosphorylation system (Coppola et al., 2014).

2.7 T2 and mitochondria

Mitochondria are the main cellular target of T2. Mechanistically, T2 interacts with the mitochondrial electron transport chain by binding to the Va subunit of cytochrome-c oxidase (COX). It has been demonstrated that T2 binding to the COX complex abolishes the allosteric ATP inhibition of COX, leading to increased respiratory flux, reduced ROS production and improved mitochondrial coupling (Moreno et al., 2003; Lanni et al., 1992). This functional modulation enhances oxygen consumption and thermogenesis by reducing the efficiency of ATP synthesis, providing a biochemical explanation for T2 rapid stimulation of mitochondrial respiration (Goglia et al., 1999). The interaction of T2 with COX is only one component of its broader influence on mitochondrial bioenergetics, as accumulating evidence indicates that T2 modulates additional respiratory pathways. T2 rapidly stimulates calcium uptake, increasing

mitochondrial dehydrogenase activity and enhancing respiratory chain activity (Hummerich & Soboll, 1989). Another target is ATP synthase. In hypothyroid rat liver, T2 was able to induce both the hydrolytic and synthetic activity of ATP synthase rapidly within one hour of administration (Cavallo et al., 2011), without altering its mRNA levels (Cavallo et al., 2013). The physiological effects of T2 on mitochondria are reflected at the whole-body level. Comparing the actions of T2 and T3 in the liver of hypothyroid rats showed that both hormones stimulated mitochondrial respiration, but with different time courses. The stimulatory effect of T2 on RMR was evident one hour after injection, resolved within 48 hours, and was not influenced by protein synthesis. In contrast, the effect of T3 appeared after 24 hours, persisted for 5-6 days, and was prevented by a protein synthesis inhibitor (O'Reilly & Murphy 1992; Moreno et al., 1997). These data confirm that the short-term effect of T2 on whole-body metabolism is due to mitochondrial activation in a protein synthesis-independent manner. T2 emerges as a pleiotropic regulator capable of restoring metabolic flexibility in steatotic hepatocytes (Senese et al., 2018).

In the last decade important advances have been achieved through the application of one-dimensional Blue Native PAGE (BN-PAGE), a technique that allows analysis of the abundance, activity, and organization of OXPHOS complexes and their assembly into supercomplexes (SCs) (Silvestri et al., 2019; Silvestri et al., 2010; Cavallo et al., 2011; Giacco et al., 2019). This approach has shown that T2 primarily modulates the kinetic properties of selected respiratory pathways, triggering a rapid and direct functional response, whereas T3 increases the abundance of respiratory chain components and promotes their assembly into SCs, leading to a slower but more sustained metabolic adaptation. Functionally, T2 enhances both coupled and uncoupled respiration in succinate-energized mitochondria in hypothyroid (Silvestri et al., 2018) and HFD rats (Lanni et al., 2005). T2 does not increase the abundance of respiratory complexes but selectively enhances complex II-linked pathways and boosts the in-gel activity of complex II. T2 preferentially activates pathways generating $FADH_2$, which yields less ATP per electron pair than NADH, representing a T2-specific thermogenic mechanism. T3 shares some effects with T2, but its actions are generally more pronounced (Cioffi et al., 2022). Importantly, T3 robustly stimulates proton leak and increases mitochondrial adenine nucleotide translocator (ANT) levels, two hallmark features of classic thyroid hormone induced thermogenesis. Finally, only T3 enhances the assembly of individual OXPHOS complexes into SCs, improving oxidative capacity and maintaining high metabolic rates (Silvestri et al., 2018).

2.8 T2: Effects on the hypothalamic pituitary-thyroid (HPT) axis

Apart from its unequivocal effects on metabolic rate, evidences from several studies have raised the possibility that T2 might also elicit side effects affecting, in particular, the HPT axis. In 1995, Horst and colleagues first showed that T2 treatment reduced, *in vivo,* TSH and T4 levels as well as, *ex vivo,* TSH secretion from rat pituitary fragments (Horst et al., 1995). *In vivo*, the used doses of T2 ranged from 20 to 200 μg/100 g body weight per day (Horst et al., 1995). When compared to T3 (used at doses of 1-15 μg /100 g per day), T2 was as effective in reducing TSH and T4 levels but did not alter body and organ weights. Some years later, Moreno and co-worker, by using T2 at doses from 2.5 to 10 μg/100 g BW, showed suppressed TSH levels also in T2-treated hypothyroid rats (Moreno et al., 1998). Very recently, as cited above, Padron and colleagues studied the effects of chronic administration of T2 to aged rats on the HPT axis, specifically monitoring the expression levels of proteins involved in thyroid biosynthesis and metabolism (Padron et al., 2014). Briefly, these authors reported a T2-induced suppression of thyroid function [i.e. reduced thyroid iodide uptake and expression and activity of thyroperoxidase, NADPH oxidase 4 (NOX4), and D1] and of TSH, T3, and T4 levels. Interestingly, serum levels responded to T2 in a dose-dependent manner (Padron et al., 2014).
As far as the effects of T2 on the HPT axis in the mouse, data are available from the two recent studies of (Goldberg et al., 2012; Jonas et al., 2015).
In the study on LDLr knockout mice, the used dose of T2, as reported above, while having similar cholesterol-lowering effects as those of T3, significantly reduced the circulating levels of T4. This result was indicative of a pituitary suppression of the thyroid function (Goldberg et al., 2012).
In the study of Jonas et al, similarly to what reported by Padron (Padron et al., 2014), T2 administration, at the higher used dose (250μg/100 g body weight), down-regulated several genes involved in the regulation of the HPT axis and dose-dependently repressed serum T4 and T3 levels, once again suggesting a T2-induced negative feedback mechanism suppressing the HPT axis (Jonas et al., 2015). In the same study, after 4 weeks of T2 treatment at the higher dose, cardiac hypertrophy was also observed. Unfortunately, the lack of a specific mouse immunoassay still limits our knowledge of T2 effects on TSH levels in mice.
All together, these studies demonstrated that T2, while increasing metabolic rate and reducing fat mass, can also lead to a suppression of the HPT axis, an effect that seems specie- and dose-dependent. This appears of particular relevance above all when our interest is to translate results obtained in animal models to humans.

2.9 The physiological and pathophysiological roles of 3,5-T2 in humans and its use as a drug

While the metabolic actions of T2 have been extensively characterized in experimental models, growing evidence suggests that 3,5-T2 may also exert physiologically relevant effects in humans.

A small case report involving two participants showed that acute administration of 3,5-T2 (1–5 μg/kg body weight) rapidly increased resting metabolic rate (RMR) within 4–6 hours. Moreover, chronic treatment for 28 days (≈5 μg/kg body weight) resulted in a ~15% increase in RMR and an average body weight reduction of approximately 4 kg, without significant alterations in major clinical parameters or detectable adverse effects, including cardiac abnormalities (Antonelli et al., 2011). Although these findings are limited by the extremely small sample size, they suggest that 3,5-T2 can exert rapid metabolic effects in humans, consistent with its non-genomic actions described in animal models. A major obstacle to the interpretation of human studies has long been the lack of reliable analytical methods for quantifying endogenous T2 (Faber et al., 1982). Earlier reports relied on assays with limited specificity, raising concerns about cross-reactivity with other iodothyronines and the robustness of the reported concentrations. Consequently, previously published human data required independent confirmation (Pinna et al., 1997).

More recently, the development of a monoclonal antibody–based competitive chemiluminescence immunoassay has enabled more accurate detection of circulating T2 (Lehmphul et al., 2014). Using this approach, Pietzner and colleagues reported measurable serum concentrations of T2 in euthyroid individuals (approximately 0.22–0.33 nM), revealing significant associations with glucose metabolism and thyroid hormone homeostasis. Subsequent metabolomic analyses identified correlations between serum T2 levels and metabolites involved in lipid metabolism, oxidative stress responses, and xenobiotic processing, in agreement with prior proteomic findings obtained in rodent liver. These observations support the notion that T2 may act as an endogenous modulator of metabolic pathways in humans (Pietzner et al., 2015a).

Altered T2 levels have also been reported in pathological conditions. Increased circulating concentrations were observed in patients with non-thyroidal illness syndrome (NTIS), including critically ill individuals, where serum T2 levels were approximately 30% higher than in healthy controls and appeared to be independent of circulating T3 or T4. These findings have led to the hypothesis that elevated T2 may contribute to the metabolic adaptations observed in NTIS and

could partially explain the limited efficacy of T4/T3 replacement therapy in low-T3 syndrome (Langouche et al., 2016).

Despite these advances, current human data remain fragmentary, and studies involving larger cohorts of euthyroid and metabolically compromised individuals are required to define the physiological range, regulation, and clinical relevance of T2 more conclusively.

Chapter III: Autophagy

Autophagy is an evolutionarily conserved catabolic process responsible for the degradation and recycling of intracellular components — including macromolecules, damaged organelles, and protein aggregates — through the lysosomal system (Klionsky & Emr, 2000; Mizushima et al., 2008). This process is essential for maintaining cellular homeostasis, as it allows cells to degrade proteins, glycogen, lipids, and organelles such as damaged mitochondria or excess endoplasmic reticulum (ER), thereby generating metabolic intermediates and biomolecular building blocks required for cell survival and adaptation to stress (Mizushima & Komatsu 2011; Youle & Narendra 2011; Liu & Czaja 2013; Mizushima 2018; Chino & Mizushima 2020).
There are three major types of autophagy, which differ mainly in the way the cellular cargo is delivered to the lysosome (Parzych & Klionsky 2014):

1. Macroautophagy (commonly referred to simply as *autophagy*) is characterized by the formation of a double-membrane vesicle, the *autophagosome*, which engulfs portions of cytoplasm or damaged organelles. The autophagosome subsequently fuses with a lysosome to form an *autolysosome*, where its contents are degraded by lysosomal hydrolases (Klionsky & Emr 2000).

2. Microautophagy involves the direct invagination of the lysosomal membrane, which engulfs small portions of cytoplasm or organelles without the intermediate formation of an autophagosome (Schuck 2020).

3. Chaperone-mediated autophagy (CMA) is a selective process through which soluble cytosolic proteins containing a specific pentapeptide motif (KFERQ) are recognized by the chaperone HSC70 and targeted to LAMP-2A (lysosome-associated membrane protein 2A). The subsequent multimerization of LAMP-2A forms a translocation complex that allows these substrates to cross the lysosomal membrane and undergo degradation (Arias & Cuervo 2011).

Through these complementary mechanisms, autophagy serves as a fundamental adaptive and quality-control system, supporting energy balance, organelle turnover, and survival under stress conditions such as nutrient deprivation or metabolic overload.
The liver is one of the most metabolically active and adaptive organs in the human body, and autophagy plays a central role in maintaining its cellular and functional homeostasis (Yin et al., 2008; Ding 2010; Rautou et al., 2010). Historically, the process of autophagy was first identified

in the liver during pioneering studies in the 1960s, when Deter and colleagues described the presence of autophagic vacuoles in hepatocytes (Deter et al., 1967). Since then, a vast body of evidence has established that autophagy is essential for hepatic metabolism, participating in the turnover of proteins, lipids, glycogen, and organelles, and in the adaptation to nutrient deprivation, oxidative stress, and xenobiotic injury.

In the healthy liver, basal autophagy contributes to metabolic homeostasis by regulating glycogenolysis, lipid turnover, and mitochondrial quality control. During fasting or stress conditions, autophagy is upregulated to provide energy substrates and maintain cellular integrity. Conversely, dysregulation of autophagy has been implicated in the pathogenesis of multiple liver diseases, including alcohol-associated liver disease (AALD) (Williams et al., 2014), non-alcoholic fatty liver disease (NAFLD) and its progressive form non-alcoholic steatohepatitis (NASH) (Gonzalez-Rodriguez et al., 2014; Tanaka et al., 2016; Fallowfield, 2011), as well as drug-induced liver injury (DILI) (Ni et al., 2012), cholestasis, viral hepatitis (Sir et al., 2008; Wang and Ou 2015), and hepatocellular carcinoma (HCC) (Chao et al., 2020).

At the mechanistic level, specific forms of selective autophagy—including mitophagy, ER-phagy, aggrephagy, and particularly lipophagy—mediate the removal of damaged mitochondria, excess endoplasmic reticulum, misfolded protein aggregates, and lipid droplets, respectively. These processes are critical for sustaining the high metabolic demands of hepatocytes and for preventing cellular injury caused by toxic accumulation of damaged organelles or lipids (Qian et al., 2021).

In pathological settings, impaired lipophagy contributes to hepatic steatosis by limiting the mobilization of triglycerides stored in lipid droplets. Likewise, defective mitophagy promotes oxidative stress and mitochondrial dysfunction, while impaired ER-phagy exacerbates endoplasmic reticulum stress and promotes apoptosis or inflammation. The crosstalk between autophagy and metabolic pathways, largely orchestrated by Beclin-1, AMPK, and SIRT1, determines whether hepatocytes adapt to or succumb under stress conditions. Recent findings have highlighted the therapeutic potential of targeting autophagy in liver diseases.

3.1 Role of autophagy in liver physiology

The liver is a central hub for systemic metabolism, orchestrating the turnover of carbohydrates, lipids, fatty acids, proteins, amino acids, and xenobiotics. Hepatocytes — the parenchymal cells that account for nearly 80% of the liver's mass — carry out most of these metabolic and

secretory functions, including glycogen storage, lipoprotein synthesis, and bile secretion. The remaining non-parenchymal cells (NPCs), such as cholangiocytes, sinusoidal endothelial cells, Kupffer macrophages, and hepatic stellate cells (HSCs), contribute to vascular regulation, immunity, and fibrosis (Uhlen et al., 2015).

Beyond its metabolic role, the liver is also a major secretory and endocrine organ: nearly 40% of its transcripts encode secreted proteins or *hepatokines*, which act as signalling molecules involved in inter-organ metabolic communication (Uhlen et al., 2015). Under physiological conditions, autophagy is crucial for maintaining hepatic homeostasis, coupling energy availability to intracellular quality control mechanisms.

Basal hepatic autophagy follows a circadian rhythm, tightly coordinated with fluctuations in nutrient status. In rodents maintained on a 12-h light/dark cycle, the expression of autophagy-related genes peaks just before the onset of activity, when energy demand rises and nutrient intake begins (Pfeifer & Strauss 1981; Ma et al., 2011; Ryzhikov et al., 2019). This rhythmic activation allows the liver to anticipate metabolic needs by mobilizing nutrients toward the brain and peripheral tissues. Autophagy also regulates the circadian clock itself through the selective degradation of core regulators, such as cryptochrome-1 (CRY1) (Toledo et al., 2018), thus reinforcing the bidirectional coupling between metabolism and circadian rhythms.

During nutrient deprivation, hepatic autophagy is strongly induced to mobilize internal reserves — promoting glycogenolysis, lipolysis, and proteolysis — and supplying glucose, fatty acids, and amino acids to sustain cellular ATP production and systemic energy balance (Schneider & Cuervo 2014; Ueno & Komatsu 2017). Conversely, in the post-prandial state, elevated circulating nutrients and hormones inhibit autophagy to favour anabolic processes such as glycogen and lipid synthesis (Mortimore & Poso 1984).

Autophagy in the liver is finely tuned by endocrine and neural signals. Hormones such as insulin, glucagon, ghrelin, and GLP-1 modulate autophagic activity according to feeding status (Yin et al., 2008; Zhang et al., 2015; He et al., 2016). The sympathetic nervous system stimulates autophagy via epinephrine release during fasting (Mortimore & Poso 1987), while glial cell line–derived neurotrophic factor (GDNF) enhances hepatocytic autophagy by inhibiting mTOR signalling (Mwangi et al., 2019).

3.2 Role of autophagy dysfunction in MASLD pathogenesis

The pathogenesis of MASLD is multifactorial, resulting from the convergence of genetic predisposition, lifestyle factors, and metabolic dysfunctions. As previously described (see Chapter I) current models describe a "multiple-hit" process that includes adipose tissue dysfunction, insulin resistance, lipotoxicity, chronic inflammation, oxidative stress, dysregulated innate immunity, and altered gut microbiota composition (Tilg & Moschen 2010; Henao-Mejia et al., 2012; Birkenfeld & Shulman 2014; Haas et al., 2016). Among these factors, defective lysosomal and autophagic function has emerged as a key pathogenic mechanism contributing to steatosis and hepatocellular injury (Choi et al., 2013).

At the cellular level, impaired autophagy reduces the degradation of lipid droplets via lipophagy, leading to excessive accumulation of triglycerides in hepatocytes. Both genetic and diet-induced models of obesity show suppression of hepatic autophagy and chaperone-mediated autophagy (CMA), which together promote steatosis and insulin resistance (Singh et al., 2009; Yang et al., 2010; Schneider et al., 2014). In humans, livers from NAFLD patients display decreased autophagic flux and lysosomal activity (Fukuo et al., 2014; Gonzalez-Rodriguez et al., 2014), confirming that defective autophagy is not merely a secondary effect but a pathophysiological driver of the disease.

Encouragingly, restoration of autophagy has been shown to ameliorate hepatic lipid accumulation and metabolic dysfunction in animal models. Genetic strategies such as Atg7 or TFEB overexpression, and pharmacological approaches using trehalose, rapamycin, carbamazepine, or other autophagy inducers, markedly reduce hepatic steatosis and improve insulin sensitivity (Singh et al., 2009; Yang et al., 2010; Sinha et al., 2014; Sun et al., 2015; DeBosch et al., 2016). Similarly, TFEB activation, which promotes lysosomal biogenesis and enhances autophagic degradation capacity, has emerged as a promising target (Wang et al., 2017).

In addition to conventional drugs, several small molecules (Rubinsztein et al., 2007; Fan et al., 2017) and autophagy-activating peptides, notably Tat-Beclin-1 (Shoji-Kawata et al., 2013), have been developed as therapeutic candidates to restore autophagic flux. Interestingly, lifestyle interventions such as caloric restriction (Marino et al., 2014) and aerobic exercise (He et al., 2012; Lira et al., 2013) — both recognized first-line strategies for NAFLD management — also activate autophagy, further underscoring the tight link between metabolic homeostasis and autophagic regulation.

Collectively, these findings indicate that autophagy serves as a metabolic checkpoint in NAFLD pathogenesis, and that enhancing autophagic or lysosomal function may represent an effective therapeutic strategy to restore hepatic lipid homeostasis and prevent disease progression.

3.3 Tat-Beclin-1 (TB) as autophagy modulator in MASLD

In MASLD, hepatocytes exhibit impaired autophagic flux and lysosomal function, which leads to the accumulation of lipid droplets, damaged mitochondria, and oxidized proteins, thereby promoting lipotoxicity, oxidative stress, and inflammatory signalling (Singh et al., 2009; Gonzalez-Rodriguez et al., 2014). Tat-Beclin-1 peptide, *a selective activator of autophagy,* acts by directly stimulating the Beclin-1–Vps34 complex, which is essential for the initiation of autophagosome formation (Shoji-Kawata et al., 2013). By enhancing this core machinery, Tat-Beclin-1 effectively restores autophagic flux, reactivating lipid degradation and improving mitochondrial turnover.

Mechanistically, TB-1 disrupts the inhibitory interaction between Beclin-1 and its negative regulators—such as Bcl-2, Bcl-xL and Rubicon—thereby promoting the assembly of the Beclin-1/Vps34/Atg14 complex and enhancing autophagosome nucleation (Wang et al., 2017). Through this selective activation of Beclin-1, TB-1 effectively restores autophagic flux in hepatocytes, facilitating lipophagy and mitophagy, two processes frequently impaired in steatotic liver.

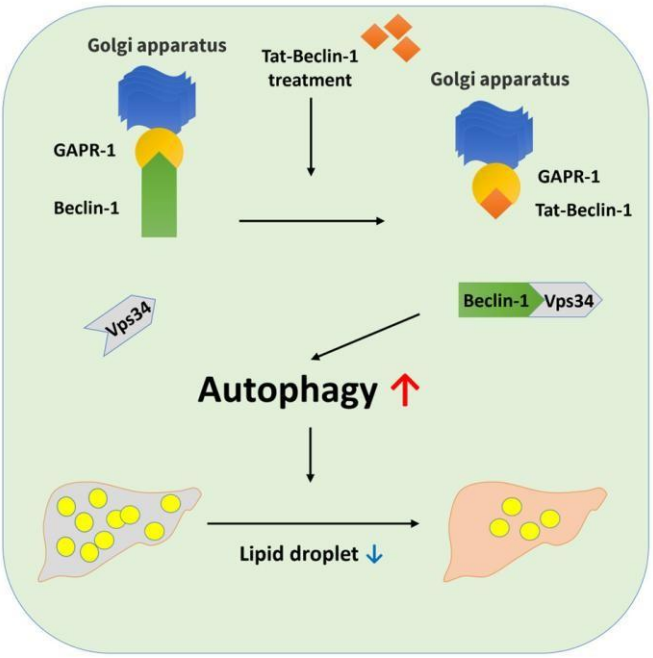

Figure 12. Proposed mechanism of action of TB-1 peptide in promoting autophagy, leading to reduced lipid droplet accumulation. GAPR-1: Golgi-Associated Plant Pathogenesis-Related Protein 1. Red arrow means increase and blue arrow means decrease (Chen et al., 2024).

Experimental evidence supports the hepatoprotective potential of TB-1 in both cellular and animal models of MASLD. In HepG2 cells, TB-1 induced the formation of autophagic vacuoles, up-regulated LC3-II and Beclin-1 expression, and markedly reduced lipid droplet accumulation. In high-fat diet-fed mice, systemic administration of TB-1 ameliorated hepatic steatosis and fibrosis, normalized transaminase levels, and improved systemic glucose and lipid metabolism (Chen et al., 2024). These effects were associated with enhanced β-oxidation, increased AMPK activation, and a concomitant reduction in inflammatory markers such as TNF-α and IL-1β, indicating a dual action on metabolic and inflammatory pathways (Chen et al., 2024).

Importantly, the therapeutic relevance of TB-1 extends beyond NAFLD/MASLD models. A pivotal study by Soria et al. (2018) demonstrated that TB-1 effectively restores autophagic flux in a murine model of ornithine transcarbamylase (OTC) deficiency, a genetic disorder characterized by chronic hyperammonemia, mitochondrial dysfunction, and impaired hepatic metabolism. In this model, TB-1 administration reactivated autophagy improved mitochondrial quality control, reduced ammonia-induced toxicity, and significantly improved liver function and survival (Soria et al., 2018). This study is particularly relevant to counteract the MASLD-linked symptoms in the liver, as hyperammonemia and impaired ammonia detoxification have recently been recognized as contributors to disease progression in advanced NAFLD and

MASH, where they exacerbate mitochondrial dysfunction, oxidative stress, and inflammation (Thomsen et al., 2023). The ability of TB-1 to correct autophagic defects and restore mitochondrial homeostasis in hyperammonemic states provides strong mechanistic support for its use in metabolic liver diseases characterized by autophagic insufficiency. Moreover, unlike non-specific autophagy inducers such as rapamycin or metformin, TB-1 acts independently of the mTOR pathway, thereby avoiding broad systemic interference with protein synthesis and growth signalling (Amaravadi et al., 2016). Its targeted mechanism confers a favourable safety profile, as evidenced by the absence of cardiac side effects in treated animals (Kheloufi et al., 2022).

Chapter IV: Aim of the project

MASLD is a leading cause of chronic disease worldwide, with a steadily increasing prevalence paralleling the rise of obesity, type 2 diabetes, and metabolic syndrome (Caturano et al., 2025). MASLD is a recently approved term to broaden diagnostic criteria and reduce the stigma with the conditions previously known as non-alcoholic fatty liver disease (NAFLD), recognising it as a systemic disease rather than limiting it to peripheral hepatic involvement (Rinella et al., 2023). It is considered a multifactorial disease, characterised by excessive hepatic lipid accumulation in the absence of significant alcohol consumption, with alterations in lipid and cholesterol metabolism, insulin resistance, mitochondrial dysfunction, oxidative stress, and inflammation contributing synergistically to drive disease progression to more severe forms (Miller et al., 2025).

Currently, lifestyle-based therapies and pharmacological treatments for diabetes and obesity have been developed, but these are palliative measures focused on controlling metabolic risk factors rather than directly addressing the molecular mechanisms underlying the systemic disease. Thus, given that MASLD prevalence is on the rise, there is an urgent need to elucidate its pathogenesis to develop specific treatments to improve liver homeostasis, reduce lipid accumulation, and restore mitochondrial and cellular function.

Thyroid hormones, particularly T3, have long been recognised as regulators of multiple physiological processes, including cell growth, homeostasis, carbohydrate, lipid, protein, and mineral metabolism (Yen 2001). The liver is one of the most important targets of thyroid hormones. In this context, exogenous T3 administration has shown encouraging results in lowering hepatic fat content in various experimental models of NAFLD, eliciting insulin-sensitising effects and preventing/reversing steatosis (Lombardi et al., 1968; Veteläinen et al., 2007; Song et al., 2003, Pucci et al., 2000). T3 regulates cholesterol metabolism by stimulating its synthesis, uptake (Lopez et al., 2007) and esterification into bile acids (Ness & Lopez 1995) and modulating both lipogenic (Cunningham et al., 1998) and lipolytic enzymes (Jackson-Hayes et al., 2003). However, chronic exposure to elevated levels of T3 induces adverse systemic effects, leading to thyrotoxicosis, which almost abolishes its use as an antilipidemic agent.

In recent years, T2, a natural derivative of thyroid hormones, has attracted rising interest as a biologically active iodothyronine and is now recognized as a metabolic modulator with specific effects on the liver. Growing evidence has indicated that T2 can improve lipid metabolism and cellular energy homeostasis in experimental models of high-fat diets, promoting increased β-

oxidation of fatty acids, reducing lipogenesis, and attenuating triglyceride accumulation in the liver (de Lange et al., 2011; Lanni et al., 2005). Moreover, T2 decreases systemic and hepatic oxidative stress and inflammation (Senese et al., 2018). Unlike T3, T2 exerts its action independently of nuclear thyroid hormones receptors activation. Specifically, T2 acts as a direct modulator of mitochondrial function, allegedly on respiratory chain complex IV (subunit Va), and stimulates mitochondrial respiration and fatty acid oxidation (Davis et al., 2016; Senese et al., 2018; Zucchi et al., 2019). In high-fat-fed rats, T2 administration decreased serum triglycerides and LDL cholesterol, as well as liver fat accumulation (Lanni et al., 2005; Mollica et al., 2009; de Lange et al., 2011; Moreno et al., 2011), suggesting potential therapeutic value for dyslipidemia or, in a broader context, MASLD.

To maintain a well-functioning mitochondrial network, MQC mechanisms, including biogenesis, dynamics, and mitophagy, are crucial. Mitochondrial dysfunction caused by oxidative stress can trigger inflammation, exacerbating MASLD condition (Einer et al., 2018; Koliaki et al., 2015; Li et al., 2019; Tumova et al., 2016). Regarding the role of iodothyronines in modulating mitochondrial dynamics, T3 enhances mitochondrial biogenesis (Giacco et al., 2024). The ability of both iodothyronines to activate several forms of autophagy (from mitophagy to lipophagy) has also been finely investigated (Sinha et al., 2015). In liver of HFD mice, T3 induces mitophagy via the ROS/AMP-activated protein kinase (AMPK)/unc-51-like autophagy activating kinase 1 (ULK1) pathway, promoting mitochondria renewal and autophagy (Sinha et al., 2015). Moreover, both T3 and T2 have been shown to be able to induce lipophagy in liver (Iannucci et al., 2017). However, studies investigating the role of T2 in regulating mitochondrial quality control and autophagic pathways remain very limited.

Under high-fat diet conditions, autophagic flux is impaired, contributing to lipid accumulation, increased oxidative stress, and disease progression. Understanding how enhancing autophagy through the administration of exogenous molecules can improve cellular function remains an interesting challenge. Beyond the iodothyronines, another excellent candidate as a potent inducer of hepatic autophagy is the Tat-Beclin 1 peptide. Tat-Beclin 1 is synthesised by fusing the HIV Tat protein signalling domain, via glycine linker, to a peptide derived from Beclin-1. Previous studies have demonstrated that Tat-Beclin1 effectively restores autophagic flux in pathological liver conditions, including an experimental model of hyperammonaemia and NAFLD, resulting in improved cellular homeostasis (Soria et al., 2018; Chen et al., 2024). In these models, Tat-Beclin 1 mediated autophagy reactivation; however, until now there have been no studies on the interaction between Tat-beclin and mitochondria, and whether this molecule can also directly influence quality control deserves to be investigated.

Based on these considerations, treatments involving exogenous administration of T2 and TB appear to represent highly innovative experimental approach to restoring liver homeostasis and counteracting the pathogenic mechanisms underlying MASLD by targeting mitochondria, the MQC, and autophagy. Furthermore, we found very interesting to investigate whether these two molecules could influence each other when administered simultaneously.

The overall aim of this project was to determine whether targeting mitochondrial dysfunction and impaired quality control through metabolic and autophagy-based interventions represents a possible effective strategy to counteract MASLD progression.

To address this aim, a 19-week high-fat diet-induced mouse model of MASLD was employed, reproducing the main metabolic and hepatic alterations of the disease. Within this experimental framework, short-term (10-day) treatments with T2, T3, and Tb, administered alone and in combination with T2 were used. The project was structured over three years, according to the following specific aims:

I. Aim 1: To evaluate whether short-term interventions modulate the main metabolic and hepatic alteration induced by long-term high-fat feeding in a mouse model of MASLD. In the first year, the study focused on the set up and validation of the HFD-induced of MASLD model and the evaluation of intervention efficacy. The thyroid axis was analysed by measuring T3, T4, and TSH levels together with the gene expression of key components of hepatic thyroid hormone signalling including transporters, deiodinases, and thyroid receptors. Phenotypic analyses were performed by analysing body weight gain and changes in white adipose tissue, liver mass and heart weight, to assess the effects of diet and treatments on fat accumulation. Hepatic lipid accumulation was evaluated by histological analysis and by quantification of serum and hepatic triglyceride and cholesterol levels and glucose serum levels. Finally, to clarify the molecular mechanisms underlying the observed alterations, the expression of markers involved in lipid and cholesterol metabolism, as well as insulin signalling was analysed.

II. Aim 2: To evaluate whether modulation of oxidative stress and antioxidant defence systems preserves hepatic mtDNA integrity in MASLD. In the second year, the study focused on the characterization of oxidative stress and the antioxidant enzyme system in the liver and on mitochondrial DNA integrity. Hepatic and systemic oxidative stress markers (i.e. H_2O_2, lipid peroxidation marker, 8-OHdG) were evaluated. In parallel, the expression and activity of key hepatic antioxidant

enzymes (MnSOD, GPX4, PRDX3) were analysed. Hepatic mitochondrial DNA was isolated to check its integrity by quantifying the presence of oxidative damage (mtDNA lesion frequency) and its amplification efficiency, alongside the analysis of molecular markers involved in the mitochondrial DNA repair system specifically the base excision repair pathway (BER).

III. Aim 3: To evaluate whether mitochondrial dysfunction-driven inflammatory signalling and impaired mitochondrial quality control contribute to MASLD progression. Based on the presence of mitochondrial DNA damage and its potential release into the cytosol, this phase of the study investigated the activation of inflammatory markers involved in the cGAS-Sting pathway. We also analysed the expression of molecular markers involved in the mitochondrial quality control system, including biogenesis, dynamics and mitophagy, as well as in the various forms autophagy.

Finally, to further explore the hepatic mitochondrial compartment, we examined i) the mitochondrial respiratory chain asset, by analysing expression of mt-complexes; ii) mitochondrial function, by determining the activity of isolated mitochondrial complexes *in vitro* (in-gel activity) and iii) mitochondrial respiratory capacity by high-resolution respiratory techniques.

This PhD project provided an integrated analysis of MASLD pathogenesis, linking high-fat diet-induced metabolic alteration to mitochondrial dysfunction and impaired mitochondrial quality control mechanisms. Overall, the findings support the therapeutic potential of targeting mitochondrial function and autophagy to restore hepatic homeostasis, as will be further discussed in the following chapters.

Chapter V: Materials and methods

5.1 Animals

Male C57BL/6J DIO mice (Mus Musculus, from Jackson Laboratory) were housed in one per cage in a temperature-controlled room at 28-30 °C (thermoneutrality for mice), under a 12:12 h dark/light cycle, with ad libitum accesss to water and food. All animal protocols were approved by the Committee on the Ethics of Animal Experiments of the University of Campania "L. Vanvitelli" (Italy) and the Italian Ministry of Health (permit number: 770/2020-PR of the 31 July 2022; project number: 83700.3 of the 23 June 2020). The minimum sample size was calculated based on a G* Power software (University of Dusseldorf: http://www.gpower.hhu.de/), with the power was of 0.90, the effect size (f) was 1.2249, and a=0.05. Every effort was made to minimize animal pain and suffering.

Mice were divided in 6 groups, (n=5 per group).

The first group, control group (Ctrl), received a standard chow diet ad libitum (percentage of total metabolizable energy: 60.4% carbohydrates, 29% proteins and 10.6% fats J −1; 15.88 kJ gross energy g −1) (Muscedola, Milan, Italy) for the entire duration of the experimental protocol (19 weeks+10 days).

The second group, the HFD group, received a high-fat diet (HFD) ad libitum for 19 weeks to induce MASLD. The HFD consistent of 280 g diet supplemented with 395 g freeze-dried lamb meat (Liomellin, Milan, Italy), 120 g cellulose (Sigma-Aldrich, St. Louis, MO, USA), 20 g mineral blend (ICN Biomedical, Solon, OH, USA), 7 g vitamin blend (ICN) and 200 g low-salt butter (Lurpak, Denmark) (percentage of total metabolizable energy: 21% carbohydrates, 29% proteins and 50% fats J −1; 19.85 kJ gross energy g −1).

After 19 weeks of HFD, mice were further divided into 5 groups and treated for additional 10 days, while continuing the HFD, as follows:

- the Hfd injected with a vehicle solution (PBS) for the last 10 days.
- the Hfd+T2 group received a daily intraperitoneal administration of 3,5-T2 (200 μg/100 g BW) (Jonas et al., 2014) during the last 10 days of HFD.
- the Hfd+T3 group received a daily intraperitoneal administration of T3 (15 μg/100 g BW) (Schneider et al., 2005) during the last 10 days of HFD;
- the Hfd+Tb group received an intraperitoneal administration of TB peptide at the dose of 15 mg/kg every 48 h (Soria et al., 2021) for a total period of 10 days;
- the Hfd+Tb+T2 group received a daily injection of 3,5-T2 (200 μg/100 g BW) and a TB peptide at the dose of 15 mg/kg every 48 h for a total period of 10 days.

During the last 10 days, the Ctrl group received injection of vehicle solution, following the same schedule as the HFD groups.

At the end of the acclimation period (19 weeks + 10 days), mice were anesthetized with pentothal (40 mg/100 g bw) and euthanized. Liver samples were processed immediately for the preparation of liver lisate and other organs were collected, weighed, and frozen in liquid nitrogen and stored at −80°C for further processing. Blood was collected via the inferior cava vein in tubes and centrifuged at 5000 g for 5 min. The serum was immediately frozen.

5.2 Serum hormones

Serum total T4 (TT4), total T3 (TT3), and TSH levels were measured using quantitative MILLIPLEX® assays platform based on Luminex® xMAP®, furnished from Prodotti Gianni (Milan, Italy).

5.3 Hematoxylin and eosin (H&E) staining

At the end of treatment, a small portion of liver tissue was excised and stored in 10% of neutral buffered formalin. The tissue samples were then dehydrated by graded ethanol sequentially and embedded in paraffin wax. Paraffin-embedded tissues were sectioned serially about 2 μm size and were stained with hematoxylin and eosin (H&E) dyes. Stained tissue sections were documented using a camera-equipped microscope (Nikon). Images were captured at 20× magnification (scale bars = 20 μm) and ×40 (scale bars = 10 μm) for the insets.

5.4 Determination of triglyceride and cholesterol levels in serum and tissue and glucose levels in serum

Quantitative determination of tissue and serum concentration of triglyceride was performed using Triglyceride (TG) Colorimetric Assay kit from Elabscience (Houston, Texas, USA). Furthermore, the quantitative determination of serum concentration of cholesterol was determined using Total Cholesterol (TC) Colorimetric Assay kit from Elabscience.

Quantitative determination of glucose levels in serum was performed using the Glucose Enzymatic Colorimetric Assay kit from Giesse Diagnostics (Rome, Italy).

5.5 Determination of H2O2, 8-OHdG and MDA in liver samples

Liver endogenous H2O2 levels were measured by using the hydrogen peroxide colorimetric assay kit (Abcam, Cambridge, UK), according to the manufacturer's instructions. Values were normalised on total protein amount, quantified by Bradford methods.

Liver lipid peroxidation products [thiobarbituric acid reactive substances (TBARS) also known as malondialdehyde-equivalents (MDA-equivalents)] were measured by Lipid peroxidation kit from Sigma. Briefly, liver samples were homogenized on ice in MDA lysis buffer, containing BHT, incubated for 5 minutes at RT and then centrifuge at 13000g for 3 minutes. To form MDA-TBA adduct, solution containing TBA was added to sample and incubated at 95° for 60 minutes, and cooled on ice for 10 minutes. Samples were pipetted onto 96-well plate and absorbance measured at 532 nm. Data were analysed through a calibration curve, obtained by plotting standards of MDA solutions at concentration of 2, 4, 6, 8 and 10 mM and respective absorbances.

8-Hydroxy-2′-deoxyguanosine (8-OHdG) levels were measured using a competitive ELISA kit (Cayman Chemical Company,Ann Arbor, MI, USA).

Standards were prepared by serial dilution in ELISA buffer. Serum samples were diluted in ELISA buffer (1:25 and 1:50) prior to analysis. Samples and standards (50 µL) were incubated with AChE-labeled tracer and monoclonal antibody in a 96-well plate and incubated at 4 °C for 18 h. After washing, Ellman's reagent was added, and the plate was incubated under shaking conditions. Absorbance was measured at 405 nm after 90–120 min. 8-OHdG concentrations were calculated from the standard curve.

5.6 Determination of MnSOD2 activity in liver samples

Mitochondria were isolated from liver tissue by homogenization in a buffer containing 20 mM HEPES, 1 mM EGTA, 70 mM sucrose and 210 mM mannitol (pH 7.2), followed by differential centrifugation (500 g for 10 min and 10,000 g for 15 min at 4 °C). The mitochondrial pellet was resuspended in 100 µL of buffer. Protein concentration of both the homogenate and mitochondrial fraction was determined by protein assay. Superoxide dismutase (SOD) activity was measured using a commercial enzymatic kit from Cayman (Cayman Chemical Company, Ann Arbor, MI, USA)

based on the xanthine/xanthine oxidase system, with appropriate preparation of standards and diluted samples. Samples (10 µL) were incubated with Radical Detector (200 µL) and the reaction was initiated by adding Xanthine Oxidase (20 µL). After incubation at room temperature for 3 minutes, absorbance was measured at 450 nm.

5.7 Reverse Transcription (RT) quantitative (q) PCR

RNA was isolated from liver using the TRIZOL standard protocol (Invitrogen, California, USA).1 μg of RNA was used to generate cDNA strands according to the Quanti Tect Reverse Transcription Kit instructions (Qiagen, Hilden, Germany). The qRT-PCR was carried out in appropriate volume of 20 μL containing cDNA samples (2 μL), 50 nM gene-specific primers and SYBR Green supermix (Applied Biosystems, Foster City, California, USA). Gene expression levels were measured using standarta cycle parameters on a QuantStudio 5 System (Thermo Fisher Scientific, Waltham, Massachusette, USA). The transcript abundance was calculated by the 2-ΔΔCT method and normalized to the expression of the housekeeping gene β-actin. PCR primers were designed using the Primer 3 program (0.4.0) and synthesized by Eurofins Genomics (Table 1).

Table 1. List of primers for RTqPCR analysis.

Gene	**Primer Sequence (5'-3')**	
	Forward	**Reverse**
Cd36	ATGGGCTGTGATCGGAACTG	AGCCAGGACTGCACCAATAAC
Dio1	CCACCTTCTTCAGCATCC	AGTCATCTACGAGTCTCTTG
Dio3	CCGACCTGATGGCTTCCA	CGCGCCATGAACGGTGGTCA
Mct8	AGAATAAGTGTGCAGGGCCT	TGGAGAGAAGTGAGTGGCAG
Pgc1α	GTCAACAGCAAA AGCCACAA	GTGTGAGGAGGGTCATCGTT
Scd1	AGGTGCCTCTTAGCCACTGA	CCAGGAGTTTCTTGGGTTGA
Spot14	ATGCAAGTGCTAACGAAACGC	CCTGCCATTCCTCCCTTGG
Tfam	CCACATGCTTTCT GGGTTT	TGCTGTGGTTTCCCAGTGTA
Thr α	GCCATTGGAAACAGAGGCGA	ATCTGGTCTTCGCAAGGCA
Thr β	AAAGTCACCCGC AACCAGT	ATTTCTGTAGCTCTTCCCGCC
β-actin	GATCATTGCTCCT CTGAGC	ACATCTGCTGGAAGGTGGAC

5.8 Liver protein extraction and western blotting

Liver Proteins extraction and quantification were performed as already reported (Giacco, A. et al., 2024). The list of the used primary antibodies is reported in Supplementary 2. Protein levels were normalized to β-actin or GAPDH. Proteins were detected by a chemiluminescence

protein-detection method based on the protocol supplied with a commercially available kit (Millipore) and by using the appropriate secondary antibodies. Signals were quantified by means of a Bio-Rad ChemiDoc™ XRS, using dedicated software (QuantityOne, Bio-Rad Laboratories) (Table 2).

Table 2. List of use antibodies for Western lot analysis.

Antibody	Cat. Number	Dilution
β-ACTIN (42 kDa)	Abcam Ab8226	1:1000 in 1XTBST with 5% BSA
ADRP (48 kDa)	Abcam Ab52356	1:1000 in 1XTBST with 5% non fat dry milk
AKT (60 kDa)	Cell Signaling #4691	1:1000 in 1XTBST with 5% BSA
AMPK (62 kDa)	Cell Signaling #2532	1:1000 in 1XTBST with 5% BSA
APE1 (37 kDa)	Novus Biologicals N.B. 100-116	1:1000 in 1XTBST with 2% non fat dry milk
ATG 9 (95 kDa)	Novus Biologicals N.B. 110-56893SS	1:500 in 1XTBST with 5% BSA
cGAS (59 kDa)	HUABIO HA 500023	1:500 in 1XTBST with 5% BSA
CPT1 (88 kDa)	Abcam Ab235841	1:1000 in 1XTBST with 5% non fat dry milk
CYP7A (60 kDa)	Invitrogen PA5-100892	1:1000 in 1XTBST with 5% non fat dry milk
DRP1 (85 kDa)	Abcam Ab56788	1:1000 in 1XTBST with 5% BSA
FAS (273 kDa)	Cell Signaling C.S. 3189	1:1000 in 1XTBST with 5% BSA
GPX4 (22 kDa)	Abcam Ab 125066	1:5000 in 1XTBST with 5% non fat dry milk
GSK3β (40-50 kDa)	Cell Signaling 9315	1:1000 in 1XTBST with 5% BSA

HMGCR (97 kDa)	Gene Tex GTX54088	1:1000 in 1XTBST with 5% non fat dry milk
HMGCS (57 kDa)	Cell Signaling C.S. 42201	1:3000 in 1XTBST with 5% non fat dry milk
IKB α (39 kDa)	Cell Signaling C.S. 4814	1:1000 in 1XTBST with 5% BSA
IL-10 (20-15 kDa)	Abcam 310329	1:500 in 1XTBST with 5% non fat dry milk
IRS1 (160 kDa)	Millipore 06-248	1:1000 in 1XTBST with 5% BSA
LC3B (14-16 kDa)	Abcam Ab 192890	1:1000 in 1XTBST with 5% non fat dry milk
MNF2 (86 kDa)	Abcam Ab 56889	1:1000 in 1XTBST with 5% non fat dry milk
MnSOD2 (26-27 kDa)	Abcam Ab 13533	1:5000 in 1XTBST 5% non fat dry milk
mTOR (289 kDa)	Cell Signaling C.S. 2983	1:1000 in 1XTBST with 5% BSA
NRF2 (97-100 kDa)	Elabscience E-AB 93081	1:1000 in 1XTBST with 5% non fat dry milk
OGG1 (39 kDa)	Cell Signaling C.S. 2983	1:1000 in 1XTBST with 2% non fat dry milk
OMA (60-58 kDa)	Elabscience E-AB 93081	1:1000 in 1XTBST with 5% BSA
OPA1 (100 kDa)	Abcam Ab 157457	1:1000 in 1XTBST 5% non fat dry milk
P62 (62 kDa)	Cell Signaling C.S. 5114	1:1000 in 1XTBST 5% BSA
PARKIN (50 kDa)	Cell Signaling C.S. 4211	1:1000 IN 1XTBST 5% BSA
PGC1α (110 kDa)	Abcam Ab 3242	1:1000 in 1XTBST 5% BSA
Phospho-AKT (60 kDa)	Cell Signaling C.S. 9271	1:1000 in 1XTBST 5% BSA
Phospho-AMPK (62 kDa)	Cell Signaling C.S. 2535	1:1000 in 1XTBST 5% BSA
Phospho-GSK3 (46-51 kDa)	Cell Signaling C.S. 9331	1:1000 in 1XTBST 5% BSA
Phospho-IKBα (40 kDa)	Cell Signaling C.S. 2859	1:500 in 1XTBST 5% BSA
Phospho-mTOR (Ser2448) (289 kDa)	Cell Signaling C.S. 5536	1:1000 in 1XTBST 5% BSA

Phospho-TBK1 (Ser 172) (84 kDa)	Cell Signaling C.S. 5483	1:300 in 1XTBST 5% BSA
Phospho-ULK1 (757) (140-150 kDa)	Cell Signaling C.S. 14202	1:500 in 1XTBST 5% BSA
PINK1 (62 kDa)	Abcam Ab 186303	1:1000 in 1XTBST 5% BSA
PNPLA3 (58 kDa)	Cell Signaling C.S. 95546	1:1000 in 1XTBST 5% BSA
POLγ (140 kDa)	Novus Biological NBPI 52300	1:1000 in 1XTBST 5% BSA
PRDX3 (28-24 kDa)	Abcam Ab 73349	1:1000 in 1XTBST 5% non fat dry milk
SOCS3 (24-25 kDa)	Abcam Ab 28481	1:1000 in 1XTBST 5% non fat dry milk
STING (PS338) (42-30 kDa)	Abcam Ab 227704	1:500 in 1XTBST 5% BSA
TBK1 (84 kDa)	Cell Signaling C.S. 3504	1:1000 in 1XTBST 5% BSA
TFAM (28 kDa)	Abcam Ab 131607	1:2000 in 1XTBST 5% non fat dry milk
TFE3 (62 kDa)	Abcam Ab 93808	1:2000 in 1XTBST 5% non fat dry milk
TFEB (53 kDa)	Abcam Ab 264421	1:500 in 1XTBST 5% non fat dry milk
TOM20 (20 kDa)	Cell Signaling C.S. 42406	1:1000 in 1XTBST 5% non fat dry milk
ULK1 (140-150 kDa)	Cell Signaling C.S. 8054	1:1000 in 1XTBST 5% BSA

5.9 Genomic DNA isolation and quantitative polymerase chain reaction

Total DNA was extracted from liver samples from 20 mg of frozen tissues (Genomic DNA Buffer Set and Genomic-tip 20/G, Qiagen, Venlo, The Netherlands) according to the manufacturer's instructions. Quality and quantity of extracted DNA was determined spectrophotometrically at 260 and 280 nm using NanoDrop One C (Thermo Fisher scientific, USA). QPCR was performed on 15 ng of liver DNA extracts as reported by Santos, with

minor modifications already described by us. Primers sequences: mtDNA long fragment (13.4 Kbp) 5'- AAAATCCCCGCAAACAATGACCACCC-3' (sense)/5'-GGCA ATTAAGAGTGGGATGGAGCCAA-3' (anti-sense); mtDNA short fragment (235 bp) 5'-CCTCCCATTCATTATCGCCGCCCTGC-3' (sense)/5'-GTCTGGGTCTCCTAGTAGGTCTGGGAA-3' (antisense). QPCR amplificates were measured using PicoGreen dye (Invitrogen, Milan, Italy) through fluorescence plate reader (Tecan, infinite pro-200, Austria). DNA damage was quantified by comparing the relative efficiency of amplification of the long mtDNA fragment normalized to the amplification of the small mtDNA fragment. Specifically, relative lesion frequencies per 10 Kbp DNA was calculated by applying the Poisson distribution according to the formula:

$$\text{Lesion frequency} = -\ln Ad{=}Ao,$$

where Ad means amplification of treated samples, and Ao represents amplification of controls.

5.10 Determination of the relative DNA mitochondrial copy number

Genomic DNA was extracted and purified from approximately 20 mg of frozen liver using QIAGEN Genomic-tip 20/G and Genomic DNA Buffer Set (Qiagen, Venlo, The Netherlands) according to the manufacturer's instructions. Purity and quantity of extracted DNA was determined spectrophotometrically at 260 and 280 nm using NanoDrop One C (ThermoFisher scientific, USA).

The mitochondrial DNA (mtDNA) content was measured by real-time PCR using a QuantStudio 5 System (Thermo Fisher Scientific, Waltham, Massachusetts, USA). The amplification of mitochondrial cytochrome c oxidase subunit II (COII, mitochondrial-encoded gene), cytochrome b (Cytb, mitochondrial-encoded gene) and β-actin (nuclear-encoded gene) were examined. The primer sequences used were as follows: COII: 5'-TGAGCCATCCCTTCACTAGG-3'(sense)/5'-TGAGCCGCAAATTTCAGAG-3'(anti-sense); Cytb:5'-TACCTGCCCCATCCAACATT-3'(sense)/5'-TAAGCCTCGTCCGACATGAA-3'(anti-sense); β-actin:5'CTGCTCTTTCCCAGATGAGG-3'(sense)/5'-CCACAGCACTGTAGGGGTTT-3'(anti-sense).

Reactions were carried out in the presence of 1x iTaq Universal SYBR Green Supermix (BioRAD), 0.5 μM of each forward and reverse primer, and 50 ng genomic DNA. The threshold cycle number (Ct) was calculated using Design and Analysis software v1 5.1 (Applied Biosystems, Thermo Fisher Scientific, US) and an automated setting of the baseline. The

relative mtDNA copy number (Rc) was determined as described in (Rooney et al, 2015), using the equations: Rc = 2 x (2^ΔCt), ΔCt = average Ct nuclear DNA − average Ct mtDNA.

5.11 Separation of respiratory complexes by Blue-Native Page (BN-PAGE) and histochemical staining for in-gel activity.

Liver fragments were immersed in ice-cold isolation buffer, consisting of 220 mM mannitol, 70 mM sucrose, 20 mM Tris-HCl, 1 mM EDTA, 5 mM EGTA, pH 7.4, and subsequently homogenized in a Potter-Elvehjem homogenizer. The homogenate was centrifuged at 500 x g for 10 min at 4°C, the resulting supernatant was centrifuged at 3000 x g for 10 min at 4°C to obtain a mitochondrial pellet. Solubilization of mitochondrial membranes by detergents, BN-PAGE, staining, and densitometric quantification of oxidative phosphorylation complexes was performed essentially as described by Scagger et al. 1995, and Lombardi et al. 2009, with minor modifications. Briefly, the mitochondria-containing sediment was suspended in a low-salt buffer (50 mM NaCl, 50 mM imidazole, pH 7.0) and solubilized with 10% (w/v) dodecyl-maltoside (for solubilization of individual respiratory chain complexes). Immediately after the electrophoretic run (carried out on 6–13% gradient polyacrylamide gels), enzymatic colorimetric reactions were performed essentially as reported by others (Zerbetto et al, 1997). Complex I activity was determined by incubating the gel slices with 2 mM Tris–HCl, pH 7.4, 0.1 mg/ml NADH, and 2.5 mg/ml nitro blue tetrazolium (NTB) at room temperature. Complex II activity was evaluated after incubating the gel slices at room temperature in a 100 mM Tris/glycine buffer at pH 7.4 containing 1 mg/mL NTB and 1 mM sodium succinate. Complex IV activity was estimated by incubating BN-PAGE gels with 5 mg 3, 3′-diaminobenzidine tetrahydrochloride (DAB) dissolved in 9 mL phosphate buffer (0.05 M, pH 7.4), 1 mL catalase (20 μg/mL), 10 mg cytochrome c, and 750 mg sucrose. The original color of the complex I, II, or IV-reacting bands was preserved by fixing the gels in 50% methanol and 10% acetic acid. In parallel, another electrophoretic run was performed to stain the gels with Coomassie Blue G and obtain the total band pattern of respiratory complexes. For densitometric analysis, electronic images of the gels were acquired by means of a GS-800 calibrated densitometer (Bio-Rad), and analyzed using QuantityOne software (Bio-Rad). Scanned gel-images were processed for the removal of background and automatic detection of bands. The areas of the bands were expressed as absolute values (arbitrary units).

5.12 Determination of mitochondrial respiration in liver

Liver fragments were weighted and immersed in ice-cold isolation buffer, consisting 220 mM mannitol, 70 mM sucrose, 20 mM Tris-HCl, 1 mM EDTA, 5 mM EGTA, and 0.1 % fatty acid-free BSA pH 7.4, and subsequently homogenized with a Potter-Elvehjem homogenizer (four strokes in 1 min). To evaluate mitochondrial function on liver homogenates a Substrate, Uncoupler, Inhibitor Titration (SUIT) protocol was used by using O2k (Oroboros Instruments, Innsbruck, Austria). Measurements were carried out at 37◦C.

Briefly, leak respiration involving complex I-linked electron flow was measured by adding malate (0.5 mM), pyruvate (5 mM), and glutamate (10 mM). Phosphorylating respiration with complex I-linked substrates was obtained after the addition of ADP (2.5 mM). The addition of succinate (10 mM) then revealed phosphorylating respiration with electron input from complexes I and II. The maximum capacity of the electron transport chain was obtained by sequentially adding oligomycin (2.5 μM) to inhibit ATP synthase, followed by the uncoupler carbonyl cyanide p-trifluoromethoxyphenylhydrazone (FCCP, 0.5 μM).

Finally, the addition of rotenone (0.5 μM) inhibited complex I, allowing calculation of the maximal capacity supported by complex II alone. Correction for non-mitochondrial respiration was performed by subtracting residual oxygen consumption obtained after the addition of the inhibitor antimycin A (2.5 μM). Mitochondrial integrity was tested by adding exogenous cytochrome c (10 mM).

All respiratory parameters were normalised to the liver homogenate protein content used in each individual measurement. Results are expressed as oxygen consumption in pmol O_2/sec × mg liver protein.

5.13 Statistical analyses

For comparisons between two groups, statistical significance was calculated using non-paired two-tailed student's t-test. For multiple comparisons one-way ANOVA (post hoc test: Student-Newman-Keuls) was performed. Graphs and calculation of statistical significance were performed using Graph Pad Prism 5 software (GraphPad). Bars are represented as the standard error of the mean (SEM). For all analyses, p value ≤ 0.05 was considered the minimum statistically significant.

Chapter VI: Results

6.1 Characterization of MASLD phenotype

At the end of the experimental period, body weight (BW), BW gain, white adipose tissue (WAT) weight, WAT weight/BW ratio, liver weight, liver weight/BW ratio, heart weight (HW) and HW/BW ratio were evaluated (**Table 3**).

Hfd mice gained significantly more weight than Ctrl mice, developing obesity. They also showed a significant increase in WAT weight/BW and liver weight/BW ratios, without showing an increase in heart weight. Compared to Hfd group, Hfd+T2, Hfd+T3, Hfd+Tb and Hfd+Tb+T2 mice exhibited a significant reduction in BW gain and WAT weight/BW ratio, with T3 showing the strongest effect among the treatments. Furthermore, only T3 treatment significantly decreased BW and increased HW and HW/BW ratio, compared to Hfd mice. Conversely, only T2 and Tb influenced the liver weight, by decreasing the liver weight/BW ratio compared to Hfd.

Table 3. Body composition parameters: body weight, adiposity, liver weight and heart weight.

	Ctrl	Hfd	Hfd+T2	Hfd+T3	Hfd+Tb	Hfd+Tb+T2
Body weight (BW) (gr)	30,7±0,65	46,03±1,22***	43,8±0,58	41,5±0,73$^{\#}$	42,16±0,44	42,82±0,94
Body weight (BW) gain (gr)	0,6±0,14	1,98±0,2**	-0,4±0,04$^{\#}$	-1,6±1 $^{\#\#,+}$	-0,2±0,2 $^{\#,\circ}$	0,27±0,28 $^{\#,\circ}$
White adipose tissue (WAT) weight (gr)	0,18±0,03	0,94±0,13***	0,60±0,08$^{\#\#}$	0,49±0,07 $^{\#\#\#}$	0,71±0,06 $^{\#}$	0,71±0,08 $^{\#}$
WAT weight/BW	0,006±0,001	0,020±0,003**	0,014±0,002$^{\#\#}$	0,01±0,001$^{\#\#,+}$	0,02±0,001$^{\#\#,\circ}$	0,016±0,002$^{\#\#,\circ}$
Liver weight (LW) (gr)	1,26±0,06	2,3±0,09***	1,69±0,03	2,003±0,11	1,72±0,152	1,97±0,07
LW/BW	0,04±0,002	0,05±0,002***	0,04±0,001$^{\#\#\#}$	0,05±0,003 $^{++}$	0,04±0,004$^{\#\#,\circ\circ}$	0,05±0,02^{++}
Heart weight (HW) (gr)	0,16±15,0	0,19±13,9	0,19±10,2	0,27±17,2$^{\#\#,++}$	0,17±6,5$^{\circ\circ}$	0,23±20,6°
HW/BW	5,31±0,38	4,2±0,36	6,50±0,42	5,84±0,81$^{*,\#}$	4,26±0,19	5,33±0,52

Values are presented as the means ± SEM from 3/5 mice in each. One-way ANOVA, Student-Newman-Keuls post-hoc test, *p<0.05 vs. Ctrl; **p< 0.01 vs. Ctrl; ***p<0.001 vs. Ctrl; #p<0.05 vs. Hfd; ##p<0.01 vs. Hfd; ###p< 0.001 vs. Hfd; +p<0.05 vs. Hfd+T2; ++p<0.01 vs. Hfd+T2; °p<0.05 vs. Hfd+T3; °°p<0.01 vs. Hfd+T3.

The accumulation of lipids in the liver was evaluated using Hematoxylin-eosin staining (**Figura 13**). Liver sections revealed a significant increase in lipid accumulation in Hfd mice, characterized by more numerous lipid droplets compared to Ctrl (**Table 4**). The number of lipid droplets (N/μm^2) were significantly reduced in all treatments compared to HFD mice.

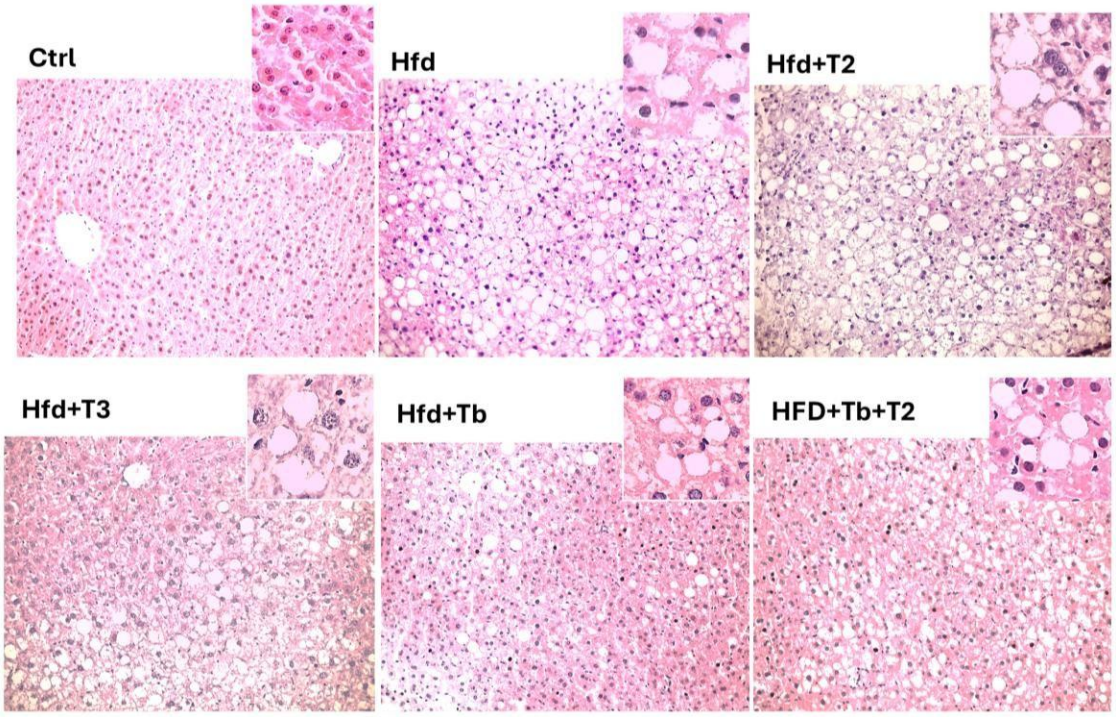

Figure 13. Hematoxylin–eosin staining of paraffin-embedded mouse liver sections from Ctrl, Hfd, Hfd+T2, Hfd+T3, Hfd+Tb and Hfd+Tb+T2 treated groups. Images were captured at 20× magnification (scale bars = 20 µm) and ×40 (scale bars = 10 µm) for the insets.

Table 4. Number per area of lipid droplets in experimental and control (Ctrl) groups.

	Number /μm^2
Ctrl	410,21±53,06
Hfd	3877,14±326,48***
Hfd+T2	2516,02±412,19#
Hfd+T3	2267,71±104,06##
Hfd+Tb	1173,41±51,02##
Hfd+Tb+T2	1246,31±267,14##

Values are presented as the means ± SEM; up to four regions of interest quantified per mouse (n = 3/group). One-way ANOVA, Student-Newman-Keuls post-hoc test, *** $p<0.001$ vs. Ctrl; #$p \leq 0.05$ vs. Hfd; ##$p \leq 0.01$, vs. Hfd.

In parallel with the histological analysis of lipid droplets, hepatic triglycerides (TG) content was assessed. As shown in Table 5, Hfd mice exhibited a marked increase in hepatic TG levels compared to the control animals, confirming pronounced lipid accumulation. Both T2 and T3 significantly reduced liver TG levels compared to the Hfd group.

Circulating TG and total cholesterol (TC) levels were also assessed. Hfd mice showed a marked increase in TG and TC levels compared to the control group. T2 significantly reduced circulating TG and TC levels and, in combination with Tb also reduced TG levels. No significant changes were observed in the other experimental groups.

Table 5. Hepatic and serum triglyceride and serum cholesterol.

	Ctrl	Hfd	Hfd+T2	Hfd+T3	Hfd+Tb	Hfd+Tb+T2
Triglyceride (TG) (mmol/gprot liver)	0,172±0,04	0,710±0,122**	0,304±0,09$^{\#\#}$	0,324±0,54$^{\#}$	0,753±0,19$^{+,\circ}$	0,765±0,17$^{+,\circ}$
Serum TG (mmol/L)	2,507±0,24	3,87±0,21*	2,755±0,001$^{\#}$	3,637±0,80	2,294±0,49	2,554±0,17$^{\#}$
Serum Total Cholesterol (TC) (mmol/L)	1,669±0,64	5,538±1,50*	2,253±0,84$^{\#}$	3,288±1,60	5,465±1,18	3,955±0,68

Values are presented as the means ± SEM from 3/5 mice in each. One-way ANOVA, Student-Newman-Keuls post-hoc test, **p< 0.01 vs. Ctrl; #p<0.05 vs. Hfd; +p<0.05 vs. Hfd+T2; °p<0.05 vs. Hfd+T3. For TG (nmol/L) Student's t-test was performed, *p<0.05 vs. Ctrl; #p<0.05 vs. Hfd.

6.2 Hepatic cholesterol and lipid metabolism

To investigate the molecular mechanisms underlying the alterations of cholesterol levels observed in Hfd, the protein expression of key hepatic enzymes involved in cholesterol synthesis and catabolism, such as HMGCS1, HMGCR and CYP7A, was evaluated (**Figure 14**).

Compared to Ctrl, Hfd mice showed a significant increase of HMGCR expression.

T2 treatment induced a reduction in both HMGCR and HMGCS1 compared to Hfd, paralleled by a strong upregulation of CYP7A, both alone and in combination with Tb, compared to the other experimental groups.

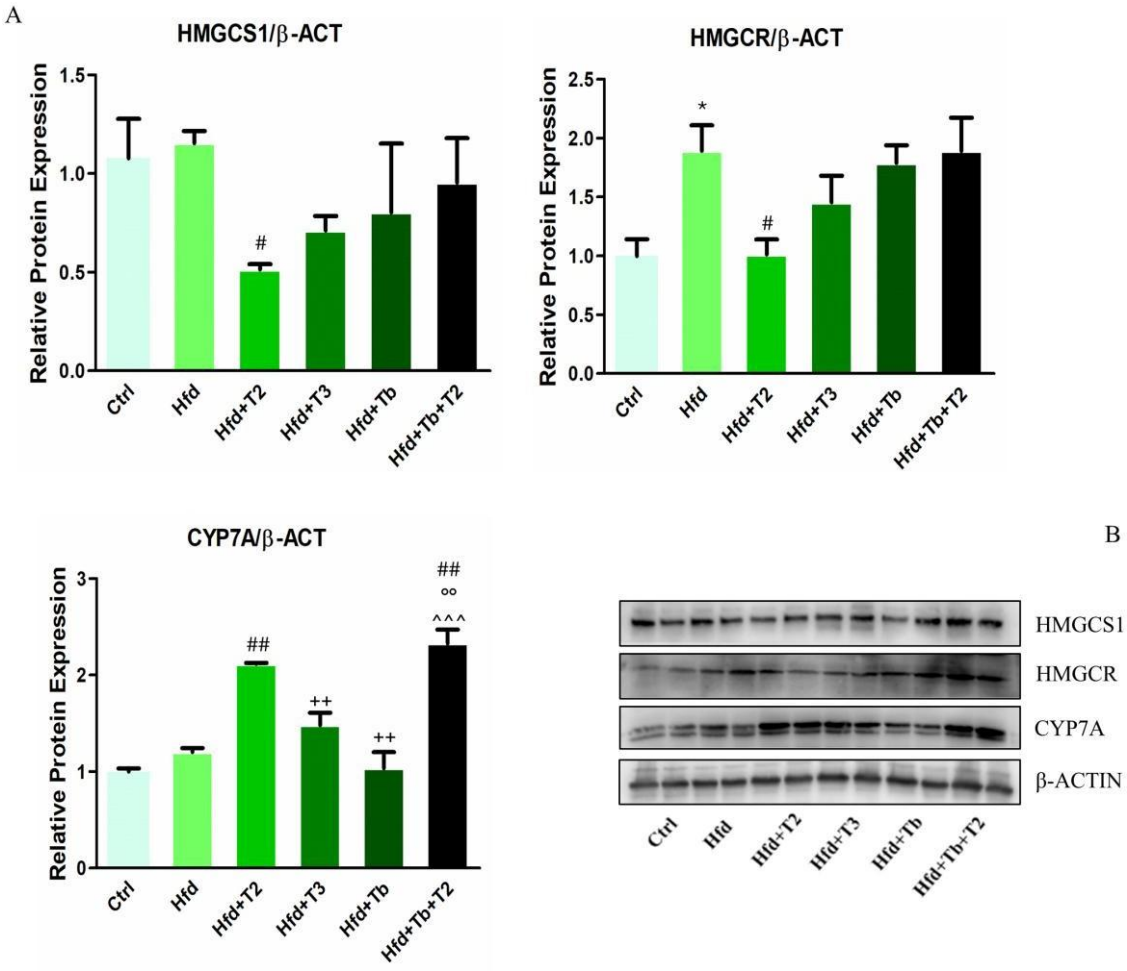

Figure 14. Cholesterol metabolism: synthesis and catabolism in liver of Ctrl, Hfd, Hfd+T2, Hfd+T3, Hfd+Tb, Hfd+Tb+T2. (A) Quantitative analysis and (B) representative Western blot of HMGCS1, HMGCR and CYP7A normalized based on β-actin. Values are presented as the means ± SEM from 3/5 mice in each group. One-way ANOVA, Student-Newman-Keuls post-hoc test, *p< 0.05 vs. Ctrl; #p<0.05 vs. Hfd; ##p<0.01 vs. Hfd; ++p<0.01 vs. Hfd+T2; °°p<0.01 vs. Hfd+T3; ^^^p<0.001 vs. Hfd+Tb. For HMGCR and HMGCS1. Student's t-test was performed, *p<0.05 vs. Ctrl; #p<0.05 vs. Hfd.

Next, gene and proteins expression of enzymes involved in lipid uptake, oxidation and synthesis was evaluated (**Figure 15**).

The expression data revealed that Hfd mice showed a marked increase in cd36 expression, accompanied by significant upregulation of CPT1 protein levels compared to Ctrl, suggesting increased lipid entry into the cell and transport to mitochondria for oxidation. In addition, compared to the control group, these mice also exhibited a significant increase in spot14 and scd1 expression, both involved in DNL, together with a reduction in the P-AMPK/AMPK ratio. Hfd+T2 and Hfd+T3 mice showed decreased cd36 expression compared to the Hfd group, while CPT1 protein levels were significantly increased. These groups showed a significant

reduction in scd1 mRNA and FASN protein expression. Both iodothyronines also increased the P-AMPK/AMPK ratio compared to Hfd. Notably, T2 significantly reduced spot14, while T3 upregulated it, consistent with its role as a T3-responsive gene. In the Hfd+Tb group, cd36 gene expression and FASN protein expression were reduced, while CPT1 protein levels were increased compared to the Hfd group.

Finally, Hfd+Tb+T2 showed reduced cd36 and FASN expression compared to Hfd. Interestingly, the combination of Tb and T2 significantly reduced CPT1 protein expression.

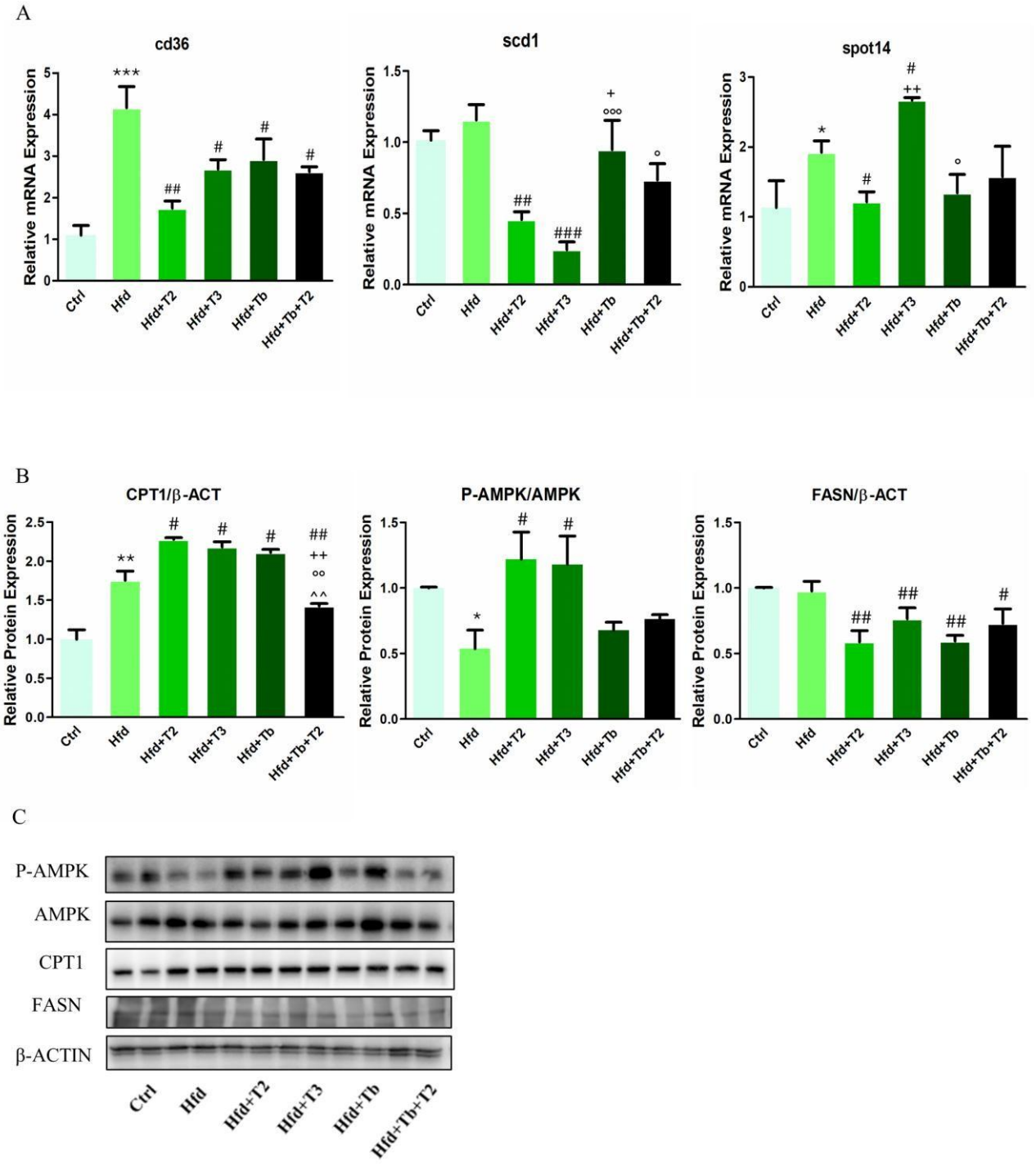

Figura 15. Lipid metabolism (uptake, oxidation and synthesis) in liver of Ctrl, Hfd, Hfd+T2, Hfd+T3, Hfd+Tb, Hfd+Tb+T2. (A) Quantification of mRNA expression of cd36, scd1 and spot14 measured by qRT-PCR. (B) Quantitative analysis and (C) representative Western blot of CPT1, P-AMPK/AMPK and FASN, normalized based on β-actin. Values are presented as the means ±SEM from 3/5 mice in each group. One-way ANOVA, Student-Newman-Keuls post-hoc test, *p<0.05 vs. Ctrl; **p<0.01 vs. Ctrl; ***p<0.001 vs. Ctrl; #p<0.05 vs. Hfd; ##p<0.01 vs. Hfd; ###p<0.001 vs. Hfd; +p<0.05 vs. Hfd+T2; ++p<0.01 vs. Hfd+T2; °p<0.05 vs. Hfd+T3; °°p<0.01 vs. Hfd+T3; °°°p<0.001 vs. Hfd+T3; ^^p<0.01 vs. Hfd+Tb. For scd1 and spot14 Student's t-test was performed, *p<0.05 vs. Ctrl; #p<0.05 vs. Hfd; ++p<0.01 vs. Hfd+T2; °p<0.05 vs. Hfd+T3.

6.3 Hepatic insulin signalling

The insulin signalling was evaluated by analysing IRS1 (insulin receptor substrate-1), P-AKT/AKT (reflecting activation of the AKT signalling cascade) and P-GSK3β/GSK3β (normally inhibited by insulin) protein levels. (**Figure 16**).

Compared to the Ctrl, Hfd mice showed a significant reduction of IRS1 protein expression, upregulation of P-GSK3β/GSK3β ratio and a trend towards reduced P-AKT/AKT ratio, indicative of hepatic insulin resistance.

Hfd+T2 group exhibited an enhanced IRS1 expression and P-AKT/AKT ratio together with a marked reduction of P-GSK3β/GSK3β ratio compared to the Hfd group.

Similar to Hfd+T2, the Hfd+T3 group showed a significant reduction of P-GSK3β/GSK3β ratio in parallel with an increase of PAKT/AKT ratio compared to the Hfd group.

Both Hfd+Tb and Hfd+Tb+T2 displayed a weak effect on insulin signalling, by reducing only the P-GSK3β/GSK3β level.

A quantitative evaluation of fasting serum glucose level was also performed. Compared to the Ctrl group, Hfd showed higher circulating glucose level. The Hfd+T2 group displayed a reduction in glycemia compared to the Hfd, as well as Tb+T2 group.

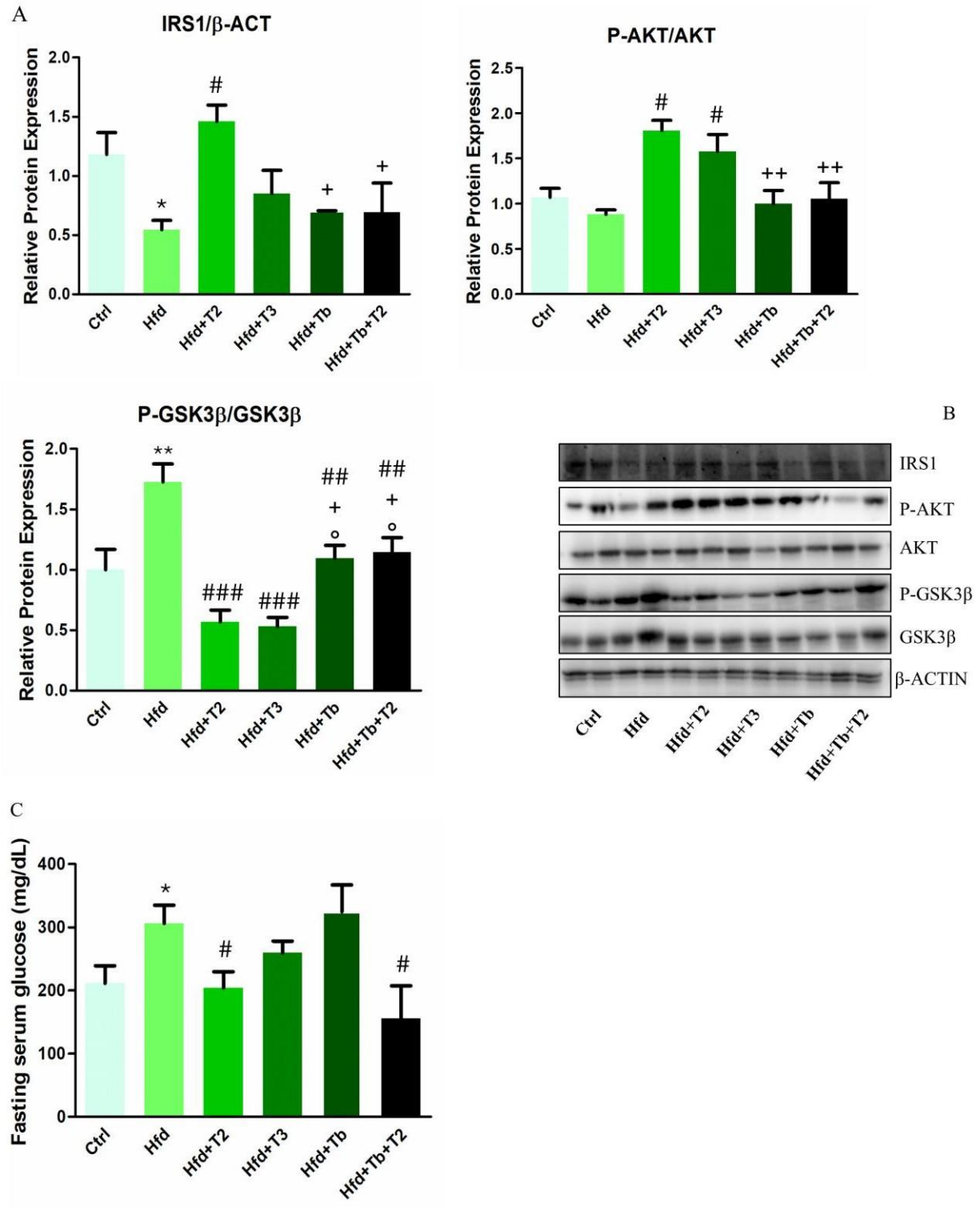

Figura 16. Insulin signalling pathway in liver of Ctrl, Hfd, Hfd+T2, Hfd+T3, Hfd+Tb, Hfd+Tb+T2. (A) Quantitative analysis and (B) representative Western blot of IRS1, P-AKT/AKT and P-GSK3β/GSK3β, normalized based on β-actin. (C) Fasting serum glucose levels. Values are presented as the means ± SEM from 3/5 mice in each group. One-way ANOVA, Student-Newman-Keuls post-hoc test, *p<0.05 vs. Ctrl; **p<0.01 vs. Ctrl; #p<0.05 vs. Hfd; ##p<0.01 vs. Hfd; ###p<0.001 vs. Hfd; +p<0.05 vs. Hfd+T2; ++p<0.01 vs. Hfd+T2; °p<0.05 vs. Hfd+T3.

6.4 Thyroid hormones homeostasis and hepatic thyroid hormones signalling

To evaluate the effects of a high-fat diet and the efficacy of iodothyronines treatments on thyroid function, total serum levels of T3 (TT3), T4 (TT4), and TSH were measured (**Table 6**).
Compared to the Ctrl mice, Hfd mice showed significantly reduced TT3 and TT4 levels, along with a significant increase in TSH levels, indicating a functional hypothyroid state induced by the high-fat diet. T2 treatment restored serum TT3 levels to values comparable to Ctrl mice, while TT4 levels remained reduced relative to Ctrl and did not differ significantly from Hfd. TSH levels were significantly decreased compared to both Ctrl and Hfd mice.
Hfd+T3 showed significantly increased circulating TT3 levels compared to all experimental groups, increased TT4 levels and decreased TSH levels compared to both Ctrl and Hfd.
Treatment with Tat-Beclin1, administered either alone or in combination with T2 acted like T2, showing reduced TT3 compared to Hfd, significantly decreased TT4 only compared to Ctrl mice and reduced TSH compared to both Ctrl and Hfd groups.

Table 6. Serum levels of T3, T4 and TSH.

	Ctrl	Hfd	Hfd+T2	Hfd+T3	Hfd+Tb	Hfd+Tb+T2
Serum T3 (TT3) pg/mL	5204,4±666,28	3253,4±371,31*	5066,4±434$^{\#}$	13470,5±2279$^{**,\#\#,++}$	4260±1377,9$^{\circ\circ}$	7163,8±1735,6$^{\#,\circ\circ}$
Serum T4 (TT4) ng/mL	98,7±5,9	32,3±0,5**	22,5±1,3**	45,6±17,5$^{**,\#}$	11,4±3,5**	40±15,4**
Serum TSH pg/mL	1569,7±28,4	2538,9±160**	826,9±34,5$^{***,\#\#\#}$	762±9,5$^{**,\#\#}$	1001,4±108,4$^{***,\#\#\#}$	846,6±12,1$^{***,\#\#\#}$

Values are presented as the means ± SEM from 3/5 mice in each group. One-way Anova, Student-Newman-Keuls post – hoc test, *p<0.05 vs. Ctrl; **p<0.01 vs. Ctrl; ***p<0.001 vs. Ctrl; #p<0.05 vs. Hfd; ##p<0.01 vs. Hfd; ###p<0.001 vs. Hfd; ++p<0.01 vs. Hfd+T2; °°p<0.01 vs. Hfd+T3.

The maintenance of circulating thyroid hormones levels and their action depend on glandular secretion and peripheral metabolism.
Hepatic gene expression of the thyroid hormone transporter, mct8, the iodothyronine deiodinases, type 1 (dio1) and type 3 (dio3), and the nuclear receptors thrα and thrβ were evaluated (**Figure 17**).

Compared to Ctrl, the expression levels of the major hepatic deiodinases, dio1 and dio3, were highly modulated under the Hfd condition. Hfd showed a significantly reduced expression level of dio1 (activating enzyme) paralleled by an increased expression of dio3 (inactivating enzyme) compared to the Ctrl group, while mct8, thrα and thrβ expression remained unchanged.

T2 treatment normalised dio1 and dio3 expression to control levels, but there were no significant changes in the expression levels of the other considered genes.

T3 treatment powerfully enhanced the dio1 expression compared to all other experimental groups, as this is a thyroid hormone response element-regulated T3-target gene. Moreover, in these mice, mct8 and thrβ increased compared to Hfd.

Tb treatment alone showed a significant increase in thrβ expression compared to Hfd. Compared to Hfd, the combined Tb+T2 treatment resulted in a significant increase of dio1 and thrβ expression accompanied by a reduction in dio3 level, resembling the effect of T3 treatment.

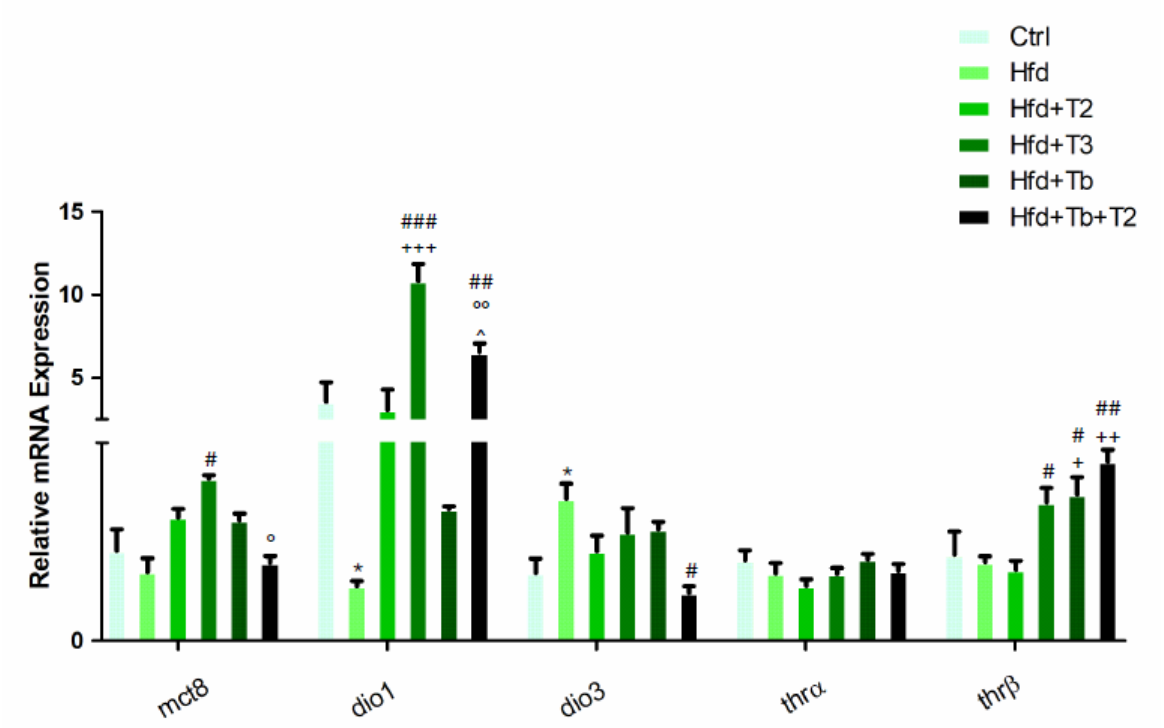

Figure 17. Hepatic gene expression of TH transporters (mct8), iodothyronine deiodinases (dio1 and dio3) and TH receptors (thrα and thrβ) in liver of Ctrl, Hfd, Hfd+T2, Hfd+T3, Hfd+Tb, Hfd+Tb+T2. Values are presented as the means ± SEM from 3/5 mice in each group. One-way Anova, Student-Newman-Keuls post – hoc test, *p<0.05 vs. Ctrl; #p<0.05 vs. Hfd; ##p<0.01 vs. Hfd; ###p<0.001 vs. Hfd; +p<0.05 vs. Hfd+T2; ++p<0.01 vs. Hfd+T2; +++p<0.001 vs. Hfd+T2; °p<0.05 vs. Hfd+T3; °°p<0.01 vs. Hfd+T3; °°°p<0.001 vs. Hfd+T3; ^p<0.05 vs. Hfd+Tb. For Dio1, Dio3 and Thrβ Student's t-test was performed, *p<0.05 vs. Ctrl; #p<0.05 vs. Hfd and ^p<0.05 vs. Hfd+Tb.

6.5 Oxidative stress and antioxidant defense

As reported in Figure 16, the Hfd group showed a marked increase in hepatic oxidative stress markers, with higher levels of hepatic H_2O_2, MDA and serum 8-OHdG compared to the control group (**Fig. 18ABCD**). In the Hfd group, MnSOD protein expression did not differ significantly from the control group, and the increase in MnSOD activity, as a compensatory response, was not sufficient to reduce oxidative stress. Accordingly, GPX4 and PRDX3 levels were significantly reduced, collectively indicating an impaired antioxidant system against oxidative damage and lipid peroxidation.

T2 administration significantly reduced H_2O_2, 8-OHdG and MDA levels compared to the Hfd group. Regarding antioxidant defence enzymes, T2 treatment resulted in a significant reduction of MnSOD expression compared to the Hfd group, paralleled by a strong stimulation of its activity. Moreover, T2 significantly increased GPX4 and PRDX3 expression levels.

T3 treatment significantly reduced hepatic H_2O_2 and MDA compared to the Hfd group but did not affect serum 8-OHdG levels. Among antioxidant defence enzymes, T3 was able only to restore GPX4 expression compared to the Hfd group.

Tb alone significantly reduced H_2O_2 levels and stimulated MnSOD activity compared to the Hfd group. Although Tb stimulated GPX4 expression compared to the Hfd group, no significant changes were observed in serum 8-OHdG and MDA levels, suggesting that Tb was unable to counteract oxidative damage to DNA and lipids.

Finally, the combination of Tb and T2 affected oxidative balance in a manner similar to T2 or Tb alone. Tb+T2, like T2, significantly reduced hepatic H_2O_2 levels compared to the Hfd, with a tendency towards reduced 8-OHdG levels. As with Tb, no differences in MDA levels were observed compared to the Hfd group, indicating ineffectiveness against lipid peroxidation.

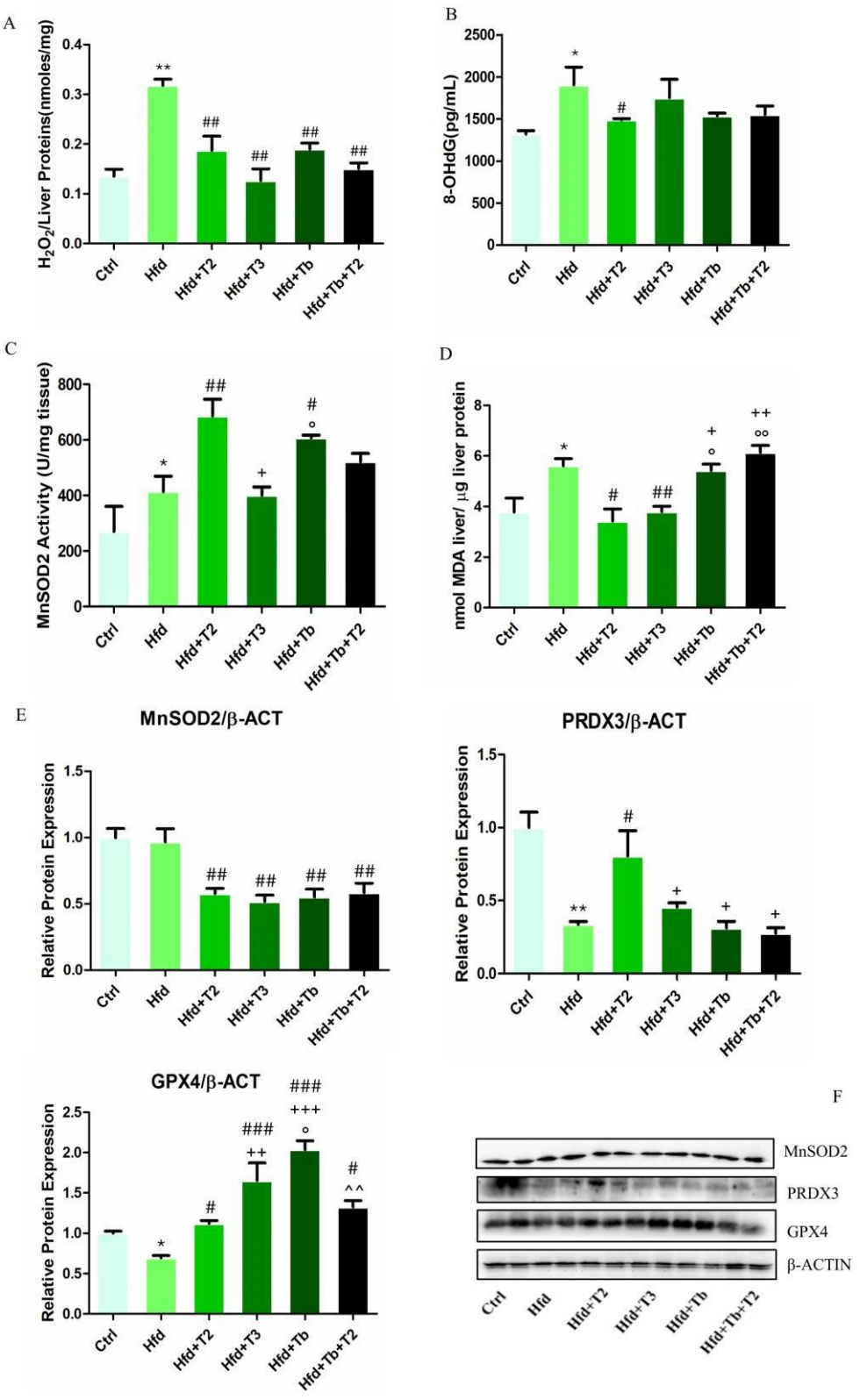

Figura 18. Oxidative stress markers and antioxidant defence enzymes in liver of Ctrl, Hfd, Hfd+T2, Hfd+T3, Hfd+Tb, Hfd+Tb+T2. (A) Hepatic H_2O_2 (nmol/proteins) level normalized on liver protein content; (B) serum levels of 8-OHdG; (C) hepatic SOD activity, (D) hepatic MDA level normalized on liver protein content, (E) quantification of bands intensity of liver protein expression of SOD2, PRDX3 and GPX4 and (F) representative western blot panel, normalized based on β-actin. Values are presented as the means ± SEM from 3/5 mice in each group. One-way Anova, Student-Newman-Keuls post – hoc test, *p<0.05 vs. Ctrl; **p<0.01 vs. Ctrl; #p<0.05 vs. Hfd, ##p<0.01 vs. Hfd; ###p<0.001 vs. Hfd; +p<0.05 vs. Hfd+T2; ++p<0.01 vs. Hfd+T2; +++p<0.001 vs. Hfd+T2; °p<0.05 vs. Hfd+T3; °°p<0.01 vs. Hfd+T3 and ^^p<0.01 vs. Hfd+Tb. For 8-OHdG Student's t-test was performed, *p<0.05 vs. Ctrl.

6.6 Mitochondrial DNA damage and repair

Mitochondria are a prominent target of oxidative damage and mtDNA is particularly susceptible due to the lack of protective histones. For this reason, the quantity, integrity and amplification of mtDNA were evaluated in the several experimental groups (**Figure 19**).

Liver from the Hfd group showed a significantly increase in mtDNA lesion frequency and reduced relative mtDNA amplification compared to the Ctrl group, indicating severe oxidative damage to mitochondrial DNA.

T2, T3, Tb alone and in combination with T2, significantly reduced the mtDNA lesions frequency compared to Hfd group.

The mtDNA copy number was used as an index of cellular mitochondrial content. The mtDNA copy number was significantly increased only by T3 treatment compared to all other experimental conditions.

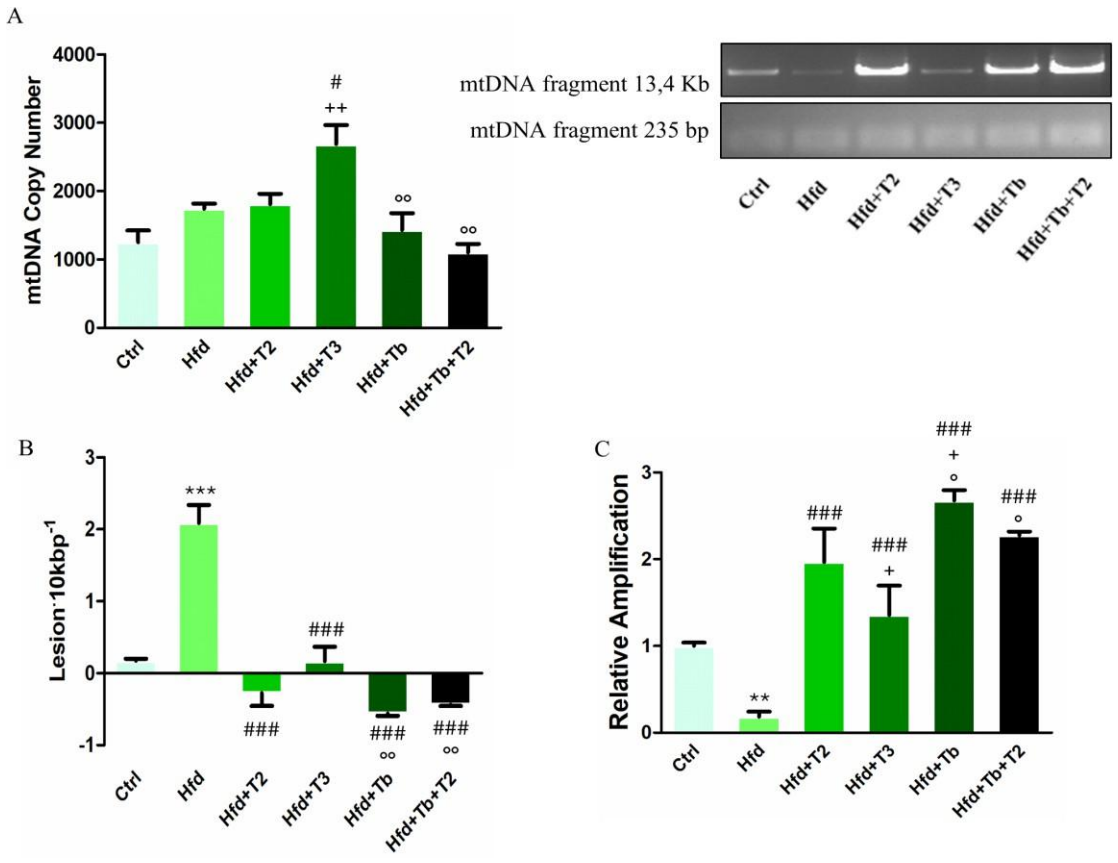

Figura 19. mtDNA copy number and mtDNA lesion frequency in liver of Ctrl, Hfd, Hfd+T2, Hfd+T3, Hfd+Tb, Hfd+Tb+T2. (A) mtDNA copy number assessed by qRT-PCR in 10 ng of genomic lier DNA using primers for mt-Cytb and β-actin; (B) frequency of mtDNA lesions per 10 kb per strand; (C) mtDNA damage evaluated by amplifying long (13.4 kb) and short (235 bp) mtDNA fragments by QPCR. Values are presented as the means ± SEM from 3/5 mice in each group. One-way Anova, Student- Newman-Keuls post – hoc test, **p<0.01 vs. Ctrl; ***p<0.001 vs. Ctrl; #p<0.05 vs. Hfd; ###p<0.001 vs. Hfd; +p<0.05 vs. Hfd+T2; ++p<0.01 vs. Hfd+T2; ° p<0.05 vs. Hfd+T3; °° p<0.01 vs. Hfd+T3.

The mtBER system plays a central role correcting mtDNA oxidative damage. The presence of BER in mitochondria is crucial for maintaining the integrity of mtDNA and overall mitochondrial function. The enzymes involved in this system are DNA glycosylase 1 (OGG1), which removes 8-oxoguanine (8-oxoG), a damaged base; apurinic/apyrimidinic endonuclease 1 (APE1), which cleaves the abasic site; and DNA polymerase gamma (POLγ), the mitochondrial polymerase that resynthesizes DNA. Protein expression levels of these enzymes were measured in all experimental groups (**Figure 20**).

Compared to the Ctrl group, Hfd treatment resulted in a significant reduction in OGG1 and APE1 protein expression, indicating impairment of the BER system. Compared to Hfd, treatment with T2 increased OGG1, APE1 and POLγ protein expression. Similarly, compared to Hfd, T3 caused a significant increase in OGG1 and APE1 protein expression, with a weaker effect on POLγ.

Finally, Tb alone and in combination with T2, compared to Hfd, significantly stimulated the expression of OGG1, APE1, and POLγ.

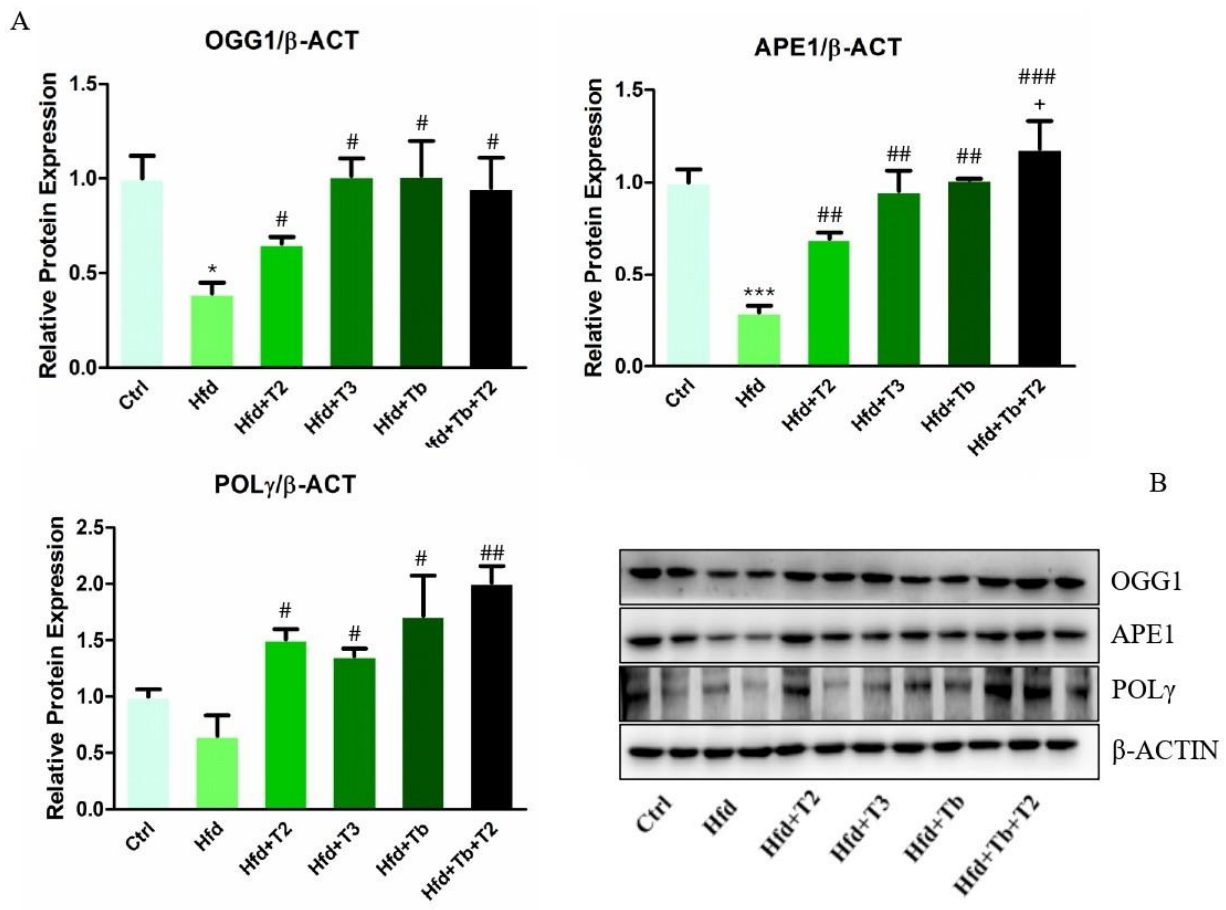

Figura 20. BER enzymes in liver of Ctrl, Hfd, Hfd+T2, Hfd+T3, Hfd+Tb, Hfd+Tb+T2 (A) Quantitative analysis and (B) representative Western blot of of OGG1, APE1 and POLγ normalized based on β-actin. Values are presented as the means ± SEM from 3/5 mice in each group. One-way ANOVA, Student-Newman- Keuls post-hoc test, *p<0.05 vs. Ctrl; **p< 0.01 vs. Ctrl; #p<0.05 vs. Hfd; ##p<0.01 vs. Hfd; ###p< 0.001 vs. Hfd.

6.7 cGAS-STING inflammatory pathway

Mitochondrial dysfunction not only promotes hepatocellular damage but can also lead to the release of mitochondrial components such as mtDNA, which act as mitochondrial damage-associated molecular patterns (mtDAMPs). These molecules are sensed by the cytosolic DNA sensor cGAS, which activates the STING pathway and promotes the inflammatory response. Based on this, the activation of the cGAS–STING axis was evaluated in the present experimental model by measuring cGAS, STING, P-TBK1/TBK1, P-IKBα/IKBα, IL-10, SOCS3 protein expression (**Figura 21**).

The Hfd diet powerfully stimulated cGAS and STING expression compared to the control. Upon activation, cGAS/STING activate TBK1 and IKBα through phosphorylation. Increased P-TBK1/TBK1 and P-IKBα/IKBα ratios were observed in the Hfd group compared to the control, suggesting the activation of the cGAS-STING inflammatory cascade induced by dietary treatment.

Treatments with T2, T3 and the combination of T2 and Tb significantly reduced the expression levels of both cGAS and STING proteins compared to the Hfd group. Tb alone significantly reduced only cGAS levels.

All treatments reduced TBK1 activation, but only T2 significantly reduced IKBα phosphorylation.

Anti-inflammatory markers such as IL-10 and SOCS3 were also analysed. A significant reduction of IL-10 and SOCS3 expression was observed in the Hfd group, consistent with hepatic inflammatory condition of these animals. T2 enhanced IL-10 protein expression as well as SOCS3 levels. Tb and T3 did not affect either marker. Notably, the anti-inflammatory effects of T2 were attenuated by Tb co-administration: Tb+T2 mice showed a significant downregulation of IL-10 protein expression compared to all experimental groups.

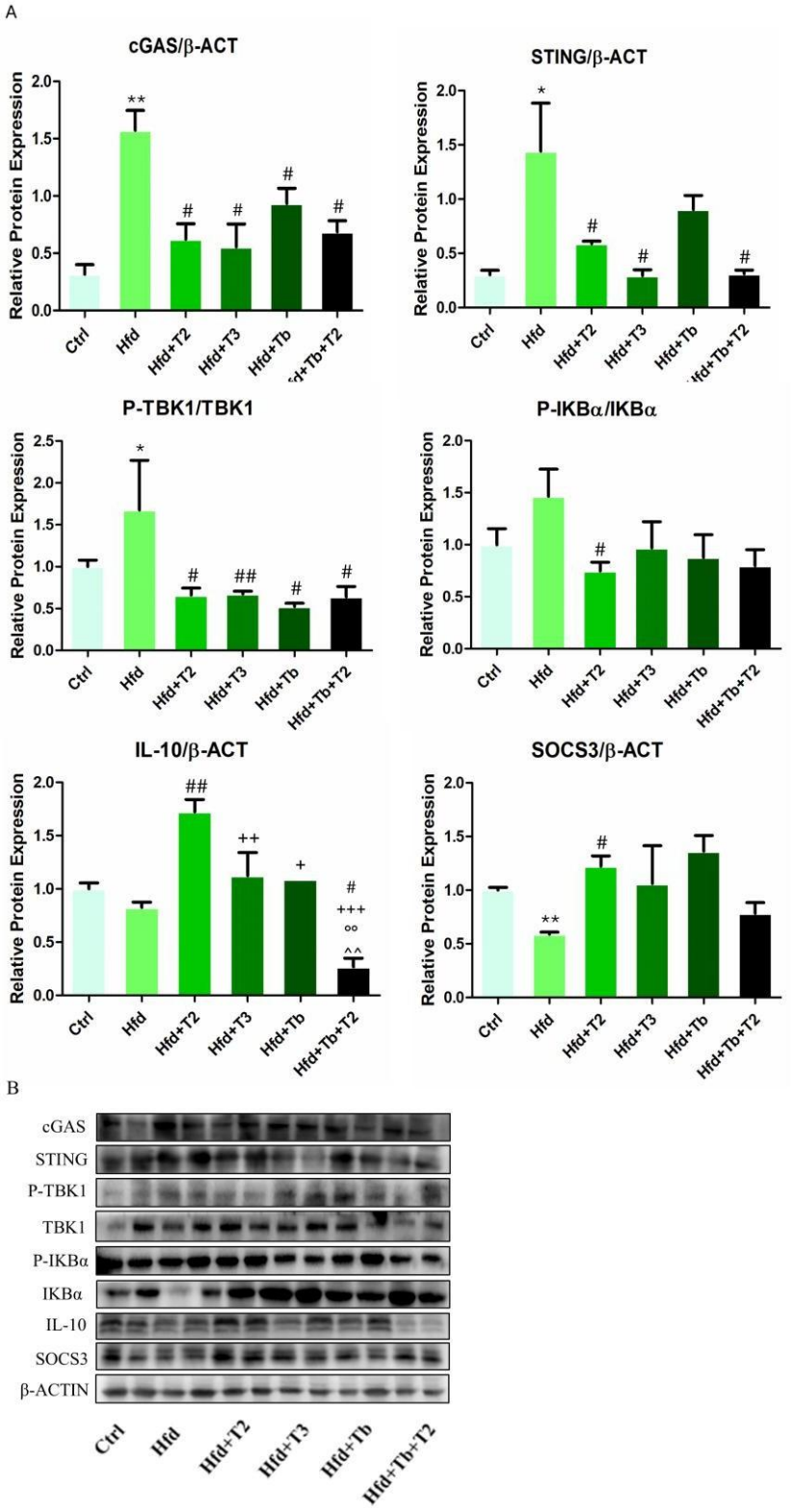

Figure 21. cGAS-STING pathway and inflammatory markers in liver of Ctrl, Hfd, Hfd+T2, Hfd+T3, Hfd+Tb, Hfd+Tb+T2. (A) Quantitative analysis and (B) representative Western blot of cGAS-STING, P-TBK1/TBK1, P-IKBα/IKBα, IL-10 and SOCS3 normalized based on β-actin. Values are presented as the means ± SEM from 3/5 mice in each group. One-way ANOVA, Student-Newman-Keuls post-hoc test, *p<0.05 vs. Ctrl; **p<0.01 vs. Ctrl; #p<0.05 vs. Hfd; ##p<0.01 vs. Hfd; +p<0.05 vs. Hfd+T2, ++p<0.01 vs. Hfd+T2; +++p<0.001 vs. Hfd+T2; °°p<0.01 vs. Hfd+T3; ^^p<0.01 vs. Hfd+Tb. For P-IKBα and SOCS3 Student's t-test was performed, **p<0.01 vs. Ctrl; # p<0.05 vs. Hfd.

6.8 General autophagy pathway and selective autophagy of lipid droplets

Autophagy represents a mechanism essential for maintaining liver homeostasis during metabolic stress. This process is known to be stimulated by Tat -beclin, which was used here for mouse treatments. Moreover, through the activation of selective autophagy programmes, such as lipophagy, autophagy enables the removal of excess lipid droplets, thereby preserving mitochondrial function and cellular energy balance. In this context, the expression of key markers involved in the regulation of autophagy and lipophagy was analysed.

In the early stages of the autophagic process, the mTOR kinase, a negative regulator of autophagy, phosphorylates pULK1 (Ser757), leading to its inactivation and blocking the initiation of the autophagic cascade (Kim et al., 2011). Autophagosome formation requires the coordinated action of ATG proteins: ATG9 transports phospholipids necessary for the formation of the autophagosome structure, allowing the intervention of LC3, which is essential for autophagic vesicle maturation (Zagkou et al., 2022). Finally, P62 acts as a selective autophagy adaptor, involved in the recognition and transport of substrates to the autophagosome. Its accumulation is generally indicative of a blockage of the autophagic flux (Bjørkøy et al., 2005).

As shown in Figure 22, compared to Ctrl, Hfd-fed mice showed higher expression levels of P-mTOR (Ser2448)/mTOR and p-ULK1(Ser757)/ULK1, indicating an upstream inhibition of autophagy. Furthermore, ATG9 was significantly increased, but the concomitant accumulation of p62 together with a reduction in LC3IIb, indicated an altered autophagic flux.

T2 treatment only removed the inhibition of autophagy, by decreasing P-mTOR (Ser2448)/mTOR, p-ULK1(Ser757)/ULK1 and ATG9 protein expression, compared to Hfd mice.

T3 and Tb restored the autophagy process under high fat diet, modulating all molecular phases of the process. Compared to Hfd, both molecules i) reduced the P-mTOR (Ser2448)/mTOR and p-ULK1(Ser757)/ULK1 ratios, ii) increased LC3IIb protein expression and iii) decreased P62 protein levels.

As reported in the following figure the combination of T2 and Tb, compared to Hfd, reduced the P-mTOR (Ser2448)/mTOR ratio, ATG9 and P62, but did not alter P-ULK1(Ser757)/ULK1 and LC3II.

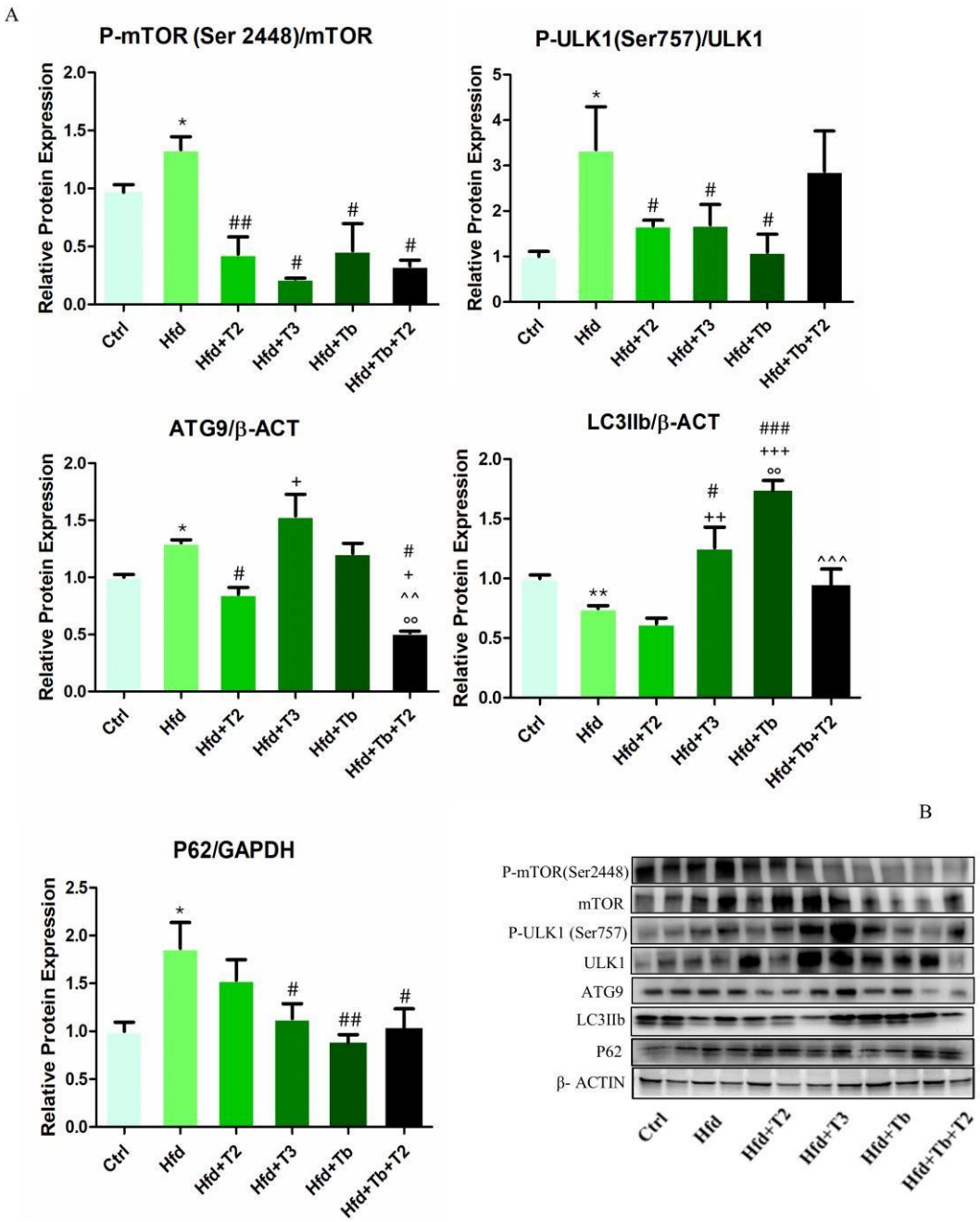

Figure 22. Autophagy markers in liver of Ctrl, Hfd, Hfd+T2, Hfd+T3, Hfd+Tb, Hfd+Tb+T2. (A) Quantitative analysis and (B) representative Western blot of P-mTOR/mTOR (Ser2448), P-ULK(Ser 757) /ULK, ATG9, LC3IIb and P62 normalized based on β-actin. Values are presented as the means ± SEM from 3/5 mice in each group. One-way ANOVA, Student-Newman-Keuls post-hoc test, *p<0.05 vs. Ctrl; # p<0.05 vs Hfd; ##p<0.05 vs. Ctrl; ###p<0.001 vs. Hfd; +p<0.05 vs. Hfd+T2; +++p<0.001 vs. Hfd+T2; °°p<0.01 vs. Hfd+T3; ^^p<0.05 vs. Hfd+Tb; ^^^p<0.001 vs. Hfd+Tb. For P-ULK, ATG9 Student's t-test was performed, *p<0.05 vs. Ctrl.

Lipophagy-specific markers were evaluated: transcription factors TFE3 and TFEB, lipid droplet lipolysis enzyme PNPLA3, and lipid droplet coat protein ADRP (**Figure 23**). In the Hfd group, TFE3 and TFEB protein levels, as well as PNPLA3, remained unchanged compared to the

controls, while there was a strong upregulation of ADRP, a known marker of hepatic lipid droplet accumulation.

Compared to the Hfd group, Hfd+T2 mice showed a significant upregulation of TFE3 and a trend towards increased TFEB expression. In addition, T2 administration significantly enhanced PNPLA3, which is involved in lipid oxidation, and conversely reduced ADRP.

Notably, compared to the Hfd group, the Hfd+T3 group displayed upregulation of TFEB and TFE3 and, like T2, significantly decreased ADRP expression.

A reduction in ADRP expression was also observed in the Hfd+Tb and Hfd+Tb+T2 groups compared to Hfd. Notably, the Hfd+Tb+T2 group, like T2, showed a significant increase in PNPLA3 compared to the Hfd group.

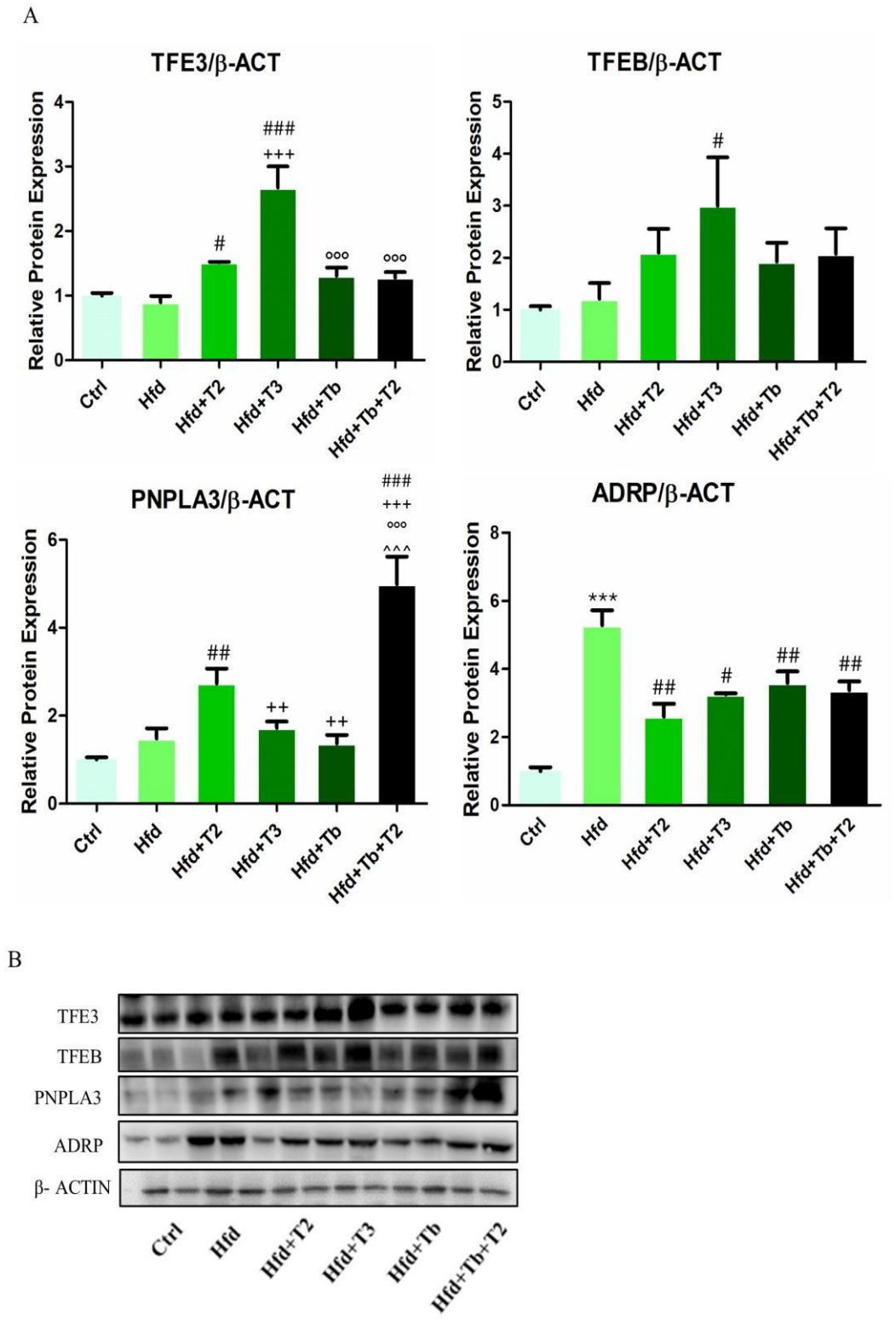

Figure 23. Lipophagy markers in liver of Ctrl, Hfd, Hfd+T2, Hfd+T3, Hfd+Tb, Hfd+Tb+T2. (A) Quantitative analysis and (B) representative Western blot of TFE3, TFEB, PNPLA3 and ADRP protein levels, normalized based on β-actin. Values are presented as the means ± SEM from 3/5 mice in each group. One-way ANOVA, Student-Newman-Keuls post-hoc test, ***p<0.001 vs. Ctrl; #p<0.05 vs. Hfd; ##p<0.01 vs. Hfd; ###p<0.001 vs. Hfd; ++p<0.01 vs. Hfd+T2; +++p<0.001 vs. Hfd+T2; °°°p<0.001 vs. Hfd+T3; ^^^p<0.001 vs. Hfd+Tb. For TFE3 Student's t-test was performed, #p<0.05 vs. Hfd.

6.9 Mitochondrial Quality Control

Since the maintenance of mitochondrial function depends on the integration of biogenesis, mitochondrial dynamics and mitophagy, collectively known as Mitochondrial Quality Control (MQC), the expression of the main markers involved in these mechanisms was analysed.

For mitochondrial biogenesis, pgc1α and tfam gene and protein expression and NRF2 and TOM20 protein expression were analysed. (**Figure 24**).

Compared to the control group, the Hfd group showed a significant reduction in tfam gene expression and TOM20 protein expression.

Hfd+T2, compared to the Hfd group, showed a significant increase in tfam gene expression together with an enhancement of PGC1α, NRF2, and TOM20 protein levels.

The Hfd+T3 group powerfully stimulated pgc1α and tfam mRNA and protein levels, compared to the Hfd group, paralleled by an enhancement of both NRF2 and TOM20, indicating a central role of T3 in the regulation of mitochondrial biogenesis.

Tb alone and in combination with T2 did not influence the biogenesis markers. Of note, the combination of Tb and T2 powered the NRF2 protein expression compared to Ctrl, Hfd, Hfd+T2 and Hfd +Tb.

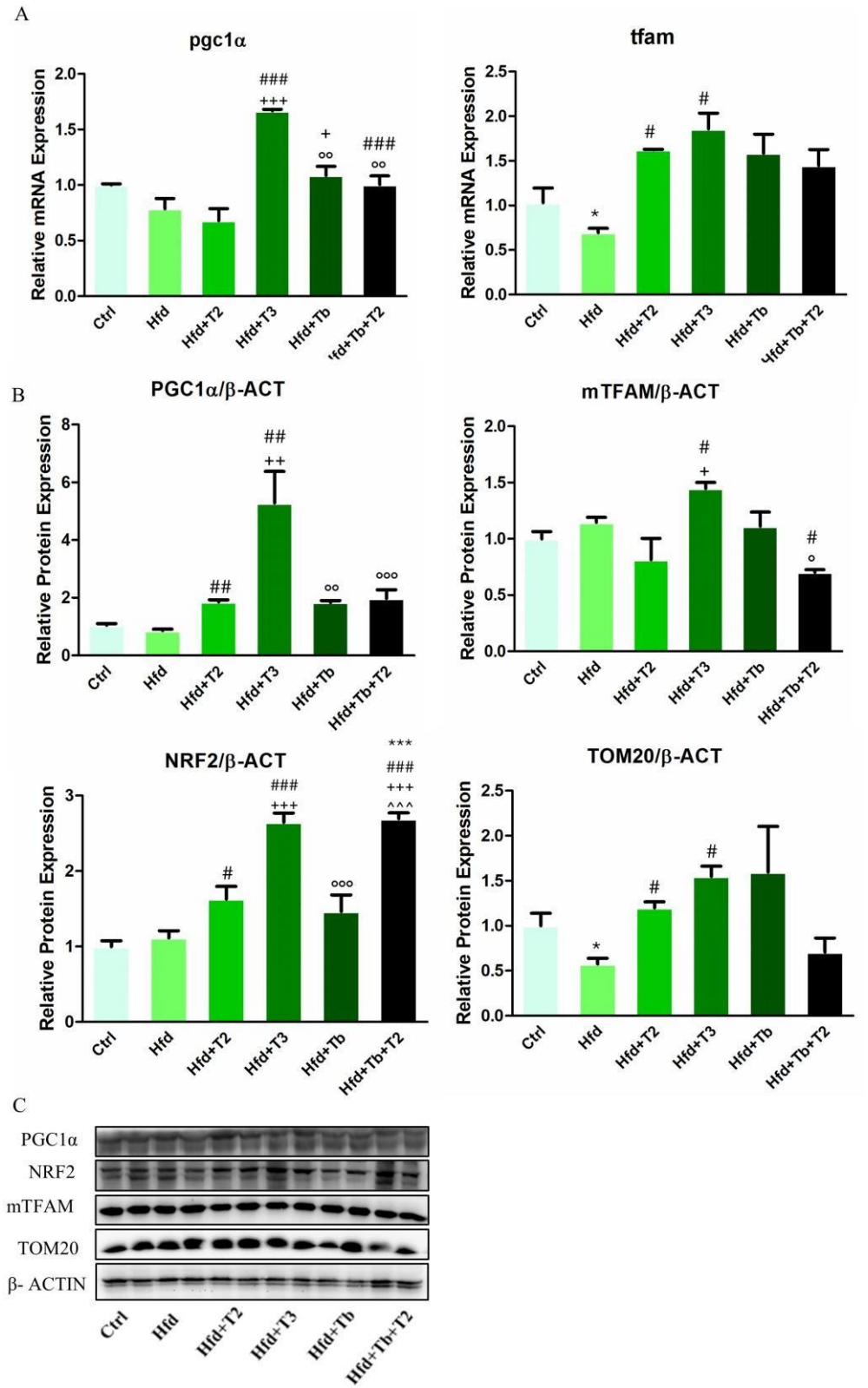

Figura 24. Mitochondrial biogenesis markers in liver of Ctrl, Hfd, Hfd+T2, Hfd+T3, Hfd+Tb, Hfd+Tb+T2. (A) Pgc1α and mTfam mRNA expression was determined by qRT-PCR. (B) Quantitative analysis and (C) representative Western blot of PGC1α, mTFAM, NRF2 and TOM20, normalized based on β-actin. Values are presented as the means ± SEM from 3/5 mice in each group. One-way ANOVA, Student-Newman-Keuls post-hoc test, *p<0.05 vs. Ctrl; #p<0.05 vs. Hfd; ##p<0.01 vs. Hfd; ###p< 0.001 vs. Hfd; +p<0.05 vs. Hfd+T2; ++p<0.01 vs. Hfd+T2; +++p<0.001 vs. Hfd+T2; °p<0.05 vs. Hfd+T3; °°p<0.01 vs. Hfd+T3; °°°p<0.001 vs. Hfd+T3; ^^^p<0.001 vs. Hfd+Tb. For tfam and TOM20 Student's t-test was performed, *p<0.05 vs. Ctrl.

The markers involved in the mitochondrial dynamics process were analysed: mitofusin 2 (MFN2), optic atrophy 1 (OPA1), and OMA1 zinc metallopeptidase (OMA1) were selected as markers of mitochondrial fusion, while dynamin-related protein 1 (DRP1) was used as a marker of mitochondrial fission (**Figure 25**). Compared to the Ctrl group, the Hfd group showed downregulation of OPA1 protein expression together with upregulation of OMA1 expression, an enzyme involved in the cleavage of OPA1, promoting mitochondrial fragmentation. Compared to the Hfd group, the Hfd+T2 group showed a significant increase in MFN2 and OPA1 expression. The Hfd+T3 group showed upregulation of OPA1 and DRP1 expression compared to the Hfd group, shifting the balance of dynamics towards fission. Tb alone did not affect these markers; notably, the combination of Tb with T2 resulted in a marked increase in MFN2, as seen with T2, and DRP1, as observed with T3.

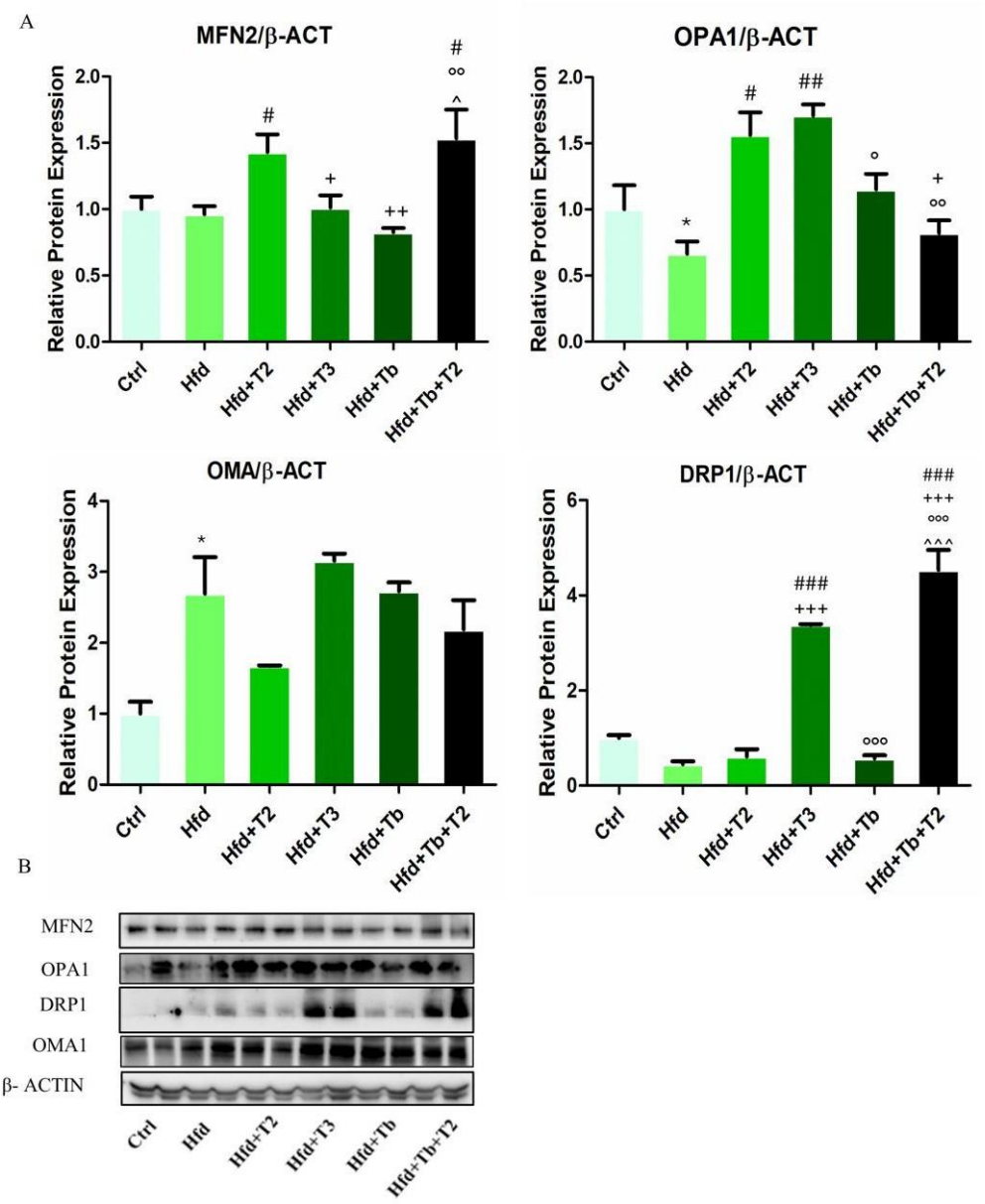

Figure 25. Mitochondrial dynamics markers in liver of Ctrl, Hfd, Hfd+T2, Hfd+T3, Hfd+Tb, Hfd+Tb+T2**.** (A) Quantitative analysis and (B) representative Western blot of MNF2, OPA1, OMA1 and DRP1 normalized based on β-actin. Values are presented as the means ± SEM from 3/5 mice in each group. One-way ANOVA, Student-Newman-Keuls post-hoc test, #p<0.05 vs. Hfd; ##p<0.01 vs. Hfd; ###p<0.001 vs. Hfd; +p<0.05 vs. Hfd+T2; ++p<0.01 vs. Hfd+T2; +++p<0.001 vs. Hfd+T2; ° p<0.05 vs. Hfd+T3; °°p<0.01 vs. Hfd+T3; °°°p<0.001 vs. Hfd+T3; ^p<0.05 vs. Hfd+Tb; ^^^p<0.001 vs. Hfd+Tb. For OPA1 Student's t-test was performed, *p<0.05 vs. Ctrl.

Mitophagy markers were subsequently analysed (**Figure 26**).

No significant differences in PINK1 and PARKIN expression levels were observed in HFD-fed mice compared to Ctrl mice.

Both the Hfd+T2 and Hfd+T3 groups exhibited increased levels of PINK1, and PARKIN compared to all other experimental groups. In contrast, treatment with Tb alone and in combination with T2 did not result in significant changes.

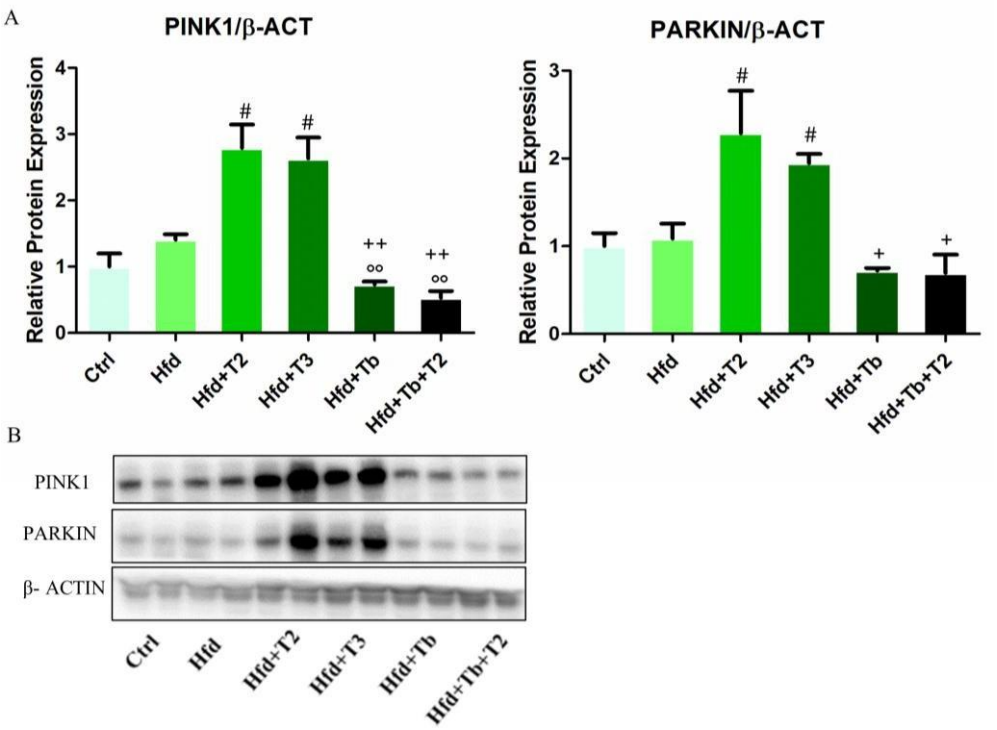

Figure 26. Mitophagy markers in liver of Ctrl, Hfd, Hfd+T2, Hfd+T3, Hfd+Tb, Hfd+Tb+T2. (A) Quantitative analysis and (B) representative Western blot of PINK1 and PARKIN, normalized based on β-actin. Values are presented as the means ± SEM from 5 mice in each groups. One-way Anova, Student-Newman-Keuls post-hoc test, #p<0.05 vs. Hfd; +p<0.05 vs. Hfd+T2; ++p<0.01 vs. Hfd+T2; °°p<0.01 vs. Hfd+T3. For PARKIN Student's t-test was performed, #p<0.05 vs. HFD.

6.10 Effects of iodothyronines and Tb on hepatic mitochondrial respiratory chain complexes abundance

Mitochondrial electron transport chain organization was evaluated by analysing the transcriptional and protein expression of respiratory chain complexes (CI–CV).

As shown in Figure 27, compared to Ctrl group, the Hfd showed a significant decrease in the CI, CIII, and CV protein expression. mRNA analysis did not show significant changes in their expression.

Compared to Hfd, the Hfd+T2 group displayed a slight increase in CII and CV expression.

Conversely, T3 strongly upregulated both gene and protein expression of all mitochondrial complexes compared to the Hfd, except for CI protein expression.

Tb treatment alone did not affect the ETC complex expression, while in combination with T2 induced a significant increase in the CII and CIV complexes compared to Hfd.

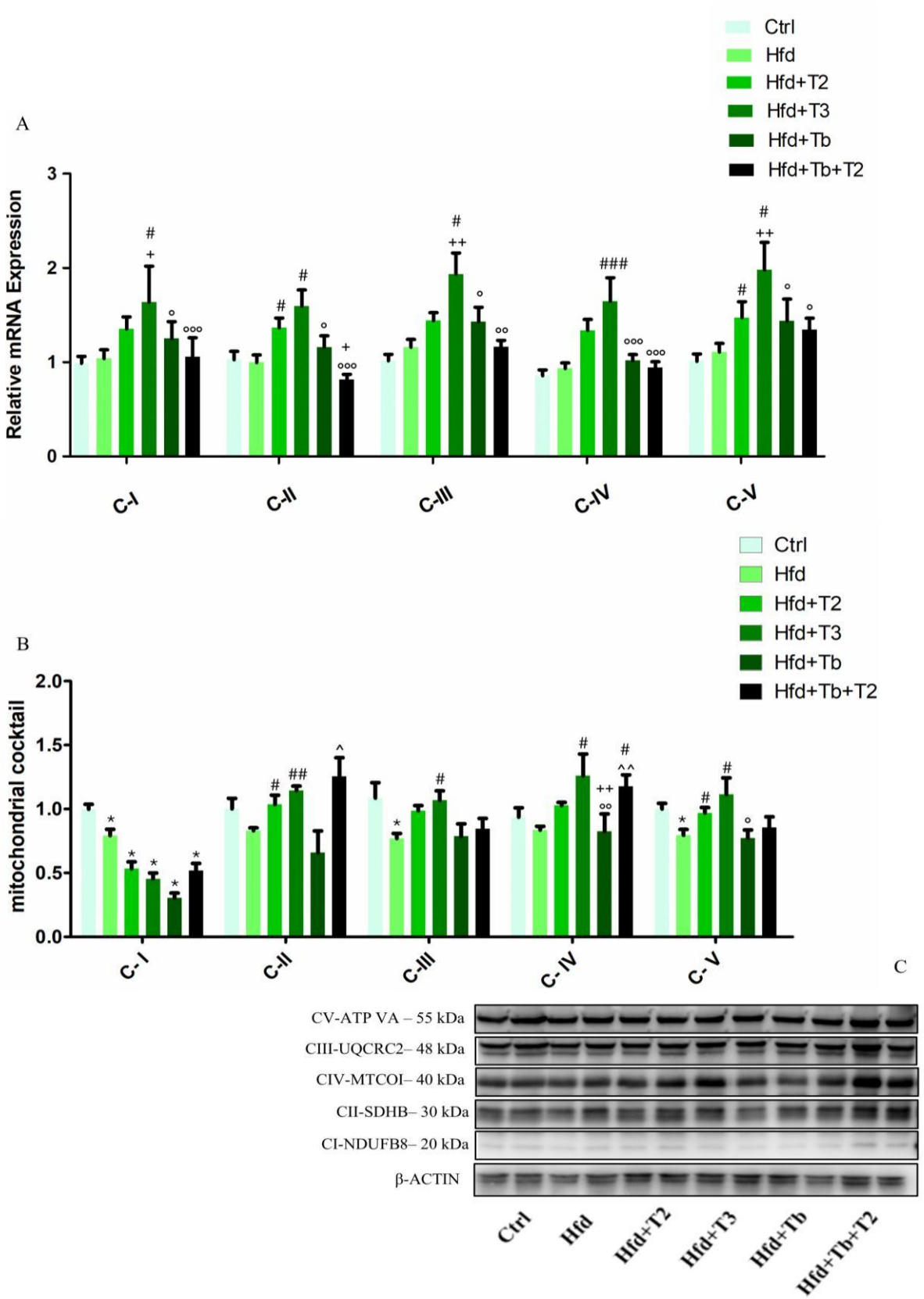

Figure 27. Respiratory complex CI-CV in liver of Ctrl, Hfd, Hfd+T2, Hfd+T3, Hfd+Tb, Hfd+Tb+T2. (A) CI–CV respiratory chain complex mRNA-expressions were determined by qRT-PCR and (B-C) quantitative analysis and representative Western Blot CI-CV respiratory chain complex protein levels. Values are presented as the means ± SEM from 3/5 mice in each group. One-way ANOVA, Student-Newman-Keuls post-hoc test, *p<0.05 vs. Ctrl; #p<0.05 vs. Hfd; ##p<0.01 vs. Hfd; ###p<0.001 vs. Hfd; +p<0.05 vs. Hfd+T2; ++p<0.01 vs. Hfd+T2; °p<0.05 vs. Hfd+T3; °°p<0.01 vs. Hfd+T3; °°°p<0.001 vs. Hfd+T3; ^p<0.05 vs. Hfd+Tb; ^^p<0.01 vs. Hfd+Tb. For CV Student's t-test was performed, *p<0.05 vs. Ctrl and for CII, CIII, CIV and CV, #<0.05 vs. Hfd.

6.11 Hepatic mitochondrial function

Given the central role of hepatic mitochondria in energy production, through the coupling of substrate oxidation and ATP synthesis, respiratory capacity in liver homogenates was assessed and corrected by antimycin subtraction.

As shown in Figure 28, 19 weeks on a high-fat diet severely impaired mitochondrial functionality. Respiration driven by complexes I and II, measured after the addition of PMG, ADP, and S, was significantly reduced compared to the control group. Specifically, a weakening of the entire electron transport chain (ETC), was observed as indicated by reduced respiration in the presence of the uncoupler FCCP, as well as after inhibition of complex I by rotenone.

T2 and T3 induced significant changes in mitochondrial respiration, restoring mitochondrial respiratory capacity, with T2 showing higher efficacy than T3. Compared to Hfd mice, both iodothyronines strongly stimulated complex I respiration alone (PMG+ADP additions) and together with complex II (S addition), in the presence of and after ATP synthase inhibition by oligomycin (O). Compared to the Hfd group, ETC activity was enhanced by T2 and T3, as indicated by increased respiration in the presence of FCCP even after exclusion of complex I.

As the effects of Tb on mitochondrial respiration have not been demonstrated here, the potentiating action of T2 was clearly distinguishable when co-administered to animals subjected to Tb. Mice treated with Tb+T2 showed stimulation of mitochondrial activity comparable to the Hfd+T2 group, with a significant increase in respiration of complex I alone and in combination with complex II, as well as in the presence of rotenone, compared to both Hfd and Hfd+Tb groups.

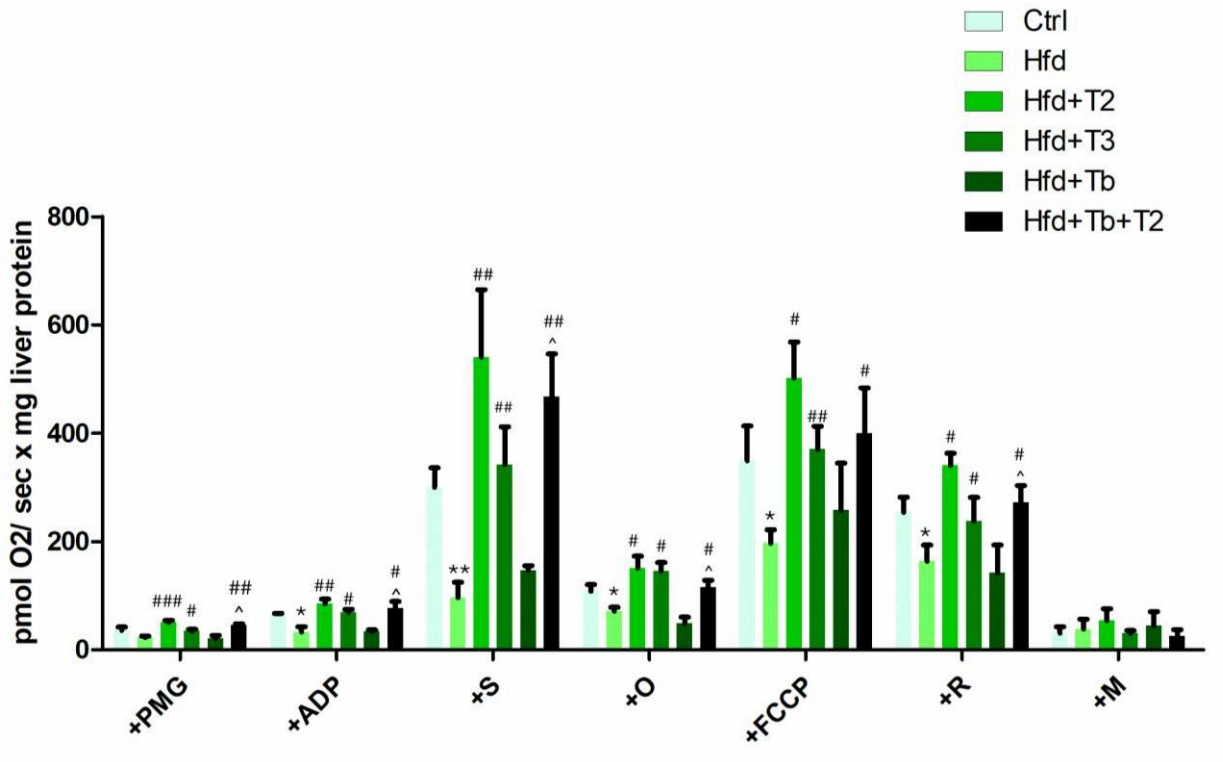

Figure 28. Mitochondrial respiratory function in liver of Ctrl, Hfd, Hfd+T2, Hfd+T3, Hfd+Tb, Hfd+Tb+T2. Mitochondrial respiration was measured in the presence of complex I-linked substrates pyruvate + glutamate + malate (PMG), adenosyntriphosphate (ATP), complex II-linked substrate succinate (S), ATP synthase inhibitor oligomycin (O), uncoupler carbonylcyanide p-trifluoromethoxyphenyl-hydrazone (FCCP) and inhibitor of complex I rotenone (R). Values are the means ± SEM from 3/5 mice in each group. One-way ANOVA, Student-Newman-Keuls post-hoc test, *p<0.05 vs. Ctrl; **p<0.01 vs. Ctrl; #p<0.05 vs. Hfd; ##p<0.01 vs. Hfd; ###p<0.001 vs. Hfd ^p<0.05 vs. Hfd+Tb. For PMG, ADP, S, O, FCCP Student's t-test was performed, *p<0.05 vs. Ctrl; *p<0.01 vs. Ctrl; #p<0.05 vs. Hfd; ##p<0.01 vs. Hfd and ^p<0.05 vs. Tb.

6.12 Effect of iodothyronines and Tb administration on the in-gel activities of liver mitochondria respiratory complexes.

To further investigate the effects of iodothyronines and Tb administration on the biochemical properties of hepatic mitochondria in MASLD, the respiratory chain complexes were extracted with dodecylmaltoside and resolved by BN-PAGE. For each individual respiratory complex (I, II, and IV) the in-gel activity was analysed (**Figure 29**).

Densitometric analysis revealed that Hfd mice showed a significant reduction in the in-gel activity of complex I compared to Ctrl, as well as a trend towards reduced activities of complexes II and IV. Compared to Hfd condition, T2 administration significantly stimulated the activities of all assayed complexes, while T3 significant activated the in-gel activities of complexes I and IV. Paralleling the *in vivo* mitochondrial respiration analysis, Tb did not influence any ETC mitochondrial activity, while T2 in combination with Tb replicated the effects elicited by T2 alone, even if the stimulatory effect on complex II did not reach statistical significance.

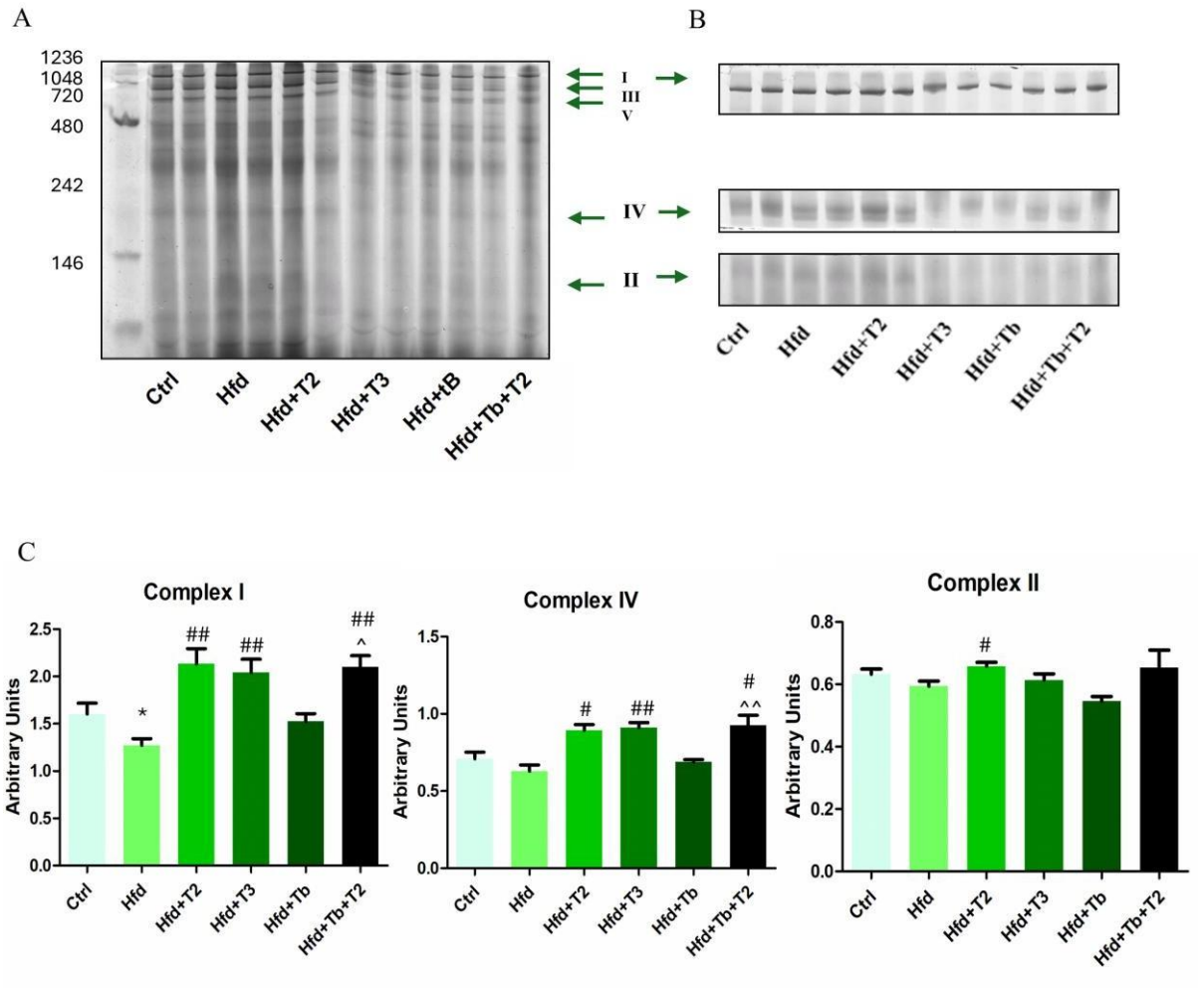

Figure 29. BN-PAGE-based analysis of individual respiratory complexes from dodecylmaltoside-solubilized crude mitochondria from liver of Ctrl, Hfd, Hfd+T2, Hfd+T3, Hfd+Tb, Hfd+Tb+T2. (A) Representative image of a Coomassie blue stained BN-PAGE gel. (B) Representative images of histochemical staining of complex I (I), complex IV (IV), and complex II (II) in-gel activity. (C) Densitometric quantification of colored bands corresponding to in gel-activity of complex I, complex IV, and complex II. Data were normalized to the value obtained for Ctrl and presented separately for each treatment (means ± SEM; n=3/5). One-way ANOVA, Student-Newman-Keuls post-hoc test ,*p< 0.05 vs. Ctrl; #p< 0.05 vs. Hfd; ##<p 0.01 vs. Hfd; ^ p < 0.05 vs. Hfd+Tb.

Chapter VII: Discussion

Metabolic dysfunction-associated steatotic liver disease (MASLD) includes patients with hepatic steatosis and at least one of five cardiometabolic risk factors such as obesity, type 2 diabetes, high blood pressure, and high circulating triglycerides or cholesterol. MASLD has very recently replaced the previous term non-alcoholic fatty liver disease (NAFLD) (Rinella et al., 2023; Powell et al., 2021). The lack of correct terminology and suitable animal models for MASLD has severely limited the study of the mechanisms underlying this multifactorial disorder, negatively affecting the development of appropriate therapeutic strategies. Therefore, establishing an animal model that adequately reflects the entire spectrum of MASLD remains a crucial need (Febbraio et al., 2019).

In the present study, chronic exposure to a high-fat diet for 19 weeks at thermoneutrality induced a broad spectrum of metabolic derangements that closely mirror the pathophysiological features of MASLD in humans. In this experimental model, we examined how several short-term pharmacological treatments based on iodothyronines and Tb modulated these pathological features. Hfd mice exhibited increased body weight, expansion of white adipose tissue and liver size, and hepatic steatosis. These morphological changes were accompanied by increased hepatic triglyceride content and elevated circulating triglyceride and cholesterol levels, parameters closely linked to MASLD severity (Xiaoxiao & Meng 2024). This phenotype is consistent with the concept that, when the storage capacity of subcutaneous adipose tissue is exceeded, lipid overflow towards visceral depots and the liver occurs, resulting in increased free fatty acid (FFA) flux to hepatocytes (Fuchs et al., 2022; Fan et al., 2023). The resulting excess delivery of FFAs – derived from adipose lipolysis, dietary intake, and de novo lipogenesis (DNL) – overwhelms hepatocellular oxidative and export capacity, promoting triglyceride storage as an initial protective mechanism. At the molecular level, Hfd mice showed dysregulated enzymes involved in DNL and fatty acid β-oxidation. Although CPT1A expression was upregulated, this compensatory response was insufficient to counterbalance lipid overload, thereby exacerbating hepatic lipid accumulation. These finding is in accordance with previous reports showing that excessive fatty acid influx, combined with dysregulated lipogenesis and impaired oxidation, is a central driver of hepatic steatosis and lipotoxicity in MASLD (Koliaki et al., 2015; Begriche et al., 2013; Friedman et al., 2018).

Pharmacological treatments produced distinct and treatment-specific metabolic profiles. T3 administration reduced body weight gain, adiposity, and hepatic liver accumulation consistent with its well-established ability to enhance lipid mobilization and oxidation. This effect was

associated with increased activation of AMPK-dependent pathways and enhanced mitochondrial fatty acid import, as indicated by CPT1A induction. However, these beneficial effects occurred in the context of a pronounced hypermetabolic state, reflected by substantial body-weight loss and systemic activation of the thyroid axis.

In contrast, T2 emerged as a metabolically selective modulator. The administration of T2 markedly attenuated visceral adipose tissue expansion and hepatic steatosis, lowered circulating triglycerides and cholesterol levels and decreased liver size without inducing excessive body-weight loss. Our data are consistent with previous results reported in animal models of HFD-induced metabolic dysfunction (Lanni et al., 2005; de Lange et al., 2004), where T2 prevented lipid accumulation in adipose tissue and liver. The metabolic improvements induced by T2 occurred in the absence of significant body weight loss, highlighting a more selective action on lipids metabolism compared to T3.

Indeed, T3 induced a more pronounced reduction in body weight, reflecting its ability to globally increase energy expenditure and metabolic rate across multiple tissues (Silvestri et al., 2018). In contrast, T2 improved hepatic lipid metabolism, likely through stimulation of hepatic fatty acid oxidation without inducing a hypermetabolic state (Senese et al., 2017). The coordinated suppression of lipid uptake and de novo lipogenesis, together with the activation of AMPK-dependent oxidative pathways, supports the hypothesis that T2 induces a complete reprogramming of hepatic lipid metabolism. This concept is further corroborated by the ability of T2 to reduce hepatic synthesis of endogenous cholesterol and to promote its disposal through bile acid synthesis. The ability of T2 to modulate cholesterol homeostasis in such a decisive manner appears unique and extremely interesting, since hypercholesterolemia is widely recognised as a key lipotoxic stress factor in MASLD (Goldberg et al., 2012).

Tb exerted a limited impact on body weight gain and adipose tissue mass, while significantly reducing hepatic steatosis, as evidenced by a marked decrease in lipid droplet number and an improvement in liver histology appearance. Since Tb alone did not modulate enzymes involved in lipid metabolism, the reduction in hepatic lipid burden observed under Tb treatment could be consistent with autophagy activation, in line with previous evidence identifying Tb as a potent autophagy inducer (Chen et al., 2024). By facilitating the removal of excess lipid droplets and damaged organelles, autophagy activation likely contributes to the restoration of cellular homeostasis and metabolic resilience (Shoji-Kawata et al., 2013; Sinha et al., 2015; Qian et al., 2021). A similar autophagy-dependent mechanism was also observed in animals treated with the combination of Tb and T2.

Chronic lipid excess disrupts hepatic insulin signalling and promotes metabolic dysfunction (Park et al., 2020; Petersen & Shulman, 2018; Solinas 2015). In accordance, Hfd feeding in our model resulted in elevated glycemia and hepatic insulin resistance, as indicated by reduced IRS1 levels, decreased AKT activation, and altered downstream GSK3 signalling, further worsening MASLD progression. Both iodothyronines improved hepatic insulin signalling, as evidenced by restoration of the IRS1-AKT-GSK3 axis, resulting in a significant reduction in circulating glucose levels. Accumulating evidence indicates that MASLD is not only associated with but can also actively contribute to the development of thyroid dysfunction (Betlejewska et al., 2025). Our data demonstrated that metabolic stress induced by high-fat diet feeding disrupts thyroid hormone homeostasis, leading to reduced circulating T3 and T4 levels, increased TSH, altered deiodinase expression, and the establishment of hepatic thyroid hormone resistance. This pattern is consistent with the model proposed by Bruinstroop et al., in which dysregulated hepatic deiodinase activity drives a liver-specific hypothyroid state that contributes to mitochondrial dysfunction, altered lipid metabolism, and inflammation in MASLD (Bruinstroop et al., 2023). In this context, MASLD appears not only as a consequence of thyroid hormone deficiency but also as a condition that may promote both systemic and hepatic hypothyroidism, which in turn amplifies lipid accumulation, cholesterol dysregulation, and metabolic stress.

Overall, the molecular response to exogenous T3 administration is consistent with a stimulatory effect on the thyroid axis, characterized by increased circulating T3 and T4 levels and decreased TSH, indicative of a hyperthyroid state. Because circulating thyroid hormone levels and tissue responsiveness depend on both glandular secretion and peripheral metabolism, this finding supports a model in which T3, acting primarily through nuclear receptor-mediated mechanisms, restores hepatic thyroid hormone signalling and modulates downstream metabolic processes (Carvalho and Ortiga-Carvalho, 2015).

T3-based interventions associated with thyrotoxicosis in the context of chronic metabolic disease have limited their use, although metabolically effective as previously discussed (Brent et al., 2012; Mullur et al., 2014). Indeed, exposure to high levels of T3 is associated with increased cardiovascular morbidity, including cardiac hypertrophy, heart failure, and arrhythmia (Vargas-Uricoechea et al., 2014).

In our study, both absolute heart weight and the heart weight to body weight ratio served as a sensitive biomarker of thyroid hormone-induced cardiac effects; therefore, T3 administration resulted in significant cardiac hypertrophy.

In contrast, T2 administration had only a minimal impact on systemic thyroid hormone homeostasis, normalizing circulating T3 levels without inducing overt activation of the thyroid axis, consistent with previous findings (Arnold et al., 1998; Goglia et al., 2005). The HW/BW ratio in T2-treated mice remained comparable to both the control and HFD-treated groups, demonstrating the absence of true cardiac hypertrophy when normalized for body weight. Treatment with Tb alone did not directly affect canonical thyroid hormone signalling and did not induce cardiac hypertrophy. Of note, the effect of the combination of Tb and T2 selectively restored hepatic thyroid hormone signalling, increasing Dio1 and TRβ while reducing Dio3 expression, without affecting Mct8, TRα, and cardiac morphology. These findings support a localized restoration of hepatic thyroid hormone action rather than a generalized activation of thyroid hormone signalling

Accumulation of hepatocellular lipids is widely recognised as a major driver of oxidative stress in MASDL; increased fatty acid oxidation does not eliminate hepatic lipid deposits but induces dysfunctional mitochondria to produce excessive ROS, thereby contributing to oxidative stress and leading to the development of liver disease (Simões et al., 2021; Li et al., 2024). This redox imbalance promotes oxidative damage to biological macromolecules, including lipids, proteins and nucleic acids (Mantena et al., 2018). In our MASLD model, chronic HFD feeding was associated with a sustained oxidative imbalance indicative of persistent mitochondrial stress. Redox homeostasis was profoundly disrupted as indicated by increased hepatic H_2O_2 and MDA levels, as well as elevated 8-OHdG. Oxidative stress is tightly linked to compromised mitochondrial genome integrity, as mtDNA is particularly susceptible to oxidative damage (Cioffi et al., 2017; Cioffi. et al., 2022). In accordance, Hfd showed increased mtDNA lesion frequency with reduced amplification efficiency, suggesting defective mitochondrial genome maintenance. This condition was further exacerbated by an inefficient repair response, impairment of BER likely favoured the persistence of oxidative mtDNA damage, reinforcing the vicious cycle between mitochondrial dysfunction, ROS accumulation, and genomic instability that characterises the transition from simple steatosis to more advanced stages of liver disease (D'Amico et al., 2022). In parallel, the antioxidant defence system appeared functionally inadequate, as indicated by reduced expression of mitochondrial antioxidant enzymes such as PRDX3 and GPX4, which limited the capacity of hepatocytes to neutralise ROS despite a compensatory increase in SOD2 activity (Kowalczyk et al., 2021).

In this pathological context, iodothyronines differentially modulated oxidative stress and mitochondrial genome integrity. T3 administration exerted only a modest effect on oxidative stress markers and associated antioxidant defences. On the other hand, T3 improved

mitochondrial DNA integrity, as indicated by reduced mtDNA lesion frequency and increased mtDNA copy number, together with the restoration of BER system. Of interest, the increase in mtDNA content is consistent with the well-established stimulatory effect of T3 on mitochondrial biogenesis, as observed in this and other studies (Cioffi. et al., 2019, Wrutniak-Cabello, et al., 2001; Weitzel et al., 2003). We can speculate that, rather than promoting mtDNA repair, T3 has a stronger stimulatory effect on mitochondrial renewal, resulting in the formation of new and healthy mitochondria. This is probably also a compensatory response to the increased energy demand (Weitzel et al., 2003), linked to the hypermetabolic state induced by T3 itself (Silvestri et al., 2018; Cioffi et al., 2022; Mullur et al., 2014).

T2 administration markedly reduced hepatic oxidative stress and was the only treatment able to also reduce systemic markers of DNA oxidation. Regarding the underlying molecular mechanisms, our results indicated that T2 acts through complementary pathways by enhancing mitochondrial antioxidant defence (i.e. PRDX3, SOD2, and GPX4) and by activating the BER system to promote the repair of mtDNA lesions. Therefore, these findings suggest that both iodothyronines are able to reduce mitochondrial oxidative damage in the liver, but through different mechanisms: T2 is more efficient in reducing oxidative insult and inducing repair (Cioffi et al., 2019), while T3 stimulates mitochondrial biogenesis, producing a mitochondrial population enriched with new and less damaged mitochondria (Cioffi et al., 2019).

By activating autophagy, Tb alleviated oxidative stress, as shown by reduced ROS accumulation, in agreement with previously studies (Lihao et al., 2022). In the present study, Tb treatment was also associated with improved mtDNA integrity, suggesting that autophagy-dependent mitochondrial quality control may contribute to the preservation of mitochondrial genome stability. Furthermore, we demonstrated for the first time that Tb treatment improves the expression of BER components, indicating that Tb not only promotes the removal of damaged mitochondria but also reinforces mitochondrial DNA repair capacity.

The combined administration of Tb and T2 showed an integrated and synergistic effect, resulting in a marked reduction of oxidative stress, restoration of mtDNA integrity, and robust activation of the BER pathway. This synergy suggests that autophagy could create a permissive cellular environment in which T2 can more effectively exert its protective actions on mitochondrial function and genome stability (Sinha et al., 2015; Senese et al., 2018).

Oxidative stress-induced mitochondrial damage promotes the release of mitochondrial damage-associated patterns (DAMPs), including mtDNA, which trigger an inflammatory response mediated by the cGAS-STING pathway (Grazioli et al., 2018, Picca et al., 2021). This signalling axis has emerged as a key mechanism linking mitochondrial dysfunction to sterile

inflammation in metabolic diseases, including MASLD (Feng et al., 2025; Yang et al., 2025). Consistent with these observations, Hfd-fed mice, in our study, showed sustained activation of the cGAS-STING-TBK1 axis, which in turn stimulated the NF-κB signalling pathway, accompanied by a reduction in anti-inflammatory regulators such as IL-10 and SOCS3, promoting hepatocyte injury.

Both iodothyronines and Tb counteract activation of the c-GAS-STING cascade; however, this attenuation may reflect a combination of improved mitochondrial quality, reduced metabolic stress, and activation of anti-inflammatory mechanisms. Among treatments, T2 administration exerted a more pronounced anti-inflammatory effect, characterised by strong inhibition of cGAS-STING signalling, decreased phosphorylation of IKBα, concomitantly with a powerfully increased level of IL-10 and SOCS3 expression, in line with previous studies (Giacco et al., 2024; Petito et al., 2021). In addition, IL-10 is known to exert insulin-sensitising effects (Gunnett et al., 2002) and its expression is reduced in obesity, metabolic syndrome, and type 2 diabetes. Accordingly, the increase in IL-10 observed following T2 treatment is consistent with the improvement in insulin sensitising reported in other studies (Petito et al., 2021).

In response to persistent oxidative stress and inflammation, autophagy represents a critical adaptive mechanism aimed at limiting cellular damage.

Consistently, our data demonstrate that autophagy was functionally impaired in HFD-fed mice, as indicated by mTOR-dependent inhibitory phosphorylation of ULK1 at Ser757, which prevents the initiation of the autophagic cascade (Kim et al., 2011). This upstream blockade limits the formation and maturation of autophagosomes and compromises the effective clearance of damaged cellular components, including mitochondria. Consistent with a functional impairment of autophagic flux, in Hfd mice reduction of LC3 expression and p62 accumulation suggested a block of autophagic flux.

Following HFD-induced impairment of autophagic flux, the different treatments modulated the autophagy pathway at distinct regulatory levels. Both iodothyronines reduced mTOR and ULK1 phosphorylation, indicating relief of the upstream inhibitory block on autophagy initiation. However, while T3 treatment was associated with increased LC3IIb and reduced p62 levels, T2 did not significantly affect these downstream markers, suggesting that normalization of upstream signalling alone was insufficient to restore effective autophagic flux. Tb treatment also fully restored autophagic flux, as evidenced by increased LC3II and reduced p62 levels. These data highlight the unique capacity of Tat–Beclin 1 to directly activate bulk autophagy under conditions of chronic metabolic stress (Chen et al., 2024). The combined administration of Tb and T2 exerted a more limited effect, reducing mTOR phosphorylation and p62 levels

without significantly affecting ULK1 or LC3IIb, indicating a partial recovery of autophagic turnover. In Hfd + Tb + T2 mice, autophagic turnover was partially restored, indicating a functional interaction rather than simple additive effects.

Beyond bulk autophagy, selective pathways such as lipophagy and mitophagy play a central role in hepatocellular adaptation to chronic lipid excess.

Lipophagy contributes to the regulation of intracellular lipid stores by targeting lipid droplets for lysosomal degradation. Under conditions of prolonged lipid overload, however, lipophagic efficiency declines, favouring lipid droplet persistence and exacerbating metabolic stress. Our data indicate an impaired activation of lipophagy in Hfd-fed mice, as suggested by upregulation of adipose differentiation–related protein (ADRP), a lipid droplet–associated protein that stabilizes triglyceride stores and limits their accessibility, and the lack of significant changes in the transcription factors TFEB and TFE3. Although this finding contrasts with evidence showing that acute lipid overload promotes lipophagy during the early stages of MASLD (El-Ashmawy et al., 2024), it is in line with reports demonstrating that prolonged lipid excess compromises hepatic lipid clearance through lipophagy, as observed after sustained HFD exposure (Schulze et al., 2017).

Within this framework, T3 treatment modulated key transcriptional regulators of lysosomal biogenesis, consistent with activation of lipophagy-related programs. Notably, T2 exerted a distinct and more selective effect on lipid handling, characterized by induction of TFE3, reduction of ADRP expression, and increased PNPLA3 levels. This molecular profile suggests enhanced accessibility of lipid droplets to catabolic pathways and improved lipid remodelling, supporting the notion that lipophagy represents a preferential mechanism for lipid clearance by iodothyronines (Sinha et al., 2012; Iannucci et al., 2017).

As a direct activator of autophagy, Tat–Beclin 1 preferentially stimulates bulk autophagic pathways. In the setting of excessive lipid accumulation associated with MASLD, autophagy activation may facilitate lipid droplet removal independently of TFEB/TFE-mediated transcriptional reprogramming, in agreement with previous studies (Singa et al., 2009; Chen et al., 2024). Notably, the combined administration of Tat–Beclin 1 and T2 enhanced autophagic activity and generated a molecular profile distinct from either treatment alone, suggesting a functional interaction between selective iodothyronine signalling and pharmacological autophagy activation that extends beyond lipid handling and may impact mitochondrial homeostasis.

The maintenance of hepatocellular function critically depends on mitochondrial integrity (Lin et al., 2020). In this context, mitochondrial quality control (MQC) mechanisms—including

mitochondrial biogenesis, dynamics, and mitophagy—are essential to preserve metabolic homeostasis and limit tissue injury under conditions of chronic metabolic stress (Pickles et al., 2018; Chen et al., 2023; Xu et al., 2025).

In HFD-fed mice, MQC was profoundly disrupted, as indicated by reduced mitochondrial mass and decreased OPA1 expression associated with OMA1 upregulation, and impaired mitophagy. This molecular profile reflects a shift toward stress-induced mitochondrial fragmentation driven by metabolic overload. However, in the setting of impaired autophagic flux, mitochondrial fragmentation failed to translate into effective mitochondrial clearance, thereby favouring the accumulation of dysfunctional mitochondria and amplifying mitochondrial stress (Rivera-Mejías et al., 2023).

T3 administration markedly reshaped MQC by strongly stimulating mitochondrial biogenesis, as demonstrated by the robust upregulation of PGC1α, TFAM, NRF2, and TOM20. In parallel, T3 induced significant changes in mitochondrial dynamics, promoting mitochondrial fission and activating PINK1–Parkin–dependent mitophagy. This coordinated response is consistent with an adaptive mechanism in which an expanded mitochondrial network facilitates the segregation and selective removal of damaged mitochondria, thereby supporting mitochondrial renewal under conditions of increased metabolic demand (Hamacher-Brady et al., 2015; Pickles et al., 2020).

In contrast, T2 exerted a more restrained and selective modulation of MQC, favouring the preservation and functional optimization of the existing mitochondrial pool rather than driving extensive mitochondrial expansion. Although T2 increased the expression of key biogenesis-related markers such as PGC1α, NRF2, and TOM20, this induction was significantly lower than that observed with T3, indicating a balanced stimulation of mitochondrial renewal. Concomitantly, T2 promoted mitochondrial fusion, as indicated by increased mitofusin-2 and OPA1 expression, a mitochondrial configuration associated with improved cristae organization, enhanced respiratory efficiency, and resistance to metabolic stress (Cipolat et al., 2006; Gomes et al., 2011; Cioffi et al., 2022). Importantly, T2 preserved the capacity for selective elimination of dysfunctional mitochondria through activation of PINK1–Parkin–mediated mitophagy, thereby supporting mitochondrial turnover without inducing a hypermetabolic state.

Unlike iodothyronines, Tb did not significantly modulate mitochondrial biogenesis, dynamics, or mitophagy in HFD-fed mice, indicating that autophagy induction alone is insufficient to directly restore MQC under chronic metabolic stress.

Notably, the combined administration of Tb and T2 selectively affected mitochondrial dynamics without promoting mitochondrial biogenesis. The reduction in TFAM expression,

together with the concomitant increase in mitofusin-2 and DRP1, suggests a remodelling of the mitochondrial network characterized by enhanced fusion–fission cycling. This balanced modulation of mitochondrial dynamics may facilitate mitochondrial adaptability and the segregation of damaged organelles, thereby supporting mitochondrial function and resilience in the absence of excessive mitochondrial expansion.

Chronic lipid overload and oxidative stress are known to profoundly impair the mitochondrial respiratory chain in MASLD, leading to defective electron transport, reduced ATP synthesis, and increased electron leakage with further ROS generation (Kowalczyk et al., 2021). HFD feeding in our model was associated with a marked reduction in both the abundance and functional competence of respiratory chain complexes, accompanied by a significant impairment of mitochondrial respiratory capacity. This pattern reflects a state of generalized mitochondrial dysfunction in which structural damage and defective quality control converge to compromise oxidative phosphorylation efficiency, a hallmark of steatotic and insulin-resistant liver described in both experimental models and human MASLD (Miller et al., 2025). T3 administration exerted a strong stimulatory effect on the respiratory chain, in part due to increased expression of electron chain complexes, consistent with the robust activation of mitochondrial biogenesis observed in this and previous studies (Cioffi et al., 2022). Furthermore, the increase in respiratory activity probably reflects more than mitochondrial uncoupling; it could indicate a hypermetabolic state resulting from a hyper-T3 condition, in which mitochondria are driven to oxidise greater quantities of fatty acids to support ATP production even in a context of mild uncoupling (Barbe et al., 2001; Silvestri et al., 2018; Lombardi et al., 2002).

In contrast, T2 preferentially improved mitochondrial respiratory chain function in a more selective manner. Our results showed increased expression of specific complexes (CII and CV), together with the marked stimulation of mitochondrial respiration and in-gel activity of individual complexes (I, II and IV), supporting the idea that T2 acts mainly by regulating electron transport efficiency and optimizing oxidative phosphorylation, consistent with previous findings (Lanni et al., 2005). As demonstrated by previous studies, our results here obtained suggest that, in the presence of lipid excess, T2 not only stimulates fatty acid oxidation but also induces a controlled reduction in mitochondrial efficiency through mild uncoupling, thereby increasing substrate oxidation without proportionally increasing ATP synthesis (Lanni et al., 2005, Cavallo 2016). This idea is strengthened by the T2-induced increase in respiration rates from FADH2- linked substrates, such as succinate, and stimulation of Complex II activity. In addition, this decreases in mitochondrial efficiency induced by T2 may depends, in the

experimental model used, on classical uncoupling proteins or on direct modulation of components of the respiratory chain, particularly cytochrome-c oxidase, a known target of T2 or other fatty acids sensitive uncoupling mitochondrial mechanisms (Goglia et al., 1994; Arnold et al., 1998; Mollica. et al., 2009; Lombardi et al., 2007). In liver T2 has been reported to upregulate UCP2 expression (Silvestri et al., 2019; Grasselli et al., 2012; Iannucci et al., 2017), and UCP2 is known to mediate mitochondrial proton leak in steatotic liver (Serviddio et al., 2008). To determine whether hepatic UCP2 is required for T2- induced mitochondrial uncoupling, further studies may be necessary to clarify its involvement. Specifically, experiments using isolated liver mitochondria and UCP2-knockout animal models are required to elucidate the relative contribution of UCP2 to these pathways. Previous in vitro studies have reported that Tb enhances mitochondrial respiration and ATP production by stimulating autophagy-dependent lipid degradation, thereby increasing substrate availability for oxidative phosphorylation. In HepG2 cells treated with oleic-albumin to induce lipid droplet accumulation, Tb administration increased basal and maximal respiration as well as ATP-linked respiration, supporting a direct coupling between autophagy activation and mitochondrial oxidative metabolism in an acute cellular setting (Chen et al., 2024).

In contrast, in our in vivo model of chronic high-fat diet-induced MASLD, Tb administration alone was unable to restore mitochondrial respiratory capacity. This divergence from in vitro observations likely reflects the profound and sustained mitochondrial dysfunction that characterizes advanced metabolic liver disease, where structural damage to the respiratory chain and impaired mitochondrial quality control limit the ability of increased substrate supply to translate into enhanced oxidative phosphorylation. Under conditions of chronic lipid overload, the activation of autophagy is insufficient to recover oxidative phosphorylation efficiency.

To determine whether autophagy-mediated lipid clearance could synergize with T2-induced mitochondrial activation, we evaluated for the first time the combined administration of Tb and T2 in MASLD. Notably, the combination generated a mitochondrial respiratory profile closely resembling that observed with T2 alone, characterized by a substantial recovery of respiratory activity and improved complex function. These findings suggest that the improvement in mitochondrial bioenergetics is primarily driven by T2, whereas autophagy activation induced by Tb may act as a complementary mechanism, facilitating mitochondrial quality control and lipid substrate turnover without directly contributing to respiratory chain activation.

Conclusions

In this study, long-term high-fat diet feeding under thermoneutral conditions successfully reproduced the main phenotypic, metabolic, and molecular features of MASLD, characterised by hepatic lipid accumulation, dysregulated lipid and cholesterol metabolism, and insulin resistance. Concomitant disruption of thyroid hormone signalling contributed to a state of functional hypothyroidism, further exacerbating metabolic inflexibility. In the liver, excess chronic lipid overload overwhelmed mitochondrial oxidative capacity, leading to oxidative stress, mitochondrial DNA damage, and activation of the cGAS–STING inflammatory pathway. Moreover, alteration in autophagic flux and mitochondrial quality control impaired the removal of dysfunctional organelles, amplifying mitochondrial dysfunction and sustaining inflammatory signalling during disease progression.

Iodothyronines treatment significantly improved multiple aspects of the MASLD phenotype. Both T3 and T2 reduced adiposity and hepatic lipid accumulation by stimulating fatty acid oxidation and lipophagy, and improved insulin signalling, although T2 exerted a more pronounced hypocholesterolaemia effect. At the molecular level, both iodothyronines improved mitochondrial fitness, but through a differential mechanism. T3 primarily acts by stimulating mitochondrial turnover. It reduced mtDNA oxidative damage through activation of BER pathways and promoted mitochondrial population renewal via coordinated induction of mitophagy and mitochondrial biogenesis. This robust activation of biogenesis was accompanied by increased abundance and activity of respiratory chain complexes, likely reflecting a compensatory response to the elevated energetic demand associated with a hypermetabolic, hyperthyroid-like state. Indeed, the systemic thyrotoxic effects observed following T3 administration, including disruption of thyroid hormone homeostasis, limit its use in chronic disease. In contrast, T2 emerged as a metabolically selective modulator that improved mitochondrial function without altering the hypothalamic-pituitary-thyroid axis or inducing cardiovascular toxicity. T2 effectively reduced oxidative stress, strengthening antioxidant defences, and preserved mtDNA integrity by stimulating DNA repair mechanisms, and exerted a marked anti-inflammatory effect. Importantly, T2 modulated MQC primarily by promoting mitochondrial fusion, and optimising functional performance of the existing mitochondrial network, thereby increasing respiratory capacity, and regulating the efficiency of the electron transport chain without excessive mitochondrial expansion.

Tb treatment acted by restoring autophagic flux, probably facilitating the clearance of lipid droplets and damaged cellular components, thereby alleviating hepatic steatosis and cellular stress. Of note, this study provides for the first time that Tb also modulates mitochondrial

genome maintenance by stimulating the expression of BER enzymes. The combined administration of Tb and T2 exerted an overall beneficial effect on MASLD, combining the autophagy-mediated clearance with T2-driven metabolic optimisation of mitochondrial function. However, the effects of the combined treatments were not always synergistic, suggesting that simultaneous modulation of autophagy and mitochondrial metabolism may involve complex regulatory interactions. In this context, excessive or asynchronous activation of mitochondrial turnover and metabolic optimization may limit the efficiency of specific quality control processes. Overall, these findings identify mitochondrial dysfunction and impaired quality control as a central pathogenic node in MASLD and highlight the therapeutic potential of strategies targeting mitochondrial metabolism and autophagic pathways. Although the mechanistic interaction between T2 and Tb remains incompletely defined, the present data suggest that the coordinated modulation of mitochondrial metabolism and autophagic flux may represent a promising and mechanistically grounded approach for the treatment of chronic metabolic liver disease, deserving further investigation through targeted in vitro and in vivo studies.

References

1. A. Lombardi, P. de Lange, E. Silvestri, R. A. Busiello, A. Lanni, F. Goglia, and M. Moreno. 3,5-Diiodo-L -thyronine rapidly enhances mitochondrial fatty acid oxidationrate and thermogenesis in rat skeletal muscle: AMP-activated proteinkinase involvement. Am J Physiol Endocrinol Metab 296: E497–E502, 2009.
2. Almanza A, Carlesso A, Chintha C, Creedican S, Doultsinos D, Leuzzi B, et al. Endoplasmic reticulum stress signalling - from basic mechanisms to clinical applications. FEBS J. 2019;286:241–78.
3. Al-Shoumer KA, Vasanthy BA, Al-Zaid MM. Effects of treatment of hyperthyroidism on glucose homeostasis, insulin secretion, and markers of bone turnover. Endocr Pract. 2006 Mar-Apr;12(2):121-30. doi: 10.4158/EP.12.2.121. PMID: 16690458
4. Amaravadi, R., Kimmelman, A. C., & White, E. (2016). Recent insights into the function of autophagy in cancer. Genes & Development, 30(17), 1913–1930.
5. Antonelli, A., Fallahi, P., Ferrari, S. M., Di Domenicantonio, A., Moreno, M., Lanni, A., & Goglia, F. (2011). 3,5-Diiodo-L-thyronine increases resting metabolic rate and reduces body weight without undesirable side effects. Journal of Biological Regulators and Homeostatic Agents, 25(4), 655–660.
6. Araki O., Ying H., Zhu X.G., Willingham M.C., Cheng S.Y. Distinct dysregulation of lipid metabolism by unliganded thyroid hormone receptor isoforms. Mol. Endocrinol. 2009;23:308–315.
7. Arias E, Cuervo AM, 2011. Chaperone-mediated autophagy in protein quality control. Curr. Opin. Cell Biol 23 (2), 184–189.
8. Arnold S, Goglia F, Kadenbach B. 3,5-Diiodothyronine binds to subunit Va of cytochrome-c oxidase and abolishes the allosteric inhibition of respiration by ATP. Eur J Biochem. 1998;252(2):325–330.
9. Atici, A.E.; Crother, T.R.; Noval Rivas, M. Mitochondrial Quality Control in Health and Cardiovascular Diseases. Front. Cell Dev. Biol. 2023, 11, 1290046.
10. Axelband, F., Dias, J., Ferrão, F.M., Einicker-Lamas, M.J., 2011. Nongenomic signaling pathways triggered by thyroid hormones and their metabolite 3-iodothyronamine on the cardiovascular system. J. Cell. Physiol. 226 (1), 21–28.
11. Baratta F, Pastori D, Del Ben M, Polimeni L, Labbadia G, Di Santo S, et al. Reduced lysosomal acid lipase activity in adult patients with non-alcoholic fatty liver disease. EBioMedicine. 2015;2:750–4.
12. Barber, G. N. (2015). STING: Infection, inflammation and cancer. Nature Reviews Immunology, 15(12), 760–770.
13. Barbhuiya, A. P., Yoshitomi, R., & Pathak, P. M. (2025). Understanding the link between sterol regulatory element-binding proteins (SREBPs) and metabolic dysfunction-associated steatotic liver disease (MASLD). Current Obesity Reports, 14(1), 36.

14. Baselli GA, Jamialahmadi O, Pelusi S, Ciociola E, Malvestiti F, Saracino M, et al. Rare ATG7 genetic variants predispose patients to severe fatty liver disease. J Hepatol. 2022;77:596–606
15. Baselli, G. A., Jamialahmadi, O., Pelusi, S., Ciociola, E., Malvestiti, F., Saracino, M., ... & Valenti, L. (2022). Rare ATG7 genetic variants predispose patients to severe fatty liver disease. Journal of Hepatology, 77(3), 596–606. Doi:10.1016/j.jhep.2022.03.031
16. Bassett, J. H., Harvey, C. B., & Williams, G. R. (2003). Mechanisms of thyroid hormone receptor-specific nuclear and extra nuclear actions. Molecular and Cellular Endocrinology, 213(1), 1–11. Doi:10.1016/j.mce
17. Begriche, K., Igoudjil, A., Pessayre, D., & Fromenty, B. (2013). Mitochondrial dysfunction in nonalcoholic steatohepatitis (NASH): Causes, consequences and possible means to prevent it. Mitochondrion, 13(1), 1–13. Doi: 10.1016/j.mito.2012.10.007
18. Begriche, K., Massart, J., Robin, M. A., Bonnet, F., & Fromenty, B. (2013). Mitochondrial adaptations and dysfunctions in nonalcoholic fatty liver disease. Journal of Hepatology, 58(1), 149–160. Doi: 10.1016/j.jhep.2012.08.027
19. Bergh, J. J., Lin, H. Y., Lansing, L., Mohamed, S. N., Davis, F. B., Mousa, S., & Davis, P. J. (2005). Integrin αVβ3 contains a cell surface receptor site for thyroid hormone that is linked to activation of mitogen-activated protein kinase and induction of angiogenesis. Endocrinology, 146(7), 2864–2871. Doi: 10.1210/en.2005-0141
20. Betlejewska, J., Hubska, J., Roszkowska, Z., Maciejczyk, A., Bachurska, D., Domański, J., Miarka, M., Raszeja-Wyszomirska, J., Bobrowicz, M., & Ambroziak, U. (2025). Endocrine disorders and metabolic dysfunction–associated steatotic liver disease: A narrative review. Endocrine Reviews.
21. Bigler, J., & Eisenman, R. N. (1988). c-erbA encodes multiple proteins in chicken erythroid cells. Molecular and Cellular Biology, 8(10), 4155–4161. Doi:10.1128/MCB.8.10.4155
22. Billingham, L. K., Stoolman, J. S., Vasan, K., Rodriguez, A. E., Poor, T. A., Szibor, M., ... & Chandel, N. S. (2022). Mitochondrial electron transport chain is necessary for NLRP3 inflammasome activation. Nature Immunology, 23(5), 692–704. https://doi.org/10.1038/s41590-022-01153-7
23. Birkenfeld AL, Shulman GI, 2014. Nonalcoholic fatty liver disease, hepatic insulin resistance, and type 2 diabetes. Hepatology 59 (2), 713–723.
24. Birkenfeld, A. L., Lee, H. Y., Majumdar, S., Jurczak, M. J., Camporez, J. P., Jornayvaz, F. R., & Shulman, G. I. (2011). Influence of the hepatic eukaryotic initiation factor 2α (eIF2α) endoplasmic reticulum (ER) stress response pathway on insulin-mediated ER stress, hepatic and peripheral glucose metabolism. Journal of Biological Chemistry, 286(41), 36163–36170. Doi: 10.1074/jbc.M111. 228817
25. Bohinc, B. N., Michelotti, G., Xie, G., Pang, H., Suzuki, A., Guy, C. D., & Diehl, A. M. (2014). Repair-related activation of Hedgehog signaling in stromal cells promotes intrahepatic hypothyroidism. Endocrinology, 155(11), 4591–4601. Doi: 10.1210/en.2014-1302

26. Bradley, D.J., Towle, H.C. & Young, W.S. III 1994. Alpha and beta thyroid hormone receptor (TR) gene expression during auditory neurogenesis: evidence for TR isoform-specific transcriptional regulation in vivo. Proc Natl Acad Sci USA 91, 439–443.
27. Brent, G. A. (2012). Mechanisms of thyroid hormone action. The Journal of Clinical Investigation, 122(9), 3035–3043.
28. Bruinstroop, E.; Dalan, R.; Cao, Y.; Bee, Y.M.; Chandran, K.; Cho, L.W.; Soh, S.B.; Teo, E.K.; Toh, S.A.; Leow, M.K.S.; et al. Low-Dose Levothyroxine Reduces Intrahepatic Lipid Content in PatientsWith Type 2 Diabetes Mellitus and NAFLD. J. Clin. Endocrinol. Metab. 2018, 103, 2698–2706.
29. C. D. A. Maldonado-Rojas, J. M. Zuarth-Vazquez, M. Uribe, and V. J. Barbero-Becerra, "Insulin Resistance and Metabolic Dysfunction-Associated Steatotic Liver Disease (MASLD): Pathways of Action of Hypoglycemic Agents," Annals of Hepatology 29, no. 2 (2024): 101182.
30. Cannon B, Nedergaard J. Brown adipose tissue: function and physiological significance. Physiol Rev 84: 277–359, 2004.
31. Carazo A., Levin J., Casas F., Seyer P., Grandemange S., Busson M., Pessemesse L., Wrutniak-Cabello C., Cabello G. Protein sequences involved in the mitochondrial import of the 3,5,3′-L-triiodothyronine receptor p43. J. Cell. Physiol. 2012;227:3768–3777. doi:10.1002/jcp.24085.
32. Casanova, A.; Wevers, A.; Navarro-Ledesma, S.; Pruimboom, L. Mitochondria: It Is All about Energy. Front. Physiol. 2023, 14, 1114231.
33. Caturano, A., Erul, E., Nilo, R., Nilo, D., Russo, V., Rinaldi, L., Acierno, C., Akkus, E., Koudelkova, K., Cerini, F., & Rizzo, A. (2025). Metabolic dysfunction-associated steatotic liver disease, insulin resistance and hepatocellular carcinoma: A deadly triad. European Journal of Clinical Investigation. Advance online publication. https://doi.org/10.1111/eci.70132
34. Cavallo, A.; Gnoni, A.; Conte, E.; Siculella, L.; Zanotti, F.; Papa, S.; Gnoni, G.V. 3,5-diiodo-L-thyronine increases FoF1-ATP synthase activity and cardiolipin level in liver mitochondria of hypothyroid rats. J. Bioenergy Biomembr. 2011, 43, 349–357.
35. Chan, I.H., Privalsky, M.L., 2010. A conserved lysine in the thyroid hormone receptor-alpha1 DNA-binding domain, mutated in hepatocellular carcinoma, serves as a sensor for transcriptional regulation. Mol. Cancer Res. 8 (1), 15–23.
36. Chao X, Qian H, Wang S, Fulte S, Ding W-X, 2020. Autophagy and liver cancer. Clin. Mol. Hepatol 26 (4), 606.
37. Chauvier D, Ankri S, Charriaut-Marlangue C, Casimir R, Jacotot E. Broad-spectrum caspase inhibitors: from myth to reality? Cell Death Differ. 2007;14:387–91.
38. Chen Q, Sun L & Chen ZJ Regulation and function of the cGAS-STING pathway of cytosolic DNA sensing. Nat. Immunol 17, 1142–1149 (2016).
39. Chen, C.-L.; Huang, F.-F.; Lin, H.-F.; Wu, C.-C.; Ni, Y.-H.; Lin, Y.-C. (2024). Tat-Beclin-1 Peptide Ameliorates Metabolic Dysfunction-Associated Steatotic Liver Disease by Enhancing Hepatic Autophagy. International Journal of Molecular Sciences, 25(22), 12372.
40. Chen, W., Zhao, H., & Li, Y. (2023). Mitochondrial dynamics in health and disease: Mechanisms and potential targets. Signal Transduction and Targeted Therapy, 8, 333.

41. Cheng SY. Multiple mechanisms for regulation of the transcriptional activity of thyroid hormone receptors. Rev Endocr Metab Disord. 2000 Jan;1(1-2):9-18.
42. Cheng, S.Y., Leonard, J.L. & Davis, P.J. 2010. Molecular aspects of thyroid hormone actions. Endocr Rev 31, 139–170.
43. Chi H.C., Chen S.L., Lin S.L., Tsai C.Y., Chuang W.Y., Lin Y.H., Huang Y.H., Tsai M.M., Yeh C.T., Lin K.H. Thyroid hormone protects hepatocytes from HBx-induced carcinogenesis by enhancing mitochondrial turnover. Oncogene. 2017;36:5274–5284. doi: 10.1038/onc.2017.136.
44. Chi H.C., Chen S.L., Lin S.L., Tsai C.Y., Chuang W.Y., Lin Y.H., Huang Y.H., Tsai M.M., Yeh C.T., Lin K.H. Thyroid hormone protects hepatocytes from HBx-induced carcinogenesis by enhancing mitochondrial turnover. Oncogene. 2017;36:5274–5284).
45. Chi H.C., Tsai C.Y., Tsai M.M., Yeh C.T., Lin K.H. Molecular functions and clinical impact of thyroid hormone-triggered autophagy in liver-related diseases. J. Biomed. Sci. 2019;26:24. doi: 10.1186/s12929-019-0517-x.
46. Chi H.C., Tsai C.Y., Tsai M.M., Yeh C.T., Lin K.H. Molecular functions and clinical impact of thyroid hormone-triggered autophagy in liver-related diseases. J. Biomed. Sci. 2019;26:24,
47. Chino H, Mizushima N, 2020. ER-phagy: quality control and turnover of endoplasmic reticulum. Trends Cell Biol. 30 (5), 384–398.
48. Chng, C.-L., Goh, G. B. B., & Yen, P. M. (2025). Metabolic and functional cross talk between the thyroid and liver. Thyroid, 35(6).
49. Choi AM, Ryter SW, Levine B, 2013. Autophagy in human health and disease. N. Engl. J. Med 368 (19), 1845–1846.
50. Choi, C.S., Savage, D.B., Kulkarni, A., Yu, X.X., Liu, Z.X., Morino, K., Kim, S., Distefano, A., Samuel, V.T., Neschen, S., et al. (2007). Suppression of diacylglycerol acyltransferase-2 (DGAT2), butnot DGAT1,withantisenseoligonucleotides reverses diet-induced hepatic steatosis and insulin resistance. J. Biol. Chem. 282, 22678–22688.
51. Chopra IJ 1976 An assessment of daily production and significance of thyroidal secretion of 3,30,50-triiodothyronine (reverse T3) in man. J Clin Invest 58:32–40.
52. Chung, G.E.; Kim, D.; Kim, W.; Yim, J.Y.; Park, M.J.; Kim, Y.J.; Yoon, J.H.; Lee, H.S. Non-Alcoholic Fatty Liver Disease across the Spectrum of Hypothyroidism. J. Hepatol. 2012, 57, 150–156.
53. Cimmino M, et al. 3,5-Diiodo-L-thyronine restores resting metabolic rate and lipid oxidation in hypothyroid rats. J Endocrinol. 1999;162(3):515–522.
54. Cioffi F, Lanni A, Goglia F. Thyroid hormones, mitochondrial bioenergetics and lipid handling. Curr Opin Endocrinol Diabetes Obes. 2010;17:402–407.
55. Cioffi F, Senese R, Lanni A, Goglia F. Thyroid hormones and mitochondria: with a brief look at derivatives and analogues. Mol Cell Endocrinol 2013; 379: 51-61.
56. Cioffi, F., Giacco, A., Petito, G., de Matteis, R., Senese, R., Lombardi, A., de Lange, P., Moreno, M., Goglia, F., & Silvestri, E. (2022). Altered mitochondrial quality control in rats with metabolic dysfunction-associated fatty liver disease (MAFLD) induced by high-fat feeding. Genes, 13(2), 315.

57. Cioffi, F., Senese, R., Lasala, P., Ziello, A., Mazzoli, A., Crescenzo, R., Liverini, G., Lanni, A., Goglia, F., & Iossa, S. (2017). Fructose-rich diet affects mitochondrial DNA damage and repair in rats. Nutrients, 9(4), 323.
58. Cioffi, F., Senese, R., Petito, G., Lasala, P., de Lange, P., Silvestri, E., et al. (2019). Both 3,3′,5-triiodothyronine and 3,5-diiodo-L-thyronine are able to repair mitochondrial DNA damage but by different mechanisms. Frontiers in Endocrinology, 10, 216.
59. Cipolat, S., Martins de Brito, O., Dal Zilio, B., & Scorrano, L. (2006). OPA1 requires mitofusin 1 to promote mitochondrial fusion. Proceedings of the National Academy of Sciences USA, 103, 11518–11523.
60. Clausen T, Van Hardeveld C, Everts ME. Significance of cation transport in control of energy metabolism and thermogenesis. Physiol Rev 71: 733–774, 1991.
61. Cody, V., Davis, P.J., Davis, F.B., 2007. Molecular modeling of the thyroid hormone interactions with alpha v beta 3 integrin. Steroids 72 (2), 165–170.
62. Cook, C.B., Kakucska, I., Lechan, R.M. & Koenig, R.J. 1992. Expression of thyroid hormone receptor beta 2 in rat hypothalamus. Endocrinology 130, 1077–1079.
63. D. Zhang, Y. Zhao, G. Zhang, et al., "Suppression of Hepatic ChREBP*a*-CYP2C50 Axis-Driven
64. da Silva Teixeira S, Filgueira C, Sieglaff DH, Benod C, Villagomez R, Minze LJ, Zhang A et al. 3,5-diiodothyronine (3,5-T2) reduces blood glucose independently of insulin sensitization in obese mice. Acta Physiol (Oxf). 2017; 220(2):238-250.
65. Dai, G., Levy, O. & Carrasco, N. 1996. Cloning and characterization of the thyroid iodide transporter. Nature 379,458–460.
66. Damiano, F.; Rochira, A.; Gnoni, A.; Siculella, L. Action of Thyroid Hormones, T3 and T2, on Hepatic Fatty Acids: Differences in Metabolic Effects and Molecular Mechanisms. Int. J. Mol. Sci. 2017, 18, 744.
67. Darras, V.M. & Van Herck, S.L. 2012. Iodothyronine deiodinase structure and function: from ascidians to humans. J Endocrinol 215, 189–206.
68. Davis PJ, Davis FB, Mousa SA, Luidens MK, Lin HY. Membrane receptor for thyroid hormone: physiologic and pharmacologic implications. *Annual Review of Pharmacology and Toxicology*. 2011;51:99–115.
69. Davis PJ, Goglia F, Leonard JL. 2016. Nongenomic actions of thyrid hormone. Nat Rev Endocrinol 17:111–121.
70. de Jesus LA, Carvalho SD, Ribeiro MO, Schneider M, Kim SW, Harney JW, Larsen PR, Bianco AC. The type 2 iodothyronine deiodinase is essential for adaptive thermogenesis in brown adipose tissue. J Clin Invest. 2001 Nov;108(9):1379-85.
71. de Lange P, Cioffi F, Senese R, et al. Nonthyrotoxic prevention of diet-induced insulin resistance by 3,5-diiodo-L-thyronine in rats. Diabetes. 2011;60:2730–2739.
72. de Lange P, Cioffi F, Senese R, Moreno M, Lombardi A, Silvestri E, De Matteis R, Lionetti L, Mollica MP, Goglia F, Lanni A. Nonthyrotoxic prevention of diet-induced insulin resistance by 3,5-diiodo-L-thyronine in rats. Diabetes 2011; 60: 2730-2739 [PMID: 21926273.
73. de Lange P, Moreno M, Silvestri E, Lombardi A, Goglia F, Lanni A. Fuel economy in food-deprived skeletal muscle: signaling pathways and regulatory mechanisms. FASEB J 2007; 21: 3431-3441. 2005.

74. de Lange P, Senese R, Moreno M, et al. The role of 3,5-diiodo-L-thyronine (T2) in energy metabolism. Front Endocrinol. 2021;12:706337.
75. De Stefani, D., Raffaello, A., Teardo, E., Szabo, I., Rizzuto, R., 2011. A forty-kilodalton protein of the inner membrane is the mitochondrial calcium uniporter. Nature 476, 336–340.
76. DeBosch BJ, Heitmeier MR, Mayer AL, Higgins CB, Crowley JR, Kraft TE, Chi M, Newberry EP, Chen Z, Finck BN, Davidson NO, Yarasheski KE, Hruz PW, Moley KH, 2016. Trehalose inhibits solute carrier 2A (SLC2A) proteins to induce autophagy and prevent hepatic steatosis. Sci. Signal 9 (416), ra21.
77. Desouza, L.A., Ladiwala, U., Daniel, S.M., Agashe, S., Vaidya, R.A., Vaidya, V.A., 2005. Thyroid hormone regulates hippocampal neurogenesis in the adult rat brain. Mol. Cell. Neurosci. 29 (3), 414–426.
78. Deter RL, Baudhuin P, De Duve C, 1967. Participation of lysosomes in cellular autophagy induced in rat liver by glucagon. J. Cell Biol 35 (2), C11–C16.
79. Dewidar B, Mastrototaro L, Englisch C, Ress C, Granata C, Rohbeck E, et al. Alterations of hepatic energy metabolism in murine models of obesity, diabetes and fatty liver diseases. EBioMedicine. 2023;94:104714.
80. Di Micco, G. Frera, J. Lugrin, Y. Jamilloux, E.T. Hsu, A. Tardivel, A. De Gassart, L. Zaffalon, B. Bujisic, S. Siegert, et al. AIM2 inflammasome is activated by pharmacological disruption of nuclear envelope integrity. Proc. Natl. Acad. Sci. USA, 113 (2016), pp. E4671-E4680.
81. Dias, K. A., Oliveira, L. A., Pereira, S. M. S., et al. (2025). Anti-inflammatory and antioxidant effects of anthocyanins in nonalcoholic fatty liver disease (NAFLD): A systematic review of in vivo studies. Critical Reviews in Food Science and Nutrition, 1–18.
82. Ding WX, 2010. Role of autophagy in liver physiology and pathophysiology. World J. Biol. Chem 1 (1), 3–12.
83. Ding, Q.; Qi, Y.; Tsang, S.-Y. Mitochondrial, Mitochondrial Dynamics, and Mitophagy in the Maturation of Cardiomyocytes. Cells 2021, 10, 2463.
84. Dinkova-Kostova, A. T., & Abramov, A. Y. (2015). The emerging role of Nrf2 in mitochondrial function. Free Radical Biology and Medicine, 88(Part B), 179–188.
85. Dummler, K.; Muller, S.; Seitz, H.J. Regulation of adenine nucleotide translocase and glycerol 3-phosphate dehydrogenase expression by thyroid hormones in different rat tissues. Biochem. J. 1996, 317, 913–918.
86. Einer C, Hohenester S, Wimmer R, Wottke L, Artmann R, Schulz S, et al. Mitochondrial adaptation in steatotic mice. Mitochondrion. 2018;40:1–12. doi: 10.1016/j.mito.2017.08.015.
87. El-Ashmawy, N. E., Khedr, E. G., Al-Ashmawy, G. M., & Kamel, A. A. (2024). Emerging role of natural lipophagy modulators in metabolic dysfunction–associated steatotic liver disease. Nutrition, 126, 112517.
88. Elbadawy, M., Tanabe, K., Yamamoto, H., et al. (2023). Evaluation of the efficacy of mitochondrial fission inhibitor (Mdivi-1) using non-alcoholic steatohepatitis (NASH) liver organoids. Frontiers in Pharmacology, 14, 1243258.

89. Erion, D. M., Ignatova, I. D., Yonemitsu, S., Nagai, Y., Chatterjee, P., Weismann, D., Hsiao, J. J., Zhang, D., Iwasaki, T., Stark, R., Flannery, C., Kahn, M., Carmean, C. M., Yu, X. X., Murray, S. F., Bhanot, S., Monia, B. P., Cline, G. W., Samuel, V. T., & Shulman, G. I. (2009). Prevention of hepatic steatosis and hepatic insulin resistance by knockdown of cAMP response element-binding protein. Cell Metabolism, 10(6), 499–511.
90. Evans RM. The steroid and thyroid hormone receptor superfamily. Science. 1988 May 13;240(4854):889-95. doi: 10.1126/science.3283939. PMID: 3283939; PMCID: PMC6159881.
91. Faber J, Kirkegaard C, Lumholtz IB, Siersbaek-Nielsen K, Friis T. Simultaneous measurement of 3,5-diiodothyronine and 3,5,3'-triiodothyronine turnover kinetics in euthyroid hyperthyroid, and hypothyroid subjects. J Clin Endocrinol Metab. (1982) 55:8–12.
92. Fan L, Gokaltun A, Maggipinto S, Kitagawa Y, Martyn J, Yeh H, et al. Alterations in Cytoskeleton and Mitochondria in the development and reversal of steatosis in human hepatocytes. Cell Mol Gastroenterol Hepatol. 2023;16:243–61.
93. Fan Y, Wang N, Rocchi A, Zhang W, Vassar R, Zhou Y, He C, 2017. Identification of natural products with neuronal and metabolic benefits through autophagy induction. Autophagy 13 (1), 41–56.
94. Farach-Carson, M.C., Davis, P.J., 2003. Steroid hormone interactions with target cells: cross talk between membrane and nuclear pathways. J. Pharmacol. Exp. Ther. 307 (3), 839–845.
95. Fatty Acid Oxidation Sensitizes Mice to Diet-Induced MASLD/MASH," Molecular Metabolism 85 (2024): 101957.
96. Feige JN, Lagouge M, Canto C, Strehle A, Houten SM, Milne JC, Lambert PD, Mataki C, Elliott PJ, Auwerx J. Specific SIRT1 activation mimics low energy levels and protects against diet-induced metabolic disorders by enhancing fat oxidation. Cell Metab 2008; 8: 347-358.
97. Fenton, A. R., Jongens, T. A., & Holzbaur, E. L. F. (2020). Mitochondrial dynamics: Shaping and remodeling an organelle network. Current Opinion in Cell Biology, 68, 28–36.
98. Ferrandino, G.; Kaspari, R.R.; Spadaro, O.; Reyna-Neyra, A.; Perry, R.J.; Cardone, R.; Kibbey, R.G.; Shulman, G.I.; Dixit, V.D.; Carrasco, N. Pathogenesis of Hypothyroidism-Induced NAFLD Is Driven by Intra- and Extrahepatic Mechanisms. Proc. Natl. Acad. Sci. USA 2017, 114, E9172–E9180.
99. Ferrer MD, Reynés C, Monserrat-Mesquida M, Quetglas-Llabrés M, Bouzas C, García S, et al. Polyunsaturated and Saturated Oxylipin plasma levels allow monitoring the non-alcoholic fatty liver disease progression to severe stages. Antioxid (Basel). 2023.
100. Folli F, Saad MJA, Backer JM, Kahn CR. Insulin stimulation of phosphatidylinositol 3-kinase activity and association with insulin receptor substrate 1 in liver and muscle of the intact rat. J Biol Chem 267: 22171–22177, 1992
101. Forini F, Nicolini G, Kusmic C, Iervasi G. Protective effects of euthyroidism restoration on mitochondria function and quality control in cardiac pathophysiology. Int J Mol Sci. (2019) 20:3377. ; Na W, Fu L, Luu N, Shi YB. Thyroid hormone directly

activates mitochondrial fission process 1 (Mtfp1) gene transcription during adult intestinal stem cell development and proliferation in Xenopus tropicalis. Gen Comp Endocrinol. (2020).

102. Frankovic, I., Zeljkovic, A., Djuricic, I., Ninic, A., Vekic, J., Derikonjic, M., Erceg, S., Tomasevic, R., Mamic, M., & Gojkovic, T. (2025). Metabolic dysfunction-associated steatotic liver disease is characterized by enhanced endogenous cholesterol synthesis and impaired synthesis/absorption balance. International Journal of Molecular Sciences, 26(15), 7462.

103. Fu, W., Wang, J., Lu, N., et al. (2025). Unveiling the crucial nexus: Mitochondrial quality control as a central driver in metabolic dysfunction-associated steatotic liver disease pathogenesis. Cell Proliferation, e70141.https://doi.org/10.1111/cpr.70141.

104. Fuchs CD, Radun R, Dixon ED, Mlitz V, Timelthaler G, Halilbasic E, et al. Hepatocyte-specific deletion of adipose triglyceride lipase (adipose triglyceride lipase/patatin-like phospholipase domain containing 2) ameliorates dietary induced steatohepatitis in mice. Hepatology (Baltimore MD). 2022;75:125–39.

105. Fukuo Y, Yamashina S, Sonoue H, Arakawa A, Nakadera E, Aoyama T, Uchiyama A, Kon K, Ikejima K, Watanabe S, 2014. Abnormality of autophagic function and cathepsin expression in the liver from patients with non-alcoholic fatty liver disease. Hepatol. Res 44 (9), 1026–1036.

106. G. Wilcox, “Insulin and Insulin Resistance,” Clinical Biochemist Reviews 26 (2005): 19–39.

107. G.P. Meares, Y. Liu, R. Rajbhandari, H. Qin, S.E. Nozell, J.A. Mobley, J.A. Corbett, E.N. Benveniste. PERK-dependent activation of JAK1 and STAT3 contributes to endoplasmic reticulum stress-induced inflammation. Mol. Cell. Biol., 34 (2014), pp. 3911-392

108. Gao, S.; Hu, J. Mitochondrial Fusion: The Machineries in and Out. Trends Cell Biol. 2021, 31, 62–74.

109. Garstka, H. L., Schmitt, W. E., Schultz, J., Sogl, B., Silakowski, B., Pérez-Martos, A., Montoya, J., & Wiesner, R. J. (2003). Import of mitochondrial transcription factor A (TFAM) into rat liver mitochondria stimulates transcription of mitochondrial DNA. Nucleic acids research, 31(17), 5039–5047.

110. Gaspari M, Larsson NG, Gustafsson CM. The transcription machinery in mammalian mitochondria. Biochim Biophys Acta 2004; 1659: 148-152.

111. Gelen V, Sengul E, Yildirim S, Cinar İ. The role of GRP78/ATF6/IRE1 and caspase-3/Bax/Bcl2 signaling pathways in the protective effects of gallic acid against cadmium-induced liver damage in rats. Iran J Basic Med Sci. 2023;26:1326–33.

112. Giacco, A., Petito, G., Silvestri, E., Scopigno, N., Vigliotti, M., Mercurio, G., de Lange, P., Lombardi, A., Moreno, M., Goglia, F., Lanni, A., Senese, R., & Cioffi, F. Comparative effects of 3,5-diiodo-L-thyronine and 3,5,3′-triiodo-L-thyronine on mitochondrial damage and cGAS/STING-driven inflammation in liver of hypothyroid rats. Frontiers in Endocrinology.

113. Giacco, A.; Delli Paoli, G.; Senese, R.; Cioffi, F.; Silvestri, E.; Moreno, M.;

of fatty acids and their derived acylcarnitines determines the direct effect of metabolically active thyroid hormones on insulin sensitivity in skeletal muscle cells. FASEB J. 2019, 33, 1811–1823.
114. Giammanco M, Di Liegro CM, Schiera G, Di Liegro I. Genomic and Non-Genomic Mechanisms of Action of Thyroid Hormones and Their Catabolite 3,5-Diiodo-L-Thyronine in Mammals. Int J Mol Sci. 2020 Jun 10;21(11):4140. doi: 10.3390/ijms21114140. PMID: 32532017; PMCID: PMC7312989.
115. Giammanco, M., Di Majo, D., La Guardia, M., Aiello, S., Crescimanno, M., Flandina, C., & Cefalù, A. B. (2016). Effects of 3,5-diiodothyronine on hepatic steatosis in high-fat diet rats. Journal of Biological Regulators and Homeostatic Agents, 30(2), 327–335.
116. Gionfra, F.; De Vito, P.; Pallottini, V.; Lin, H.-Y.; Davis, P.J.; Pedersen, J.Z.; Incerpi, S. The Role of Thyroid Hormones in Hepatocyte Proliferation and Liver Cancer. Front. Endocrinol. 2019, 10, 532.
117. Gnocchi D, et al. 3,5-Diiodo-L-thyronine activates Akt signaling and reduces lipid accumulation in primary rat hepatocytes. Mol Cell Endocrinol. 2016;425:1–11.
118. Goglia F, et al. Biological effects of 3,5-diiodo-L-thyronine (T2): new insights into thyroid hormone action. Mol Cell Endocrinol. 2016;458:95–102.
119. Goglia F, Moreno M, Lanni A, et al. Thyroid hormone metabolites and mitochondrial metabolism. Biochim Biophys Acta. 1980;639(1):1–17.
120. Goglia F, Moreno M, Lanni A. Action of thyroid hormones at the cellular level: the mitochondrial target. FEBS Lett 1999; 452: 115-120.
121. Goglia F, Torresani J, Bugli P, Barletta A, Liverini G. In vitro binding of triiodothyronine to rat liver mitochondria. Pflugers Arch 1981; 390: 120-124.
122. Goglia, F., Silvestri, E., & Lanni, A. (2002). Thyroid hormones and mitochondria. Bioscience Reports, 22(1), 17–32.
123. Goglia, F., Torresani, J., Bugli, P., Barletta, A. & Liverini, G. In vitro binding of triiodothyronine to rat liver mitochondria. Pflugers Arch. 390, 120–124 (1981).
124. Goglia, F.; Skulachev, V.P. A function for novel uncoupling proteins: Antioxidant defense of mitochondrial matrix by translocating fatty acid peroxides from the inner to the outer membrane leaflet. FASEB J. 2003, 17, 1585–1591.
125. Goh, E. C., Kim, D., Kim, W., Yim, J. Y., Park, M. J., Kim, Y. J., Yoon, J.-H., & Lee, H.-S. (2013). Non-alcoholic fatty liver disease across the spectrum of hypothyroidism. Journal of Hepatology, 57(1), 150–156.
126. Goldberg IJ, Huang LS, Huggins LA, Yu S, Nagareddy PR, Scanlan TS, Ehrenkranz JR. Thyroid hormone reduces cholesterol via a non-LDL receptor-mediated pathway. Endocrinology 2012; 153: 5143-5149.
127. Goldstein JL, DeBose-Boyd RA, Brown MS. Protein sensors for membrane sterols. Cell 124: 35–46, 2006.
128. Gomes, L. C., Di Benedetto, G., & Scorrano, L. (2011). During autophagy mitochondria elongate to sustain cellular ATP levels. Nature Cell Biology, 13, 589–598.
129. Gonzalez-Rodriguez A, Mayoral R, Agra N, Valdecantos MP, Pardo V, Miquilena-Colina ME, Vargas-Castrillon J, Lo Iacono O, Corazzari M, Fimia GM, Piacentini M, Muntane J, Bosca L, Garcia-Monzon C, Martin-Sanz P, Valverde AM,

2014. Impaired autophagic flux is associated with increased endoplasmic reticulum stress during the development of NAFLD. Cell Death Dis. 5, e1179.

130. Grasselli E, Canesi L, Voci A, De Matteis R, Demori I, Fugassa E, Vergani L. Effects of 3,5-diiodo-L-thyronine administration on the liver of high fat diet-fed rats. Exp Biol Med (Maywood) 2008; 233: 549-557.

131. Grasselli E, Voci A, Canesi L, Goglia F, Ravera S, Panfoli I, Gallo G, Vergani L. Non-receptor-mediated actions are responsible for the lipid-lowering effects of iodothyronines in FaO rat hepatoma cells. *Journal of Endocrinology*. 2011;210(1):59–69.

132. Grasselli E, Voci A, Canesi L, et al. Direct mitochondrial actions of 3,5-Diiodo- L-thyronine (T2) in hepatoma cells lacking thyroid hormone receptors. Cell Physiol Biochem. 2011b;28(5):743–752.

133. Grasselli E, Voci A, Demori I, et al. 3,5-Diiodo-L-thyronine modulates lipid-handling proteins and stimulates mitochondrial oxidative metabolism in fatty hepatocytes. J Endocrinol. 2016;228(1):1–12.

134. Grattagliano I, de Bari O, Bernardo TC, Oliveira PJ, Wang DQ, Portincasa P. Role of mitochondria in nonalcoholic fatty liver disease--from origin to propagation. Clin Biochem 2012; 45: 610-618 [PMID: 22484459.

135. Grazioli, S., & Pugin, J. (2018). Mitochondrial damage-associated molecular patterns: From inflammatory signaling to human diseases. Frontiers in Immunology, 9, 832.

136. Greatorex S, Kaur S, Xirouchaki CE, Goh PK, Wiede F, Genders AJ, et al. Mito- chondria- and NOX4-dependent antioxidant defense mitigates progression to nonalcoholic steatohepatitis in obesity. J Clin Invest. 2023;134.

137. Green, A.; Hossain, T.; Eckmann, D.M. Mitochondrial Dynamics Involves Molecular and Mechanical Events in Motility, Fusion and Fission. Front. Cell Dev. Biol. 2022, 10, 1010232.

138. Gregory, R. B., & Berry, M. N. (1991). Administration of triiodothyronine lowers mitochondrial membrane potential in hepatocytes. Biochimica et Biophysica Acta, 1133(1), 89–94.

139. Gross, D. N., van den Heuvel, A. P. J., & Birnbaum, M. J. (2008). The role of FoxO in the regulation of metabolism. Oncogene, 27(16), 2320–2336.

140. Gunnett, C. A., Heistad, D. D., & Faraci, F. M. (2002). Interleukin-10 protects nitric oxide–dependent relaxation during diabetes: Role of superoxide. Diabetes, 51(6), 1931–1937.

141. Guo Z., Li M., Han B., Qi X. Association of Non-Alcoholic Fatty Liver Disease with Thyroid Function: A Systematic Review and Meta-Analysis. Dig. Liver Dis. 2018;50:1153–1162.

142. Haas JT, Francque S, Staels B, 2016. Pathophysiology and mechanisms of nonalcoholic fatty liver disease. Annu. Rev. Physiol 78, 181–205.

143. Haeusler RA, Hartil K, Vaitheesvaran B, Arrieta-Cruz I, Knight CM, Cook JR, Kammoun HL, Febbraio MA, Gutierrez-Juarez R, Kurland IJ, Accili D. Integrated control of hepatic lipogenesis versus glucose production requires FoxO transcription factors. Nat Commun 5: 1–8, 2014.

144. Hamacher-Brady, A., & Brady, N. R. (2016). Mitophagy programs: Mechanisms and physiological implications of mitochondrial targeting by autophagy. Cellular and Molecular Life Sciences, 73(4), 775–795.
145. Harper ME, Seifert EL. Thyroid hormone effects on mitochondrial energetics. Thyroid 18: 145–156, 2008.
146. Harris, A.R., Fang, S.L., Azizi, F., Lipworth, L., Vagenakis, A.G. & Barverman, L.E. 1978. Effect of starvation on hypothalamic-pituitary-thyroid function in the rat. Metabolism 27, 1074–1083.
147. He C, Bassik MC, Moresi V, Sun K, Wei Y, Zou Z, An Z, Loh J, Fisher J, Sun Q, Korsmeyer S, Packer M, May HI, Hill JA, Virgin HW, Gilpin C, Xiao G, Bassel-Duby R, Scherer PE, Levine B, 2012. Exercise-induced BCL2-regulated autophagy is required for muscle glucose homeostasis. Nature 481 (7382), 511–515.
148. He Q, Sha S, Sun L, Zhang J, Dong M, 2016. GLP-1 analogue improves hepatic lipid accumulation by inducing autophagy via AMPK/mTOR pathway. Biochem. Biophys. Res. Commun 476 (4), 196–203.
149. He, Y., Jiang, J., Shi, Z., et al. (2021). Chemical activators of the Nrf2 signaling pathway in nonalcoholic fatty liver disease. Journal of Cellular Biochemistry, 122, 1160–1173.
150. Henao-Mejia J, Elinav E, Jin C, Hao L, Mehal WZ, Strowig T, Thaiss CA, Kau AL, Eisenbarth SC, Jurczak MJ, Camporez JP, Shulman GI, Gordon JI, Hoffman HM, Flavell RA, 2012. Inflammasome-mediated dysbiosis regulates progression of NAFLD and obesity. Nature 482 (7384), 179–185.
151. Herz, C.T.; Kiefer, F.W. Adipose tissue browning in mice and humans. J. Endocrinol. 2019, 241, R97–R109.
152. Hess, B.; Martius, C. The mode of action of thyroxin. Arch. Biochem. Biophys. 1951, 33, 486–487.
153. Hess, B.; Martius, C. The mode of action of thyroxin. Arch. Biochem. Biophys. 1951, 33, 486–487.
154. Hodin, R.A., Lazar, M.A. & Chin, W.W. 1990. Differential and tissue-specific regulation of the multiple rat c-erbA messenger RNA species by thyroid hormone. J Clin Invest 85, 101–105.
155. Iannucci L.F., Cioffi F., Senese R., Goglia F., Lanni A., Yen P.M., Sinha R.A. Metabolomic analysis shows differential hepatic effects of T2 and T3 in rats after short-term feeding with high fat diet. Sci. Rep. 2017;7:2023. doi: 10.1038/s41598-017-02205-1.
156. Iannucci L.F., Cioffi F., Senese R., Goglia F., Lanni A., Yen P.M., Sinha R.A. Metabolomic analysis shows differential hepatic effects of T2 and T3 in rats after short-term feeding with high fat diet. Sci. Rep. 2017;7:2023. doi: 10.1038/s41598-017-02205-1..)
157. Iannucci, A., Senese, R., Cioffi, F., Goglia, F., Lanni, A., & de Lange, P. (2017). Action of Thyroid Hormones, T3 and T2, on Hepatic Fatty Acids. Frontiers in Endocrinology, 8, 66.
158. Iracheta-Vellve, A., Petrasek, J., Gyongyosi, B., Satishchandran, A., Lowe, P., Kodys, K., Catalano, D., Calenda, C. D., Kurt-Jones, E. A., Fitzgerald, K. A., &

Szabo,

G. (2016). Endoplasmic Reticulum Stress-induced Hepatocellular Death Pathways Mediate Liver Injury and Fibrosis via Stimulator of Interferon Genes. The Journal of biological chemistry, 291(52), 26794–26805.

159. Iwen, K. A., Schröder, E., & Brabant, G. (2018). Thyroid hormones and the metabolic syndrome. European Thyroid Journal, 7(3), 135–148.

160. J. Grootjans, A. Kaser, R.J. Kaufman, R.S. Blumberg. The unfolded protein response in immunity and inflammation. Nat. Rev. Immunol., 16 (2016), pp. 469-484

161. Jeremy J. Buzzard, John R. Morrison, Moira K. O'Bryan, Qing Song, Nigel G. Wreford, Developmental Expression of Thyroid Hormone Receptors in the Rat Testis, Biology of Reproduction, Volume 62, Issue 3, 1 March 2000, Pages 664–669.

162. Jiang M, Xu A, Tokmakejian S, Narayanan N. Thyroid hormone-induced overexpression of functional ryanodine receptors in the rabbit heart. Am J Physiol Heart Circ Physiol 278: H1429–H1438, 2000.

163. Jomova, K.; Raptova, R.; Alomar, S.Y.; Alwasel, S.H.; Nepovimova, E.; Kuca, K.; Valko, M. Reactive Oxygen Species, Toxicity, Oxidative Stress, and Antioxidants: Chronic Diseases and Aging. Arch. Toxicol. 2023, 97, 2499–2574.

164. Jonas W, Lietzow, J, Wohlgemuth, F, Hoefig CS, Wiedmer, P, Schweizer U, Köhrle J, Schürmann A. 3,5-Diiodo-L-thyronine (3,5-T2) exerts thyromimetic effects on hypothalamus-pituitary-thyroid axis, body composition, and energy metabolism in male diet-induced obese mice. Endocrinol. 2015; 156(7): 389-399.

165. Jornayvaz, F.R., Birkenfeld, A.L., Jurczak, M.J., Kanda, S., Guigni, B.A., Jiang, D.C., Zhang, D., Lee, H.Y., Samuel, V.T., and Shulman, G.I. (2011). Hepatic insulin resistance in mice with hepatic overexpression of diacylglycerol acyltransferase 2. Proc. Natl. Acad. Sci. USA 108, 5748–5752.

166. K.V. Swanson, M. Deng, J.P. Ting. The NLRP3 inflammasome: molecular activation and regulation to therapeutics. Nat. Rev. Immunol., 19 (2019), pp. 477-489.

167. Kadenbach B, Hüttemann M, Arnold S, Lee I, Bender E. Mitochondrial energy metabolism is regulated via nuclearcoded subunits of cytochrome c oxidase. Free Radic Biol Med 2000; 29: 211-221.

168. Kalra, S., Unnikrishnan, A. G., & Sahay, R. (2014). The hypoglycemic side of hypothyroidism. Indian journal of endocrinology and metabolism, 18(1), 1–3. https://doi.org/10.4103/2230-8210.126517

169. Kalyanaraman H., Schwappacher R., Joshua J., Zhuang S., Scott B.T., Klos M., Casteel D.E., Frangos J.A., Dillmann W., Boss G.R., et al. Nongenomic thyroid hormone signaling occurs through a plasma membrane-localized receptor. Sci. Signal. 2014;7:ra48. doi: 10.1126/scisignal.2004911.

170. Kapoor, R., van Hogerlinden, M., Wallis, K., Ghosh, H., Nordstrom, K., Vennstrom, B., Vaidya, V.A., 2010. Unliganded thyroid hormone receptor alpha1 impairs adult hippocampal neurogenesis. FASEB J. 24 (12), 4793–4805.

171. Kaushik S, Wang Y, Xiang Y, Novak I, Komatsu M, Tanaka K, Cuervo AM, Czaja MJ, 2009. Autophagy regulates lipid metabolism. Nature 458 (7242), 1131–1135.

172. Kaushik, S., & Cuervo, A. M. (2015). Proteostasis and aging. Nature Medicine,

21, 1406–1415.

173. Kent, A.C.; El Baradie, K.B.Y.; Hamrick, M.W. Targeting the Mitochondrial Permeability Transition Pore to Prevent Age-Associated Cell Damage and Neurodegeneration. Oxidative Med. Cell. Longev. 2021, 2021, 6626484.
174. Kheloufi, M., Das, S., & Brenner, C. (2022). Autophagy in liver physiology and disease. Journal of Hepatology, 77(5), 1234–1250.
175. Klionsky DJ, Emr SD, 2000. Autophagy as a regulated pathway of cellular degradation. Science 290 (5497), 1717–1721.
176. Koliaki C, Szendroedi J, Kaul K, Jelenik T, Nowotny P, Jankowiak F, et al. Adaptation of hepatic mitochondrial function in humans with non-alcoholic fatty liver is lost in steatohepatitis. Cell Metab. 2015;21:739–46.
177. Kowalczyk, P.; Sulejczak, D.; Kleczkowska, P.; Bukowska-O´sko, I.; Kucia, M.; Popiel, M.; Wietrak, E.; Kramkowski, K.; Wrzosek, K.; Kaczy´ nska, K. Mitochondrial Oxidative Stress-A Causative Factor and Therapeutic Target in Many Diseases. Int. J. Mol. Sci. 2021, 22, 13384.
178. Kowalik, M.A.; Columbano, A.; Perra, A. Thyroid Hormones, Thyromimetics and Their Metabolites in the Treatment of Liver Disease. Front. Endocrinol. 2018, 9, 382.
179. Krause, K. Novel Aspects of White Adipose Tissue Browning by Thyroid Hormones. Exp. Clin. Endocrinol. Diabetes 2020, 128, 446–449.
180. Krysko, D. V., Agostinis, P., Krysko, O., Garg, A. D., Bachert, C., Lambrecht, B. N., & Vandenabeele, P. (2011). Emerging role of damage-associated molecular patterns derived from mitochondria in inflammation. Trends in Immunology, 32(4), 157–164.
181. Kuusi T, Taskinen MR, Nikkila EA. Lipoproteins, lipolytic enzymes, and hormonal status in hypothyroid women at different levels of substitution. J Clin Endocrinol Metab. 1988;66:51–56.
182. L. Beucher, C. Gabillard-Lefort, O.R. Baris, J. Mialet-Perez. Monoamine oxidases: a missing link between mitochondria and inflammation in chronic diseases. Redox Biol., 77 (2024), Article 103393
183. Langouche L, Lehmphul I, Perre SV, Kohrle J, Van den Berghe G. Circulating 3-T1AM and 3,5-T2 in critically ill patients: a cross-sectional observational study. Thyroid (2016) 26:1674–80.
184. Lanni A, Moreno M, Cioffi M, Goglia F. Effect of 3,3'-diiodothyronine and 3,5- diiodothyronine on rat liver oxidative capacity. Mol Cell Endocrinol 1992; 86: 143-148.
185. Lanni A, Moreno M, Goglia F. 3,5-Diiodo-L-thyronine and energy metabolism: non-genomic regulation of mitochondrial respiration. Am J Physiol Endocrinol Metab. 1998;274:E951–E957.
186. Lanni A, Moreno M, Goglia F. 3,5-Diiodo-L-thyronine and mitochondrial metabolism: new perspectives. Front Biosci. 2005;10:994–1004.
187. Lanni A, Moreno M, Lombardi A, de Lange P, Silvestri E, Ragni M, Farina P, Baccari GC, Fallahi P, Antonelli A, Goglia F. 3,5-diiodo-L-thyronine powerfully reduces adiposity in rats by increasing the burning of fats. FASEB J 2005; 19: 1552- 1554.

188. Lanni A, Moreno M, Lombardi A, Goglia F. Rapid stimulation of energy metabolism by 3,5-diiodo-L-thyronine in hypothyroid rats. J Endocrinol Invest. 1994;17(5):293–298.
189. Lanni A, Moreno M, Lombardi A, Goglia F. Rapid stimulation of mitochondrial respiration and thermogenesis by 3,5-diiodo-L-thyronine in perfused rat liver and human cells. J Endocrinol Invest. 1992;15(5):379-386.
190. Lanni, A.; Moreno, M.; Goglia, F. Mitochondrial Actions of Thyroid Hormone. Compr. Physiol. 2016, 6, 1591–1607.
191. Laplante, M., & Sabatini, D. M. (2012). mTOR signaling in growth control and disease. Cell, 149(2), 274–293.
192. Lardy, H.A.; Feldcott, G. Metabolic effects of thyroxine in vitro. Ann. N. Y. Acad. Sci. 1951, 54, 636–648.
193. Lazar MA. Nuclear receptor corepressors. *Nuclear Receptor Signaling*. 2003;1:e001. doi:10.1621/nrs.01001
194. Lazar, M.A. & Berrodin, T.J. 1990. Thyroid hormone receptors form distinct nuclear protein-dependent and independent complexes with a thyroid hormone response element. Mol Endocrinol 4, 1627–1635.
195. Lazar, M.A. & Chin, W.W. 1990. Nuclear thyroid hormone receptors. J Clin Invest 86, 1777–1782.
196. Lazarus JV, Mark HE, Anstee QM, Arab JP, Batterham RL, Castera L, et al. Advancing the global public health agenda for NAFLD: a consensus statement. Nat Rev Gastroenterol Hepatol. 2022;19:60–78.
197. Lechan, R.M., Qi, Y., Berrodin, T.J., Davis, K.D., Schwartz, H.L., Strait, K.A., Oppenheimer, J.H. & Lazar, M.A. 1993. Immunocytochemical delineation of thyroid hormone receptor beta 2-like immunoreactivity in the rat central nervous system. Endocrinology 132, 2461–2469.
198. Lehmphul I, Brabant G, Wallaschofski H, Ruchala M, Strasburger CJ, Kohrle J, et al. Detection of 3,5-diiodothyronine in sera of patients with altered thyroid status using a new monoclonal antibody-based chemiluminescence immunoassay. Thyroid (2014) 24:1350–60.
199. Leo, T., Meo, S., Barletta, A., Martino, G., Goglia, F., 1976. Modification of nucleic acid levels per mitochondrion induced by thyroidectomy or triiodothyronine administration. Pflug. Arch. 366 (1), 73–77.
200. Lesmana R., Sinha R.A., Singh B.K., Zhou J., Ohba K., Wu Y., Yau W.W., Bay B.H., Yen P.M. Thyroid Hormone Stimulation of Autophagy Is Essential for Mitochondrial Biogenesis and Activity in Skeletal Muscle. Endocrinology. 2016;157:23–38. doi: 10.1210/en.2015-1632.
201. Li Z, Li Y, Zhang HX, Guo JR, Lam CW, Wang CY, et al. Mitochondria-mediated pathogenesis and therapeutics for non-alcoholic fatty liver disease. Mol Nutr Food Res. 2019;63:e1900043. doi: 10.1002/mnfr.201900043.
202. Li, H., Jia, Y., Yao, D., Gao, M., Wang, L., & Liu, J. (2020). Rhein alleviates myocardial ischemic injury by inhibiting mitochondrial division, activating mitochondrial autophagy and suppressing myocardial cell apoptosis through the

Drp1/PINK1/Parkin pathway. Molecular Biology Reports, 47(8), 6101–6113.

203. Li, X., & Li, M. (2024). Unlocking cholesterol metabolism in metabolic-associated steatotic liver disease: Molecular targets and natural product interventions. Pharmaceuticals, 17(8), 1073.
204. Li, X., Chen, W., Jia, Z., Xiao, Y., Shi, A., & Ma, X. (2025). Mitochondrial dysfunction as a pathogenesis and therapeutic strategy for metabolic-dysfunction-associated steatotic liver disease. International Journal of Molecular Sciences, 26(9), 4256.
205. Li, Y., Chen, Y., & Johnstone, C. N. (2020). Autophagy and inflammasome regulation in liver injury. Cell Death & Disease, 11, 879.
206. Linton SD, Aja T, Armstrong RA, Bai X, Chen L-S, Chen N, et al. First-in-class pan caspase inhibitor developed for the treatment of liver disease. J Med Chem. 2005;48:6779–82.
207. Lira VA, Okutsu M, Zhang M, Greene NP, Laker RC, Breen DS, Hoehn KL, Yan Z, 2013. Autophagy is required for exercise training-induced skeletal muscle adaptation and improvement of physical performance. Faseb. J 27 (10), 4184–4193.
208. Liu K, Czaja MJ, 2013. Regulation of lipid stores and metabolism by lipophagy. Cell Death Differ. 20 (1), 3–11.
209. Liu YY, Brent GA. Thyroid hormone crosstalk with nuclear receptor signaling in metabolic regulation. Trends Endocrinol Metab. 2010;21(3):166–173. doi: 10.1016/j.tem.2009.11.004.
210. Liu YY, Heymann RS, Moatamed F, Schultz JJ, Sobel D, Brent GA. A mutant thyroid hormone receptor alpha antagonizes peroxisome proliferator-activated receptor alpha signaling in vivo and impairs fatty acid oxidation. Endocrinology 148: 1206– 1217, 2007.
211. Liu, J.; Han, X.; Zhang, T.; Tian, K.; Li, Z.; Luo, F. Reactive Oxygen Species (ROS) Scavenging Biomaterials for Anti-Inflammatory Diseases: From Mechanism to Therapy. J. Hematol. Oncol. 2023, 16, 116.
212. Lombardi A, de Lange P, Silvestri E, Busiello RA, Goglia F, Lanni A. 3,5- Diiodo-L-thyronine: a metabolically active thyroid hormone metabolite. J Endocrinol. 2015;226(1): R1–R12.
213. Lombardi A, Silvestri E, Moreno M, De Lange P, Farina P, Goglia F, Lanni A. Skeletal muscle mitochondrial free-fatty-acid content and membrane potential sensitivity in different thyroid states: involvement of uncoupling protein-3 and adenine nucleotide translocase. *FEBS Letters*. 2002;532(1-2):179-183.
214. Lombardi, A., de Lange, P., Silvestri, E., Busiello, R. A., Lanni, A., Goglia, F., & Moreno, M. (2009). 3,5-Diiodo-L-thyronine rapidly enhances mitochondrial fatty acid oxidation rate and thermogenesis in rat skeletal muscle: AMP-activated protein kinase involvement. American Journal of Physiology – Endocrinology and Metabolism, 296(3), E497–E502.
215. Lombardi, A.; Busiello, R.A.; Napolitano, L.; Cioffi, F.; Moreno, M.; de Lange, P.; Silvestri, E.; Lanni, A.; Goglia, F. UCP3 translocates lipid hydroperoxide and

mediates lipid hydroperoxide-dependent mitochondrial uncoupling. J. Biol. Chem. 2010, 285, 16599–16605.
216. Lonard DM, O'malley BW. Nuclear receptor coregulators: judges, juries, and executioners of cellular regulation. Mol Cell. 2007 Sep 7;27(5):691-700.
217. Lopez D, Abisambra Socarras JF, Bedi M, Ness GC. Activation of the hepatic LDL receptor promoter by thyroid hormone. Biochim Biophys Acta 1771: 1216–1225, 2007.
218. Lu Z, Li Y, Chowdhury N, Yu H, Syn W-K, Lopes-Virella M, et al. The Presence of Periodontitis exacerbates non-alcoholic fatty liver Disease via Sphingolipid Metabolism-Associated Insulin Resistance and hepatic inflammation in mice with metabolic syndrome. Int J Mol Sci. 2023.
219. Luo, Y.; Lin, H. Inflammation Initiates a Vicious Cycle between Obesity and Nonalcoholic Fatty Liver Disease. Immun. Inflamm. Dis. 2021, 9, 59–73.
220. M. M. Syed-Abdul, "Lipid Metabolism in Metabolic-Associated Steatotic Liver Disease (MASLD)," Metabolites 14, no. 1 (2023): 12.
221. M. Zhou, J. Lv, X. Chen, Y. Shi, G. Chao, and S. Zhang, "From Gut to Liver: Exploring the Crosstalk Between Gut-Liver Axis and Oxidative Stress in Metabolic Dysfunction-Associated Steatotic Liver Disease," Annals of Hepatology 30, no. 1 (2025): 101777.
222. Ma D, Panda S, Lin JD, 2011. Temporal orchestration of circadian autophagy rhythm by C/EBPbeta. EMBO J. 30 (22), 4642–4651.
223. Mandato C., D'Acunzo I., Vajro P. Thyroid Dysfunction and Its Role as a Risk Factor for Non-Alcoholic Fatty Liver Disease: What's New. Dig. Liver Dis. 2018;50:1163–1165.
224. Mantena, S. K., Vaughn, D. P., Andringa, K., Eccleston, H. B., King, A. L., Abrams, G. A., Doeller, J. E., Kraus, D. W., Darley-Usmar, V. M., & Bailey, S. M. (2008). High fat diet induces dysregulation of hepatic oxygen gradients and mitochondrial function in vivo. Biochemical Journal, 417, 183–193.
225. Mantovani, A.; Nascimbeni, F.; Lonardo, A.; Zoppini, G.; Bonora, E.; Mantzoros, C.S.; Targher, G. Association Between Primary Hypothyroidism and Nonalcoholic Fatty Liver Disease: A Systematic Review and Meta-Analysis. Thyroid. 2018, 28, 1270–1284.
226. Marino G, Pietrocola F, Madeo F, Kroemer G, 2014. Caloric restriction mimetics: natural/physiological pharmacological autophagy inducers. Autophagy 10 (11), 1879–1882.
227. Marino, L., Kim, A., Ni, B., & Celi, F. S. (2023). Thyroid hormone action and liver disease: A complex interplay. Hepatology.
228. McKenna, N.J., Cooney, A.J., DeMayo, F.J., Downes, M., Glass, C.K., Lanz, R.B., Lazar, M.A., Mangelsdorf, D.J., Moore, D.D., Qin, J. et al. 2009. Minireview: evolution of NURSA, the Nuclear Receptor Signaling Atlas. Mol Endocrinol 23, 740–746.
229. Mendoza, A., Tang, C., Choi, J., Acuña, M., Logan, M., Martin, A. G., Al-Sowaimel, L., Desai, B. N., Tenen, D. E., Jacobs, C., Lyubetskaya, A., Fu, Y., Liu, H., Tsai, L., Cohen, D. E., Forrest, D., Wilson, A. A., & Hollenberg, A. N. (2021). Thyroid

hormone signaling promotes hepatic lipogenesis through the transcription factor ChREBP. Science Signaling, 14(709), eabh3839.

230. Miller, D. M., McCauley, K. F., & Dunham-Snary, K. J. (2025). Metabolic dysfunction–associated steatotic liver disease (MASLD): Mechanisms, clinical implications and therapeutic advances. Endocrinology, Diabetes & Metabolism, 8(6), e70132.

231. Mizushima N, 2018. A brief history of autophagy from cell biology to physiology and disease. Nat. Cell Biol 20 (5), 521–527.

232. Mizushima N, Komatsu M, 2011. Autophagy: renovation of cells and tissues. Cell 147 (4), 728–741.

233. Mizushima N, Levine B, Cuervo AM, Klionsky DJ, 2008. Autophagy fights disease through cellular self-digestion. Nature 451 (7182), 1069–1075.

234. Mollica MP, Lionetti L, Moreno M, Lombardi A, De Lange P, Antonelli A, Lanni A, Cavaliere G, Barletta A, Goglia F. 3,5-diiodo-l-thyronine, by modulating mitochondrial functions, reverses hepatic fat accumulation in rats fed a highfat diet. J Hepatol 2009; 51: 363-370.

235. Moreno M, de Lange P, Lombardi A, Silvestri E, Lanni A, Goglia F. Metabolic effects of thyroid hormone derivatives. Thyroid. 2008;18:239–253.

236. Moreno M, Lombardi A, De Lange P, Silvestri E, Ragni M, Lanni A, Goglia F. Fasting, lipid metabolism, and triiodothyronine in rat gastrocnemius muscle: interrelated roles ofuncoupling protein 3, mitochondrial thioesterase, and coenzyme Q. FASEB J 2003; 17: 1112-1114.

237. Moreno M, Silvestri E, De Matteis R, de Lange P, Lombardi A, Glinni D, Senese R, Cioffi F, Salzano AM, Scaloni A, Lanni A, Goglia F. 3,5-Diiodo-L-thyronine prevents highfat- diet-induced insulin resistance in rat skeletal muscle through metabolic and structural adaptations. FASEB J 2011; 25: 3312-3324.

238. Moreno M, Lombardi A, Beneduce L, Silvestri E, Pinna G, Goglia F & Lanni A 2002 Are the effects of T3 on resting metabolic rate in euthyroid rats entirely caused by T3 itself? Endocrinology 143 504–510.

239. Mortimore GE, Poso AR, 1984. Lysosomal pathways in hepatic protein degradation: regulatory role of amino acids. Fed. Proc 43 (5), 1289–1294.

240. Mortimore GE, Poso AR, 1987. Intracellular protein catabolism and its control during nutrient deprivation and supply. Annu. Rev. Nutr 7, 539–564.

241. Mota M, Banini BA, Cazanave SC, Sanyal AJ. Molecular mechanisms of lipotoxicity and glucotoxicity in nonalcoholic fatty liver disease. Metabolism. 2016;65:1049–61.

242. Mullur, R., Liu, Y.-Y., & Brent, G. A. (2014). Thyroid hormone regulation of metabolism. Physiological Reviews, 94(2), 355–382.

243. Muñoz-Planillo, R., Kuffa, P., Martínez-Colón, G., Smith, B. L., Rajendiran, T. M., & Núñez, G. (2013). K^+ efflux is the common trigger of NLRP3 inflammasome activation by bacterial toxins and particulate matter. Immunity, 38(6), 1142–1153. https://doi.org/10.1016/j.immuni.2013.05.016.

244. Murphy, M. P. (2009). How mitochondria produce reactive oxygen species. Biochemical Journal, 417(1), 1–13.

245. Mwangi SM, Li G, Ye L, Liu Y, Reichardt F, Yeligar SM, Hart CM, Czaja MJ, Srinivasan S, 2019. Glial cell line-derived neurotrophic factor enhances autophagic flux in mouse and rat hepatocytes and protects against palmitate lipotoxicity. Hepatology 69 (6), 2455–2470.
246. Ng MYW, Wai T, Simonsen A. Quality control of the mitochondrion. Dev Cell. 2021;56(7):881–905.
247. Ni H-M, Boggess N, McGill MR, Lebofsky M, Borude P, Apte U, Jaeschke H, Ding W-X, 2012. Liver-specific loss of Atg5 causes persistent activation of Nrf2 and protects against acetaminophen-induced liver injury. Toxicol. Sci 127 (2), 438–450.
248. Oppenheimer JH, Koerner D, Schwartz HL, Surks MI 1972 Specific nuclear triiodothyronine binding sites in rat liver and kidney. J Clin Endocrinol Metab 35:330–333.
249. Oppenheimer JH, Schwartz HL, Lane JT, Thompson MP. Functional relationship of thyroid hormone-induced lipogenesis, lipolysis, and thermogenesis in the rat. J Clin Invest 87: 125–132, 1991.
250. Oppenheimer JH, Schwartz HL, Mariash CN, Kinlaw WB, Wong NC, Freake HC. Advances in our understanding of thyroid hormone action at the cellular level. *Endocrine Reviews*. 1987;8(3):288–308. doi:10.1210/edrv-8-3-288.
251. Ordonez-Moran, P. & Munoz, A. 2009. Nuclear receptors: genomic and non-genomic effects converge. Cell Cycle 8, 1675–1680.
252. Ore, A., & Akinloye, O. A. (2019). Oxidative stress and antioxidant biomarkers in clinical and experimental models of non-alcoholic fatty liver disease. Medicina, 55(2), 26.
253. Ortiga-Carvalho, T. M., Sidhaye, A. R., & Wondisford, F. E. (2014). Thyroid hormone receptors and resistance to thyroid hormone disorders. Nature Reviews Endocrinology, 10(10), 582–591.
254. Padron AS, Neto RA, Pantaleão TU, de Souza dos Santos MC, Araujo RL, de Andrade BM et al.. Administration of 3,5-diiodothyronine (3,5-T2) causes central hypothyroidism and stimulates thyroid-sensitive tissues. J Endocrinol. 2014;221(3):415-27.
255. Pajares, M., Jiménez-Moreno, N., García-Yagüe, Á. J., Escoll, M., de Ceballos, M. L., Van Leuven, F., Rábano, A., Yamamoto, M., Rojo, A. I., & Cuadrado, A. (2016). Transcription factor NFE2L2/NRF2 is a regulator of macroautophagy genes. Autophagy, 12(10), 1902–1916.
256. Park, S. S., & Seo, Y. K. (2020). Excess Accumulation of Lipid Impairs Insulin Sensitivity in Skeletal Muscle. International journal of molecular sciences, 21(6), 1949.
257. Parzych KR, Klionsky DJ, 2014. An overview of autophagy: morphology, mechanism, and regulation. Antioxidants Redox Signal. 20 (3), 460–473.
258. Pessayre, D., Fromenty, B., & Berson, A. (2012). Mitochondria in steatohepatitis. Journal of Hepatology, 56(3), 726–734.
259. Petersen, M. C., & Shulman, G. I. (2018). Mechanisms of insulin action and insulin resistance. Physiological Reviews, 98(4), 2133–2223.
260. Petito, G., Cioffi, F., Silvestri, E., De Matteis, R., Lattanzi, D., de Lange, P., et al. (2021). 3,5-Diiodo-L-thyronine (T2) administration affects visceral adipose tissue

inflammatory state in rats receiving long-lasting high-fat diet. Frontiers in Endocrinology, 12, 703170.
261. Pfeifer U, Strauss P, 1981. Autophagic vacuoles in heart muscle and liver. A comparative morphometric study including circadian variations in meal-fed rats. J. Mol. Cell. Cardiol 13 (1), 37–49.
262. Pham TH, Lee GH, Jin SW, Lee SY, Han EH, Kim ND, et al. Sesamin ameliorates lipotoxicity and lipid accumulation through the activation of the estrogen receptor alpha signaling pathway. Biochem Pharmacol. 2023;216:115768.
263. Picard F, Kurtev M, Chung N, Topark-Ngarm A, Senawong T, Machado De Oliveira R, Leid M, McBurney MW, Guarente L. Sirt1 promotes fat mobilization in white adipocytes by repressing PPAR-gamma. Nature 2004; 429: 771-776.
264. Picca, A., Calvani, R., & Coelho-Junior, H. J. (2021). Cell death and inflammation: The role of mitochondria in health and disease. Cells, 10, 537.
265. Pickles, S., Vigié, P., & Youle, R. J. (2018). Mitophagy and quality control mechanisms in mitochondrial maintenance. Current Biology, 28, R170–R185.
266. Pierantonelli I., Svegliati-Baroni G. Nonalcoholic Fatty Liver Disease: Basic Pathogenetic Mechanisms in the Progression From NAFLD to NASH. Transplantation. 2019;103:e1–e13. doi: 10.1097/TP.0000000000002480.
267. Pietzner M, Homuth G, Budde K, Lehmphul I, Volker U, Volzke H, et al. Urine metabolomics by (1)H-NMR spectroscopy indicates associations between serum 3,5- T2 concentrations and intermediary metabolism in euthyroid humans. Eur Thyroid
J. (2015a) 4(Suppl. 1):92–100.
268. Pihlajamäki, J.; Boes, T.; Kim, E.Y.; Dearie, F.; Kim, B.W.; Schroeder, J.; Mun, E.; Nasser, I.; Park, P.J.; Bianco, A.C.; et al. Thyroid Hormone-Related Regulation of Gene Expression in Human Fatty Liver. J. Clin. Endocrinol. Metab. 2009, 94, 3521– 3529.
269. Pinna G, Meinhold H, Hiedra L, Thoma R, Hoell T, Graf KJ, et al. Elevated 3,5- diiodothyronine concentrations in the sera of patients with nonthyroidal illnesses and brain tumors. J Clin Endocrinol Metab. (1997) 82:1535–42.
270. Pohl J, Ring A, Hermann T, Stremmel W. Role of FATP in parenchymal cell fatty acid uptake. Biochim Biophys Acta. 2004;1686:1–6.
271. Popov, L.-D. (2020). Mitochondrial biogenesis: An update. Journal of Cellular and Molecular Medicine, 24(9), 4892–4899.
272. Popov, L.-D. Mitochondrial Biogenesis: An Update. J. Cell. Mol. Med. 2020, 24, 4892–4899.
273. Powell, E. E., Wong, V. W. S. & Rinella, M. Non-alcoholic fatty liver disease. Lancet397, 2212–2224 (2021).
274. Prieur X, Huby T, Coste H, Schaap FG, Chapman MJ, Rodriguez JC. Thyroid hormone regulates the hypotriglyceridemic gene APOA5. J Biol Chem. 2005;280:27533–43. doi: 10.1074/jbc.M503139200.
275. Psarra AM, Solakidi S, Sekeris CE. The mitochondrion as a primary site of action of steroid and thyroid hormones: presence and action of steroid and thyroid hormone receptors in mitochondria of animal cells. Mol Cell Endocrinol 2006; 246: 21-

33.

276. Qian, H., Chao, X., Williams, J., Fulte, S., Li, T., Yang, L., & Ding, W.-X. (2021).
Autophagy in liver diseases: A review. Molecular Aspects of Medicine, 82, 100973. https://doi.org/10.1016/j.mam.2021.100973.
277. Radosavljevic, T.; Brankovic, M.; Samardzic, J.; Djureti´c, J.; Vukicevic, D.; Vucevic, D.; Jakovljevic, V. Altered Mitochondrial Function in MASLD: Key Features and Promising Therapeutic Approaches. Antioxidants 2024, 13, 906.
278. Ramanathan, R.; Patwa, S.A.; Ali, A.H.; Ibdah, J.A. Thyroid Hormone and Mitochondrial Dysfunction: Therapeutic Implications for Metabolic Dysfunction-Associated Steatotic Liver Disease (MASLD). Cells 2023, 12, 2806.
279. Rautou PE, Mansouri A, Lebrec D, Durand F, Valla D, Moreau R, 2010. Autophagy in liver diseases. J. Hepatol 53 (6), 1123–1134.
280. Rensen PC, van Dijk KW, Havekes LM. Apolipoprotein AV: low concentration, high impact. Arterioscler Thromb Vasc Biol. 2005;25:2445–7. doi: 10.1161/01.ATV.0000193889.65915.f9.
281. Rinella ME, Lazarus JV, Ratziu V, et al.; NAFLD Nomenclature consensus group. A multisociety Delphi consensus statement on new fatty liver disease nomenclature. Hepatology 2023;78: 1966–1986.
282. Rinella, M. E. et al. A multisociety Delphi consensus statement on new fatty liver disease nomenclature. J. Hepatol.79, 1542–1556 (2023).
283. Rivera-Mejías, P., Narbona-Pérez, Á. J., Hasberg, L., Kroczek, L., Bahat, A., Lawo, S., Folz-Donahue, K., Schumacher, A.-L., Ahola, S., Mayer, F. C., Giavalisco, P., Nolte, H., Lavandero, S., & Langer, T. (2016). The mitochondrial protease OMA1 acts as a metabolic safeguard upon nuclear DNA damage. Cellular and Molecular Life Sciences, 73(4), 775–795.
284. Rivkees, S.A., Bode, H.H. & Crawford, J.D. 1988. Longterm growth in juvenile acquired hypothyroidism: the failure to achieve normal adult stature. N Engl J Med 318, 599–602.
285. Roca-Agujetas, V.; de Dios, C.; Lestón, L.; Marí, M.; Morales, A.; Colell, A. Recent Insights into the Mitochondrial Role in Autophagy and Its Regulation by Oxidative Stress. Oxidative Med. Cell. Longev. 2019, 2019, 1–16.
286. Rocha VZ, Libby P. The multiple facets of the fat tissue. Thyroid 18: 175–183, 2008
287. Roers A, Hiller B & Hornung V Recognition of endogenous nucleic acids by the innate immune system. Immunity 44, 739–754.
288. Rosen, M.D., Chan, I.H., Privalsky, M.L., 2011. Mutant thyroid hormone receptors (TRs) isolated from distinct cancer types display distinct target gene specificities: a unique regulatory repertoire associated with two renal clear cell carcinomas. Mol. Endocrinol. 25 (8), 1311–1325.
289. Rubic, T., Lametschwandtner, G., Jost, S., Hinteregger, S., Kund, J., Carballido-Perrig, N., et al. (2008). Triggering the succinate receptor GPR91 on dendritic cells enhances immunity. Nature Immunology, 9, 1261–1269.
290. Rubinsztein DC, Gestwicki JE, Murphy LO, Klionsky DJ, 2007. Potential therapeutic applications of autophagy. Nat. Rev. Drug Discov 6 (4), 304–312.

291. Ryzhikov M, Ehlers A, Steinberg D, Xie W, Oberlander E, Brown S, Gilmore PE, Townsend RR, Lane WS, Dolinay T, Nakahira K, Choi AMK, Haspel JA, 2019. Diurnal rhythms spatially and temporally organize autophagy. Cell Rep. 26 (7), 1880–1892 e1886.
292. Sabatino, L., Vassalle, C., Del Seppia, C., & Iervasi, G. (2021). Deiodinases and the three types of thyroid hormone deiodination reactions. Endocrinology and Metabolism, 36(5), 952–964.
293. Saelim, N., John, L.M., Wu, J., Park, J.S., Bai, Y., Camacho, P., Lechleiter, J.D., 2004. Nontranscriptional modulation of intracellular Ca2+ signaling by ligand stimulated thyroid hormone receptor. J. Cell Biol. 167 (5), 915–924.
294. Sagliocchi, S., Restolfer, F., Cossidente, A., & Dentice, M. (2024). The key roles of thyroid hormone in mitochondrial regulation, at interface of human health and disease. Journal of Basic and Clinical Physiology and Pharmacology, 35(4– 5), 231–240. https://doi.org/10.1515/jbcpp-2024-0108.
295. Samuel VT, Liu ZX, Wang A, Beddow SA, Geisler JG, Kahn M, et al. Inhibition of protein kinase Cepsilon prevents hepatic insulin resistance in nonalcoholic fatty liver disease. J Clin Invest. 2007;117:739–745. doi: 10.1172/JCI30400.
296. Samuel, V. T., Liu, Z. X., Qu, X., Elder, B. D., Bilz, S., Befroy, D., Romanelli, A. J., & Shulman, G. I. (2004). Mechanism of hepatic insulin resistance in non-alcoholic fatty liver disease. Journal of Biological Chemistry, 279(31), 32345–32353. doi:10.1074/jbc.M313478200.
297. Samuels, H.H., Forman, B.M., Horowitz, Z.D. & Ye, Z.S. 1988. Regulation of gene expression by thyroid hormone. J Clin Invest 81, 957–967.
298. Saponaro F, Sestito S, Runfola M, Rapposelli S and Chiellini G (2020) Selective Thyroid Hormone Receptor Beta (TRβ) Agonists: New Perspectives for the Treatment of Metabolic and Neurodegenerative Disorders. Front. Med. 7:331.doi:10.3389/fmed.2020.331.
299. Scapin S, Leoni S, Spagnuolo S, Gnocchi D, De Vito P, Luly P, Pedersen JZ, Incerpi S. Short-term effects of thyroid hormones during development: Focus on signal transduction. Steroids 2010; 75: 576-584.
300. Scarpulla RC. Nuclear control of respiratory gene expression in mammalian cells. J Cell Biochem 2006; 97: 673-683.
301. Schneider JL, Cuervo AM, 2014. Liver autophagy: much more than just taking out the trash. Nat. Rev. Gastroenterol. Hepatol 11 (3), 187–200.
302. Schönfeld, P.;Wiêckowski, M.R.;Wojtczak, L. Thyroid hormone-induced expression of the ADP/ATP carrier and its effect on fatty acid-induced uncoupling of oxidative phosphorylation. FEBS Lett. 1997, 416, 19–22.
303. Schuck S, 2020. Microautophagy–distinct molecular mechanisms handle cargoes of many sizes. J. Cell Sci 133 (17).
304. Schulze, R. J., Sathyanarayan, A., & Mashek, D. G. (2017). Breaking fat: The regulation and mechanisms of lipophagy. Biochimica et Biophysica Acta – Molecular and Cell Biology of Lipids, 1862, 1178–1187.
305. Scorletti E, Carr RM. A new perspective on NAFLD: focusing on lipid

droplets. J Hepatol. 2022;76:934–45

306. Senese R, Cioffi F, de Lange P, Goglia F, Lanni A. Thyroid: biological actions of ‘nonclassical’ thyroid hormones. J Endocrinol. 2018;236(2):R43–R58.
307. Senese R, de Lange P, Petito G, Moreno M, Goglia F, Lanni A. 2018. 3,5-diiodothyronine: a novel thyroid hormone metabolite and a potent modulator of energy metabolism. Front Endocrinol (Lausanne) 9:427.
308. Sethi, P., Mishra, A. K., Ghosh, S., Singh, K. K., Sharma, S., Stojchevski, R., Avtanski, D., & Sinha, J. K. (2025). Lipid metabolism–signaling crosstalk in metabolic disease and aging: Mechanisms and therapeutic targets. Cells.
309. Shao, S.-S., Zhao, Y.-F., Song, Y.-F., Xu, C., Yang, J.-M., Xuan, S.-M., Yan, H.-L., Yu, C.-X., Zhao, M., Xu, J., & Zhao, J.-J. (2014). Dietary high-fat lard intake induces thyroid dysfunction and abnormal morphology in rats. Acta Pharmacologica Sinica, 35(11), 1411–1420.
310. Sheikh, M. Y., Younus, M. F., Shergill, A., & Hasan, M. N. (2025). Diet and lifestyle interventions in metabolic dysfunction–associated fatty liver disease: A comprehensive review. International Journal of Molecular Sciences, 26(19), 9625.
311. Shi W, Xu G, Gao Y, Zhao J, Liu T, Zhao J, et al. Novel role for epalrestat: protecting against NLRP3 inflammasome-driven NASH by targeting aldose reductase. J Transl Med. 2023;21:700.
312. Shi, Y., Wu, Z., Liu, S., Zuo, D., Niu, Y., Qiu, Y., et al. (2023). Targeting PRMT3 impairs methylation and oligomerization of HSP60 to boost anti-tumor immunity by activating cGAS–STING signaling. Cell Reports, 42(6), 112566. https://doi.org/10.1016/j.celrep.2023.112566.
313. Shin, S. M., Yang, J. H., & Ki, S. H. (2013). Role of the Nrf2-ARE pathway in liver diseases. Oxidative Medicine and Cellular Longevity, 2013, 763257.
314. Shoji-Kawata S, Sumpter R, Leveno M, Campbell GR, Zou Z, Kinch L, Wilkins AD, Sun Q, Pallauf K, MacDuff D, Huerta C, Virgin HW, Helms JB, Eerland R, Tooze SA, Xavier R, Lenschow DJ, Yamamoto A, King D, Lichtarge O, Grishin NV, Spector SA, Kaloyanova DV, Levine B, 2013. Identification of a candidate therapeutic autophagy-inducing peptide. Nature 494 (7436), 201–206.
315. Silva, J. E. (2006). Thermogenic mechanisms and their hormonal regulation. Physiological Reviews, 86(2), 435–464.
316. Silvestri E, Cioffi F, Glinni D, Ceccarelli M, Lombardi A, de Lange P, Chambery A, Severino V, Lanni A, Goglia F, Moreno M. Pathways affected by 3,5-diiodo-l- thyronine in liver of high fat-fed rats: evidence from two-dimensional electrophoresis, blue-native PAGE, and mass spectrometry. Mol Biosyst 2010; 6: 2256-2271.
317. Silvestri, E.; Lombardi, A.; Coppola, M.; Gentile, A.; Cioffi, F.; Senese, R.; Goglia, F.; Lanni, A.; Moreno, M.; de Lange, P. Differential Effects of 3,5-Diiodo-L- Thyronine and 3,5,30-Triiodo-L-Thyronine on Mitochondrial Respiratory Pathways in Liver from Hypothyroid Rats. Cell. Physiol. Biochem. 2018, 47, 2471–2483.
318. Simões ICM, Amorim R, Teixeira J, Karkucinska-Wieckowska A, Carvalho A, Pereira SP, et al. The alterations of mitochondrial function during NAFLD Progression-An Independent Effect of mitochondrial ROS production. Int J Mol Sci. 2021.
319. Simões, I. C. M., Fontes, A., Pinton, P., Zischka, H., & Wieckowski, M.

R. (2021).

Mitochondria in non-alcoholic fatty liver disease. International Journal of Biochemistry & Cell Biology, 131, 105874.

320. Simonides WS, Thelen MH, van der Linden CG, Muller A, van Hardeveld C. Mechanism of thyroid-hormone regulated expression of the SERCA genes in skeletal muscle: implications for thermogenesis. Biosci Rep 21: 139–154, 2001.

321. Singh, B. K., Sinha, R. A., Tripathi, M., Mendoza, A., Ohba, K., Sy, J. A. C., Xie, S. Y., Zhou, J., Ho, J. P., Chang, C. Y., et al. (2018). Thyroid hormone receptor and ERRα coordinately regulate mitochondrial fission, mitophagy, biogenesis, and function. Science Signaling, 11, aam5855.

322. Singh, R., Kaushik, S., Wang, Y., Xiang, Y., Novak, I., Komatsu, M., Tanaka, K., Cuervo, A. M., & Czaja, M. J. (2009). Autophagy regulates lipid metabolism. Nature, 458, 1131–1135.

323. Sinha R.A., You S.H., Zhou J., Siddique M.M., Bay B.H., Zhu X., Privalsky M.L., Cheng S.Y., Stevens R.D., Summers S.A., et al. Thyroid hormone stimulates hepatic lipid catabolism via activation of autophagy. J. Clin. Investig. 2012;122:2428– 2438.]

324. Sinha RA, Farah BL, Singh BK, Siddique MM, Li Y, Wu Y, Ilkayeva OR, Gooding J, Ching J, Zhou J, Martinez L, Xie S, Bay BH, Summers SA, Newgard CB, Yen PM, 2014. Caffeine stimulates hepatic lipid metabolism by the autophagy-lysosomal pathway in mice. Hepatology 59 (4), 1366–1380.

325. Sinha, R. A., et al. (2015). "Thyroid hormone induction of mitochondrial activity is coupled to mitophagy via ROS-AMPK-ULK1 signaling". Autophagy.

326. Sinha, R. A., You, S.-H., Zhou, J., Siddique, M. M., Bay, B.-H., Zhu, X., Privalsky, M. L., Cheng, S.-Y., Stevens, R. D., Summers, S. A., Newgard, C. B., Lazar, M. A., & Yen, P. M. (2012). Thyroid hormone stimulates hepatic lipid catabolism via activation of autophagy. Journal of Clinical Investigation, 122, 2428–2438.

327. Sinha, R.A.; Bruinstroop, E.; Singh, B.K.; Yen, P.M. Nonalcoholic Fatty Liver Disease and Hypercholesterolemia: Roles of Thyroid Hormones, Metabolites, and Agonists. Thyroid 2019, 29, 1173–1191.

328. Sinha, R.A.; Singh, B.K.; Yen, P.M. Reciprocal Crosstalk Between Autophagic and Endocrine Signaling in Metabolic Homeostasis. Endocr. Rev. 2017, 38, 69–102.

329. Sir D, Chen WL, Choi J, Wakita T, Yen TS, Ou JH, 2008a. Induction of incomplete autophagic response by hepatitis C virus via the unfolded protein response. Hepatology 48 (4), 1054–1061.

330. Soria LR, Brunetti-Pierri N. Targeting autophagy for therapy of hyperammonemia. Autophagy. 2018;14(7):1273–1275. doi:10.1080/15548627.2018.1444312.

331. Sterling, K. & Milch, P. O. Thyroid hormone binding by a component of mitochondrial membrane. Proc. Natl Acad. Sci. USA 72, 3225–3229 (1975).

332. Sterling, K., Milch, P.O., 1975. Thyroid hormone binding by a component of mitochondrial membrane. Proc. Natl. Acad. Sci. USA 72 (8), 3225–3229.

333. Sun L, Zhang S, Yu C, Pan Z, Liu Y, Zhao J, Wang X, Yun F, Zhao H, Yan S, Yuan Y, Wang D, Ding X, Liu G, Li W, Zhao X, Liu Z, Li Y, 2015. Hydrogen sulfide

reduces serum triglyceride by activating liver autophagy via the AMPK-mTOR pathway. Am. J. Physiol. Endocrinol. Metab 309 (11), E925–E935.

334. T. Radosavljevic, M. Brankovic, J. Samardzic, et al., "Altered Mitochondrial Function in MASLD: Key Features and Promising Therapeutic Approaches," Antioxidants 13, no. 8 (2024): 906.

335. Tang, J.X.; Thompson, K.; Taylor, R.W.; Oláhová, M. Mitochondrial OXPHOS Biogenesis: Co-Regulation of Protein Synthesis, Import, and Assembly Pathways. Int.
J. Mol. Sci. 2020, 21, 3820.

336. Tata JR, Ernster L, Lindberg O 1962 Control of basal metabolic rate by thyroid hormonesandcellular function. Nature 193:1058–1060.

337. Tata JR, Ernster L, Lindberg O, Arrhenius E, Pedersen S, Hedman R. The action of thyroid hormones at the cell level. *Biochemical Journal*. 1963;86(3):408–428. doi:10.1042/bj0860408

338. Tata JR. The early phase of thyroid hormone action: metabolic rate and mitochondrial response. Biochim Biophys Acta. 1960;40:145-152.

339. Tilg H, Moschen AR, 2010. Evolution of inflammation in nonalcoholic fatty liver disease: the multiple parallel hits hypothesis. Hepatology 52 (5), 1836–1846.

340. Titchenell, P. M., Chu, Q., Monks, B. R., & Birnbaum, M. J. (2015). Hepatic insulin signalling is required for suppression of gluconeogenesis and regulation of lipid metabolism. Nature Communications, 6, 7078.

341. Toledo M, Batista-Gonzalez A, Merheb E, Aoun ML, Tarabra E, Feng D, Sarparanta J, Merlo P, Botre F, Schwartz GJ, Pessin JE, Singh R, 2018. Autophagy regulates the liver clock and glucose metabolism by degrading CRY1. Cell Metabol. 28 (2), 268–281 e264.

342. Tumova J, Andel M, Trnka J. Excess of free fatty acids as a cause of metabolic dysfunction in skeletal muscle. Physiol Res. 2016;65:193–207. doi: 10.33549/physiolres.932993.

343. Uehara, K., Santoleri, D., Whitlock, A. E. G., & Titchenell, P. M. (2023). Insulin Regulation of Hepatic Lipid Homeostasis. Comprehensive Physiology, 13(3), 4785– 4809. https://doi.org/10.1002/cphy.c220015

344. Ueno T, Komatsu M, 2017. Autophagy in the liver: functions in health and disease. Nat. Rev. Gastroenterol. Hepatol 14 (3), 170–184.

345. Uhlen M, Fagerberg L, Hallstrom BM, Lindskog C, Oksvold P, Mardinoglu A, Sivertsson A, Kampf C, Sjostedt E, Asplund A, Olsson I, Edlund K, Lundberg E, Navani S, Szigyarto CA, Odeberg J, Djureinovic D, Takanen JO, Hober S, Alm T, Edqvist PH, Berling H, Tegel H, Mulder J, Rockberg J, Nilsson P, Schwenk JM, Hamsten M, von Feilitzen K, Forsberg M, Persson L, Johansson F, Zwahlen M, von Heijne G, Nielsen J, Ponten F, 2015. Proteomics. Tissue-based map of the human proteome. Science 347 (6220), 1260419.

346. V.T. Samuel, Z.X. Liu, X. Qu, B.D. Elder, S. Bilz, D. Befroy, A.J. Romanelli, G.I. Shulman. Mechanism of hepatic insulin resistance in non-alcoholic fatty liver disease.

347. Van Houten, B., Hunter, S. E., & Meyer, J. N. (2016). Mitochondrial DNA damage and repair: New insights into DNA damage responses. Free Radical Biology and Medicine, 100, 10–19.
348. Van Rooyen, D. M., Larter, C. Z., Haigh, W. G., Yeh, M. M., Ioannou, G., Kuver, R., Lee, S. P., Teoh, N. C., & Farrell, G. C. (2011). Hepatic free cholesterol accumulates in obese, diabetic mice and causes nonalcoholic steatohepatitis. Gastroenterology, 141(4), 1393–1403.e5.
349. Vargas-Uricoechea H, Bonelo-Perdomo A, Sierra-Torres CH. Effects of thyroid hormones on the heart. *Arteriosclerosis*. 2014;26(6):296-309.
350. Ventura-Clapier, R., Garnier, A., & Veksler, V. (2008). Transcriptional control of mitochondrial biogenesis: The central role of PGC-1α. Cardiovascular Research, 79, 208–217.
351. Veskovic, M.; Mladenovic, D.; Milenkovic, M.; Tosic, J.; Borozan, S.; Gopcevic, K.; Labudovic-Borovic, M.; Dragutinovic, V.; Vucevic, D.; Jorgacevic, B.; et al. Betaine Modulates Oxidative Stress, Inflammation, Apoptosis, Autophagy, and Akt/mTOR Signaling in Methionine-Choline Deficiency-Induced Fatty Liver Disease. Eur. J. Pharmacol. 2019, 848, 39–48.
352. W. Fu, J. Wang, N. Lu, et al., " Unveiling the Crucial Nexus: Mitochondrial Quality Control as a Central Driver in Metabolic Dysfunction-Associated Steatotic Liver Disease Pathogenesis," Cell Proliferation (2025): e70141.
353. Wang C, Niederstrasser H, Douglas PM, Lin R, Jaramillo J, Li Y, Oswald NW, Zhou A, McMillan EA, Mendiratta S, Wang Z, Zhao T, Lin Z, Luo M, Huang G, Brekken RA, Posner BA, MacMillan JB, Gao J, White MA, 2017. Small-molecule TFEB pathway agonists that ameliorate metabolic syndrome in mice and extend C. elegans lifespan. Nat. Commun 8 (1), 2270.
354. Wang L, Ou JH, 2015. Hepatitis C virus and autophagy. Biol. Chem 396 (11), 1215–1222.
355. Wang Y, Ding Y, Li J, Chavan H, Matye D, Ni HM, Chiang JY, Krishnamurthy P, Ding WX, Li T, 2017. Targeting the enterohepatic bile acid signaling induces hepatic autophagy via a CYP7A1-AKT-mTOR Axis in mice. Cell Mol Gastroenterol Hepatol 3 (2), 245–260.
356. Wang Y., Yang J., Zhang Y., Zhou J. Focus on Mitochondrial Respiratory Chain: Potential Therapeutic Target for Chronic Renal Failure. Int. J. Mol. Sci. 2024;25:949. doi: 10.3390/ijms25020949.
357. Weitzel J.M., Iwen K.A. Coordination of Mitochondrial Biogenesis by Thyroid Hormone. Mol. Cell Endocrinol. 2011;342:1–7.
358. Wenceslau, C. F., McCarthy, C. G., Szasz, T., Spitler, K., Goulopoulou, S., & Webb, R. C. (2014). Mitochondrial damage-associated molecular patterns and vascular function. European Heart Journal, 35(18), 1172–1177. https://doi.org/10.1093/eurheartj/ehu047.
359. West, A. P., & Shadel, G. S. (2017). Mitochondrial DNA in innate immune responses and inflammatory pathology. Nature Reviews Immunology, 17(6), 363–375.
360. West, A.P., Shadel, G.S., Ghosh, S., 2011. Mitochondria in innate immune responses. Nat. Rev. Immunol. 11 (6), 389–402.

361. Westermann, B., 2010. Mitochondrial fusion and fission in cell life and death. Nat. Rev. Mol. Cell Biol. 11 (12), 872–884.
362. White MF. Insulin signaling in health and disease. Science (1979) 302: 1710–1711, 2003.
363. Williams JA, Manley S, Ding WX, 2014. New advances in molecular mechanisms and emerging therapeutic targets in alcoholic liver diseases. World J. Gastroenterol 20 (36), 12908–12933.
364. Wirth E.K., Meyer F. Neuronal effects of thyroid hormone metabolites. Mol. Cell. Endocrinol. 2017;458:136–142. doi: 10.1016/j.mce.2017.01.007.
365. Wolff G, Sakurai M, Mhamane A, Troullinaki M, Maida A, Deligiannis IK, et al. Hepatocyte-specific activity of TSC22D4 triggers progressive NAFLD by impairing mitochondrial function. Mol Metab. 2022;60:101487.
366. Wrutniak C., Cassar-Malek I., Marchal S., Rascle A., Heusser S., Keller J.M., Fléchon J., Dauça M., Samarut J., Ghysdael J., et al. A 43-kDa protein related to c-Erb A alpha 1 is located in the mitochondrial matrix of rat liver. J. Biol. Chem. 1995;270:16347–16354. doi: 10.1074/jbc.270.27.16347.
367. Wrutniak-Cabello C., Casas F., Cabello G. Mitochondrial T3 receptor and targets. Mol. Cell. Endocrinol. 2017;458:112–120. doi: 10.1016/j.mce.2017.01.054
368. Wulf A, Harneit A, Kröger M, Kebenko M, Wetzel MG, Weitzel JM. T3-mediated expression of PGC-1alpha via a far upstream located thyroid hormone response element. Mol Cell Endocrinol. 2008 Jun 11;287(1-2):90-5. doi: 10.1016/j.mce.2008.01.017.
369. Xu, M., Feng, P., Yan, J., & Li, L. (2025). Mitochondrial quality control: A pathophysiological mechanism and potential therapeutic target for chronic obstructive pulmonary disease. Frontiers in Pharmacology, 15, 1474310.
370. Y.H. Chen, S. Lin, S.Y. Jin, T.M. Gao. Extracellular ATP is a homeostatic messenger that mediates Cell-Cell communication in physiological processes and psychiatric diseases. Biol. Psychiatry, 97 (2025), pp. 41-53.
371. Yakes, F. M., & Van Houten, B. (1997). Mitochondrial DNA damage is more extensive and persists longer than nuclear DNA damage in human cells following oxidative stress. Proceedings of the National Academy of Sciences of the United States of America, 94(2), 514–519.
372. Yan, Y., Niu, Z., Sun, C., Li, P., Shen, S., Liu, S., Wu, Y., Yun, C., Jiao, T., Jia, S., Li, Y., Fang, Z. Z., Zhao, L., Wang, J., Xie, C., Jiang, C., Li, Y., Feng, X., Hu, C., Jiang, J., … Ying, H. (2022). Hepatic thyroid hormone signalling modulates glucose homeostasis through the regulation of GLP-1 production via bile acid-mediated FXR antagonism. Nature communications, 13(1), 6408.
373. Yang J, Zhang Y, Yuan Y, Xie Z, Li L. Investigation of the Association between Air Pollution and non-alcoholic fatty liver disease in the European Population: a mendelian randomization study. Toxics. 2024
374. Yang JD, Roberts LR, 2010. Hepatocellular carcinoma: a global view. Nat. Rev. Gastroenterol. Hepatol 7 (8), 448–458.

375. Yang, Z., Guo, G., Li, J., & Sun, C. (2025). The role of cGAS–STING pathway in chronic liver diseases: Mechanisms and therapeutic perspectives. The FASEB Journal.
376. Yau W.W., Singh B.K., Lesmana R., Zhou J., Sinha R.A., Wong K.A., Wu Y., Bay B.H., Sugii S., Sun L., et al. Thyroid hormone (T3) stimulates brown adipose tissue activation via mitochondrial biogenesis and MTOR-mediated mitophagy. Autophagy. 2019;15:131–150.
377. Ye, L., Fu, X., & Li, Q. (2025). Mitochondrial quality control in health and disease. MedComm, 6(8), e70319.
378. Yen, P.M. 2001. Physiological and molecular basis of thyroid hormone action. Physiol Rev 81, 1097–1142.
379. Yin XM, Ding WX, Gao W, 2008. Autophagy in the liver. Hepatology 47 (5), 1773–1785.
380. Youle RJ, Narendra DP, 2011. Mechanisms of mitophagy. Nat. Rev. Mol. Cell Biol 12 (1), 9–14.
381. Z. Shao, X. Ding, Y. Zhou, J. Zhou, Y. Luo, D. Wu, et al. The role and mechanism of P2X7R in cirrhotic cardiomyopathy. Mol. Immunol., 176 (2024), pp. 49-59.
382. Zhang M-H, Li J, Zhu X-Y, Zhang Y-Q, Ye S-T, Leng Y-R, et al. Physalin B ameliorates nonalcoholic steatohepatitis by stimulating autophagy and NRF2 activation mediated improvement in oxidative stress. Free Radic Biol Med. 2021.
383. Zhang Q, Li F, Ge Q, Wang Y, Shen Z, Guo Y, Wang J, Zhangdi H, Lu J, Gao J, Chen G, Zhang Q, Wang X, Dong H, Lu L. YBX1/CD36 positive feedback loop-mediated lipid accumulation drives metabolic dysfunction-associated steatotic liver disease. Int J Biol Sci. 2025 Feb 18;21(5):2118-2134. doi: 10.7150/ijbs.105798. PMID: 40083711; PMCID: PMC11900817.
384. Zhang XK, Kahl M. Regulation of retinoid and thyroid hormone action through homodimeric and heterodimeric receptors. Trends Endocrinol Metab. 1993 Jul;4(5):156-62. doi: 10.1016/1043-2760(93)90105-n. PMID: 18407151.
385. Zhang Y, Fang F, Goldstein JL, Brown MS, Zhao TJ, 2015. Reduced autophagy in livers of fasted, fat-depleted, ghrelin-deficient mice: reversal by growth hormone. Proc. Natl. Acad. Sci. U. S. A 112 (4), 1226–1231.
386. Zhao L, Zhang C, Luo X, Wang P, Zhou W, Zhong S, et al. CD36 palmitoylation disrupts free fatty acid metabolism and promotes tissue inflammation in non-alcoholic steatohepatitis. J Hepatol. 2018;69:705–17.
387. Zhao, F.; Zou, M.-H. Role of the Mitochondrial Protein Import Machinery and Protein Processing in Heart Disease. Front. Cardiovasc. Med. 2021, 8, 749756.
388. Zick, M.; Rabl, R.; Reichert, A.S. Cristae formation—Linking ultrastructure and function of mitochondria. Biochim. Biophys. Acta Mol. Cell Res. 2009, 1793, 5–19.
389. Zucchi R, Rutigliano G, Saponaro F. 2019. Novel thyroid hormones. Endocrine 66:95–104.